KENTUCKY

TRANSPORTATION

CENTER

College of Engineering

STRUCTURAL EVALUATION OF THE HISTORIC JOHN A. ROEBLING SUSPENSION BRIDGE

UK

UNIVERSITY OF KENTUCKY

KTC03-10/MSC97-1F

STRUCTURAL EVALUATION OF THE HISTORIC
JOHN A. ROEBLING SUSPENSION BRIDGE

by

Wei-Xin Ren
Former Visiting Professor, Kentucky Transportation Center

Issam E. Harik
Professor of Civil Engineering and Head, Structures Section,
Kentucky Transportation Center

George E. Blandford
Professor of Civil Engineering, University of Kentucky

Michael Lenett
Former Research Professor of Civil Engineering, University of Cincinnati

and

T. Michael Baseheart
Professor of Civil Engineering, University of Cincinnati

Kentucky Transportation Center
College of Engineering, University of Kentucky

in cooperation with

Transportation Cabinet
Commonwealth of Kentucky

and

Federal Highway Administration
U.S. Department of Transportation

The contents of this report reflect the views of the authors who are responsible for the facts and accuracy of the data presented herein. The contents do not necessarily reflect the official views or policies of the University of Kentucky, the Kentucky Transportation Cabinet, nor the Federal Highway Administration. This report does not constitute a standard, specification or regulation. Manufacturer or trade names are included for identification purposes only and are not to be considered an endorsement.

April 2003

1. Report No. KTC03-10/MSC97-1F	2. Government Accession No.	3. Recipient's Catalog No.

4. Title and Subtitle	5. Report Date
STRUCTURAL EVALUATION OF THE HISTORIC JOHN A. ROEBLING SUSPENSION BRIDGE	April 2003
	6. Performing Organization Code

7. Author(s): Wei-Xin Ren, Issam E. Harik, George E. Blandford, Michael Lenett, and T. Michael Baseheart	8. Performing Organization Report No. KTC03-10/MSC97-AF

9. Performing Organization Name and Address	10. Work Unit No. (TRAIS)
Kentucky Transportation Center College of Engineering University of Kentucky Lexington, Kentucky 40506-0281	
	11. Contract or Grant No.

12. Sponsoring Agency Name and Address	13. Type of Report and Period Covered
Kentucky Transportation Cabinet State Office Building Frankfort, Kentucky 40622	Final
	14. Sponsoring Agency Code

15. Supplementary Notes

Prepared in cooperation with the Kentucky Transportation Cabinet and the U.S. Department of Transportation, Federal Highway Administration.

16. Abstract

The John A. Roebling suspension bridge, formerly the Covington-Cincinnati suspension bridge over the Ohio River was completed in 1867 and is still serving the Northern Kentucky community. The objective of this study is to assess the bridge load capacity via the dynamics-based technique. The scope of research includes finite element modeling and modal analysis, field ambient vibration testing, finite element model calibration to field test results, and bridge load-capacity evaluation. It is demonstrated that stress stiffening of cable elements plays an important role in both static and dynamic analyses of the Roebling suspension bridge. Large deflection behavior has been shown to have a limited effect on the member forces and deflections. Dominant vibration modes in the low frequency range are shown to be in the transverse direction. Higher free vibration modes of the bridge are coupled. In the structural evaluation under dead loading, the main cable area is reduced by 10% to 40% to simulate deterioration and corrosion of the cables. It is observed that the safety margin of the main cables remains fair (larger than one) even for the conservative 40% cable area reduction and extreme live loading pattern that equals 40% of uniform dead loading. Similarly, the truss member forces are within the maximum capacity.

The current load limit posting for the Roebling bridge is adequate. In case the load limit will be increased in the future, it is recommended that a detailed study be conducted to evaluate the need to strengthen the top chord truss members in order to increase the loading capacity of the truss.

17. Key Words	18. Distribution Statement
suspension bridge; finite element; modal analysis; ambient vibration testing; natural frequency; load-carrying capacity; structural evaluation.	Unlimited with approval of Kentucky Transportation Cabinet

19. Security Classif. (of this report) Unclassified	20. Security Classif. (of this page) Unclassified	21. No. of Pages 123	22. Price

Form DOT 1700.7(8-72)   **Reproduction of Completed Page Authorized**

TABLE OF CONTENTS

EXECUTIVE SUMMARY

1. INTRODUCTION

2. THE JOHN A. ROEBLING SUSPENSION BRIDGE

3. FINITE ELEMENT MODELING AND MODAL ANALYSIS

4. FIELD DYNAMIC TESTING AND MODEL CALIBRATION

5. BRIDGE CAPACITY

6. CONCLUSIONS AND RECOMMENDATIONS

EXECUTIVE SUMMARY

Research Objectives

The John A. Roebling suspension bridge, formerly the Covington-Cincinnati suspension bridge, over the Ohio River between Covington, Kentucky, and Cincinnati, Ohio, was completed in 1867. This bridge has provided 135 years of continuous service. Obviously, it was designed for live loads quite different from the loading it has to carry today. It is therefore essential to evaluate the current load-carrying capacity of the bridge and to bring the bridge up to current standards of safety, if necessary. Thus, the objectives of this investigation are

- ❑ Assess the current load capacity; and
- ❑ Evaluate the safety factors under live loading.

Structural evaluation of the John A. Roebling suspension bridge uses a dynamics-based methodology. This has become an increasingly popular strategy over the past twenty years even though dynamics-based structural evaluation requires improvements in instrumentation for sensing and recording, data acquisition, algorithms for system identification, finite element model calibration and structure evaluation. It does provide a 'global' approach to evaluate the current state of the structure. This study is composed of the following four tasks:

1) Finite element modeling and modal analysis;
2) On-site ambient vibration testing;
3) Finite element model updating (calibration) using field test results; and
4) Evaluation of the load-carrying capacity of the bridge components to assess the current levels of safety.

This study assesses the response of the bridge to current and projected traffic loads. The outcomes should assist in the preservation of the Roebling suspension bridge, which is regarded by many as a "National Treasure."

Background

Civil infrastructure structures, such as highway/railway bridges, water/gas/petroleum pipelines, electrical transmission towers, offshore structural foundations, etc., serve as the underpinnings of our highly industrialized society. Many such structures are deteriorating because of age, misuse and lack of repair. Much of the old infrastructure was not designed for current demands. Thus, evaluation is in order to prevent potential catastrophic events.

Many of the suspension bridges built in the U.S. in the 19th century are still in service today, e.g., the John A. Roebling suspension bridge, completed in 1867, over the Ohio River between Covington, Kentucky and Cincinnati, Ohio. The bridge was originally designed for the pedestrian traffic and horse-drawn wagons. Considering the live loads these bridges carry today, it is necessary to determine the current safely levels of these bridges.

Visual inspection has been and still is the most common method used in the structure evaluation. However, the increased size and complexity of structures can reduce the efficiency of the visual inspections. Conventional visual inspection might be costly and time consuming, especially when disassembly is necessary to provide access to the area being inspected. Structural evaluation using dynamics-based methods, on the other hand, has become an increasing popular in infrastructure evaluation.

Dynamics-based evaluation is based on comparing the experimental modal analysis data obtained from in situ field tests with the finite element predictions. One of the difficulties with such dynamics-based evaluations is the fact that it is difficult to establish a finite element model for aging or damaged structures since the current structural properties are typically unknown. Use of incorrect properties (material and cross section) in the FE models for dynamic performance predictions may result in relatively large differences between the experimental and analytical predictions. Some of the differences can be attributed to modeling errors resulting from the simplified assumptions that are necessary in modeling such complex structures, but much of the differences come from parameter errors due to structural damage as well as uncertainties in material and geometric properties. Thus, FE model calibration using the field dynamic test results plays an important role in dynamics-based structural evaluation. Such a calibrated FE model is the basis for load-carrying capacity evaluations of the bridge.

Finite Element Modeling and Modal Analysis

A three-dimensional finite element model is constructed in ANSYS, one of the most powerful engineering design and analysis software. The established finite element model is used to conduct both static and dynamic analyses of the Roebling suspension bridge. Since dead loading has a significant influence on the stiffness of a suspension bridge, static analysis due to dead loading is used to predict the deformed equilibrium configuration of the bridge and the level of "pre-stressing" in the structural members. Modal (dynamic) analysis is performed on the deformed equilibrium configuration and "pre-stressed" state predicted in the static dead load analysis. The modal analysis of a suspension bridge is therefore a "pre-stressed" modal analysis. All possible frequencies and mode shapes could be obtained from such a model, but only the lower frequency response modes are significant in predicting bridge response. Coupled modes are predicted from the finite element modal analyses, which provide a comprehensive understanding of the dynamic behavior of the bridge.

One major advantage of finite element modeling and analysis is that parametric studies are possible. The structural and material parameters that significantly affect the modal properties of the bridge can be identified through the parametric studies. Throughout the parametric studies, the key parameters affecting the vertical modal properties of the Roebling suspension bridge are the mass, cable elastic modulus and stiffening truss stiffness. The key parameters affecting the transverse modal properties are the mass, cable elastic modulus, stiffening truss stiffness and the transverse bending stiffness of the deck system. The parametric studies reported here not only prove the efficiency of the finite element methodology, but also demonstrate the extent and variation in modal properties due to variations in the input parameters.

Field Ambient Vibration Testing and Model Calibration

On site ambient vibration testing provides a fast and inexpensive methodology to obtain the current dynamic properties of a structure. The ambient vibration testing does not affect the traffic on the bridge because it uses the traffics and winds as natural excitation. This method is obviously cheaper than the forced vibration testing since no extra equipment is needed to excite the structure. Furthermore, on-site dynamic testing of a bridge provides an accurate and reliable description of the current bridge dynamic characteristics. Matching the current bridge dynamic characteristics with the analytical (FE) predictions has become an integral part of dynamics-based structure evaluation in order to minimize as much as possible the uncertainties and assumptions involved in analytical modeling.

Current dynamic characteristics (frequencies and mode shapes) of the Roebling suspension bridge are obtained from field ambient vibration testing under "natural" excitation such as traffic and wind. FE model calibration is then carried out by adjusting the structural and/or material parameters that significantly affect the modal responses of the bridge to match the analytic predicted frequencies and mode shapes with the field test results.

The first five vertical frequencies and transverse frequencies obtained from system identification through ambient vibration measurements and FEM predictions are summarized in Tables E-1 and E-2, respectively. Good agreement is observed in the tables.

Table E-1   Vertical Frequencies (Hz)

Order	v1	v2	v3	v4	v5
Test	0.563	0.904	1.218	1.931	2.308
FEM	0.561	0.971	1.240	1.843	2.282

Table E-2   Transverse Frequencies (Hz)

Order	t1	t2	t3	t4	t5
Test	0.186	0.447	0.602	0.938	1.254
FEM	0.189	0.418	0.617	0.875	1.091

It is shown that the dominant response mode shapes for the Roebling suspension bridge in the low-frequency (0 – 1.0 Hz) range are in the transverse direction. This reveals that the lateral stiffness of the bridge is relatively weak, which is due to using a single truss system to provide lateral stiffness unlike the lateral systems of modern bridges that use two lateral trusses. It is also observed that at least one of the dominant response modes is coupled, i.e., interaction among the transverse, vertical or torsion responses.

Bridge Load Capacity and Safety Factor Evaluation

An extreme live loading is considered in the study, defined as a live load pattern that equals 40% of the uniform dead loading. In addition, cable areas are reduced by 10 – 40% to simulate the deterioration of the cables. The load-carrying capacity of cable members and stiffening truss members are summarized in Tables E-3 and E-4, respectively.

It can be observed from the tables that the safety of the primary cables, secondary cables and suspenders remains above three under the extreme distributed live load condition. If in addition, the effective primary and secondary cable section areas are reduced 40%, the cable safety factors still remain above two. Thus, the reduction in the safely of the cables is not significantly affected by such drastic reductions in cable areas, which is good since these members sustain the majority of the bridge load. However, the reductions in the primary and secondary cable areas do result in significant increases in bridge deflection.

Table E-3   Capacity of Cable Members

Member		Maximum Force (kips)	Allowable Capacity (kips)	Safety Factor
Dead load + live load	Primary cable	2,620	8,392	3.20
	Secondary cable	1,947	12,040	6.18
	Suspender	46	150	3.26
Dead load +live load +40% cable area reduction	Primary cable	2,122	5,035	2.37
	Secondary cable	1,567	7,224	4.61
	Suspender	37	150	4.05

Table E-4   Capacity of Stiffening Truss Members

Member		Maximum Force (kips)	Allowable Capacity (kips)	Safety Factor
Dead load + live load	Bottom chord	138.8	828	5.97
	Top Chord	-367.7	985	2.68
	Diagonal	79.9	330	4.13
Dead load +live load +40% cable area reduction	Bottom chord	254.9	828	3.25
	Top Chord	-712.6	985	1.38
	Diagonal	150.0	330	2.20

Note: Tension is positive

The truss member forces induced under uniformly distributed live loading of 40% of dead load are well within the maximum load-carrying capacity, first set of rows in Table E-4. Critical truss members are shown to be the top chord members. For the primary and secondary cable area reduction of 40%, the induced forces in the critical truss members approach the design limit (safety factor of only 1.38). However, this level of loading and cable area reduction is considered improbable.

Recommendations

The current load limit posting for the Roebling bridge is adequate. In case the load limit will be increased in the future, it is recommended that a detailed study be conducted to evaluate the need to strengthen the top chord truss members in order to increase the loading capacity of the truss.

1. INTRODUCTION

1.1 General

Civil infrastructure structures, such as highway/railway bridges, water/gas/petroleum pipelines, electrical transmission towers, offshore structural foundations, etc., serve as the underpinnings of our highly industrialized society. Many infrastructures are now decaying because of age, deterioration, misuse, and lack of repair. Some of old infrastructures were originally not designed for current demands. It is the time to consider how to evaluate these widely spread infrastructures in order to prevent potential catastrophic events.

Structural decaying is considered as a weakening of the structure that negatively affects its performance. Structural decaying may also be defined as any deviation in the structure's original geometric or material properties that may cause undesirable stresses, displacements or vibrations on the structure. These weakening and deviations may be due to cracks, loose bolts, broken welds, corrosion, fatigue, etc.

Visual inspection has been and still is the most common method used in the structure evaluation. The increased size and complexity of today's structures can reduce the efficiency of the visual inspections. Conventional visual inspection might be costly and time consuming, especially when disassembly is necessary to provide access to the area being inspected. In addition, these visual inspection techniques are often inadequate for identifying the status of a structure invisible to the human eyes. For this reason, nondestructive damage detection techniques have been developed such as

- ❑ Ultrasonic and eddy current scanning;
- ❑ Acoustic emission;
- ❑ X-ray inspection, etc.

These techniques, although useful in many instances, are very expensive and involve bulky equipment. Moreover, they all require good access to the structure, and cause a great amount of down-time for the structure. A possible disadvantage is also that the place of potential damage should be known in advance. The methods are obviously "local" inspection techniques.

Structural evaluation using dynamics-based methods, on the other hand, has become an increasing concern due to their infrastructural roles (Friswell and Mottershead 1995; Brownjogn and Xia 2000). It is difficult to establish the finite element model for the aging or damaged structures as the current structural properties are unknown. Confidence in using FE models for dynamic performance predictions may be lacking due to relatively large difference between experimental and analytical modes. The differences come not only from the modeling errors resulting from simplified assumptions made in modeling the complicated structures but also parameter errors due to structural damage, uncertainties in material and geometric properties. Dynamics-based evaluation is therefore based on a comparison of the experimental modal analysis data obtained from in situ field tests with the finite element predictions. The FEM model calibration through the field dynamic testing plays an important role in the dynamics-based structural evaluation. The calibrated FEM model will be the basis for future load-carrying capacity evaluations of the bridge.

The dynamics-based structural evaluation requires improvements in instrumentation for sensing and recording, data acquisition, algorithms for system identification, model updating and structure evaluation. It provides a "global" way to evaluate the structural state. Detailed literature reviews have been provided by Doebling et al (1996), Salawu (1997) and Stubbs et al (1999). The applications have scattered over various areas (Casas and Aparicio 1994; Chen et al. 1995; Hearn and Testa 1991; Harik et al. 1997; Harik et al. 1999; Juneja et al. 1997; Liu 1995; Mazurek and Dewolf 1990; Ren and De Roeck 2000a; Ren and De Roeck 2000b). It has demonstrated that structural vibration based method is powerful and can significantly reduce the cost and increase the accuracy of nondestructive structure evaluation in aging large-scale structures.

Many of the suspension bridges built in the States in the 19th century still stand today. These suspension bridges were obviously designed for live loads that are quite different from automobile traffic they carry today. A good example is the John A. Roebling suspension bridge, completed in 1867, over the Ohio River between Covington, Kentucky and Cincinnati, Ohio. It is necessary to bring these bridges up to current standards of safety. The present study focuses on the load-carry capacity and safety evaluation of the John A. Roebling suspension bridge through a dynamics-based method. A three-dimensional finite element model is created in the ANSYS. Starting from the deformed configuration due to dead load, the modal analysis is followed up to provide all possible frequencies and mode shapes. The results of the finite element modal analysis have been compared with in situ ambient vibration measurements, and initial finite element model is updated. This finite element model, after calibrated with experimental measurements, is used to evaluate the safety of the bridge under extreme live load condition. The outcome assists in the preservation of the Roebling suspension bridge. The methodology developed could be applied to wide range of old cable-supported bridges.

1.2   On-Site Dynamic Testing

On-site dynamic testing of a bridge provides an accurate and reliable description of its real dynamic characteristics. Matching the real dynamic characteristics of bridges has become an integral part of aging structure evaluation in order to eliminate the uncertainties and assumptions involved in analytical modeling. There are two main types of dynamic bridge testing: forced vibration test and ambient vibration test. In the forced vibration testing, the structure is excited by artificial means such as shakers or drop weights. The disadvantage of this method is that traffic has to be shut down for a rather long time. It is clear that this can be a serious problem for intensively used bridges.

In contrast, the ambient vibration testing does not affect the traffic on the bridge because it uses the traffics and winds as natural excitation. This method is obviously cheaper than the forced vibration testing since no extra equipment is needed to excite the structure. However, relatively long records of response measurements are required and the measurement data are highly stochastic. Consequently, the system identification results are not always that good.

In the context of ambient vibration testing only response data of ambient vibrations are measurable while actual loading conditions are unknown. A system identification procedure will therefore need to base itself on output-only data. System identification using ambient vibration measurements presents a challenge requiring use of special identification techniques, which can deal with very small magnitudes of ambient vibration contaminated by noise without the knowledge of

input forces.

For the Roebling suspension bridge, on-site dynamic testing was performed in the way of ambient vibration testing under "natural" excitation such as traffic, wind and their association. Since the bridge is symmetric, ambient vibration measurements is carried out only on one-half of the bridge (one-half main span and one side span). The measured data are the acceleration-time histories. The dynamic characteristics (frequencies and mode shapes) of the Roebling suspension bridge were extracted from the peak of the average normalized power spectral densities (ANPSDs). These vibration properties are subsequently used as a basis for updating the original finite element model of the bridge.

1.3   Finite Element Modeling and Model Calibration

Nowadays, it is no longer a question to predict accurately both static and dynamic structural behavior of suspension bridges. The discretized finite element method (FEM) of continua provides a convenient and reliable idealization of the structure. Thanks to rapid computer developments and the accumulation matrix analysis studies on nonlinear problems, the finite deformation theory with a discrete finite element model has been the most powerful tool used in the analysis and design of suspension bridges. An important advantage of the finite element method is that structural complexities can be considered effectively. The application of the finite deformation theory can include the effect of all nonlinear sources of suspension bridges such as cable sags, large deflections, axial force and bending moment interaction. Another advantage of the finite element method lies in the capability of in-depth dynamic analysis.

A completed three-dimensional finite element model of the Roebling suspension bridge is conceived in the ANSYS, one of the most powerful engineering design and analysis software (ANSYS5.6 1999). The ANSYS is chosen because of the program's significant capability to account for the cable stress stiffening and the pre-stressed modal analysis capability. The FEM model of the Reobling suspension bridge is composed of four element types: 3-D beam element, 3-D truss element, 3-D tension-only truss element and membrane shell element, which consists of 1756 nodes and 3482 finite elements. The active degree of freedom (DOF) is totally 7515.

In the design of suspension bridges, the dead load often contributes most of bridge loads. It was realized in the early 1850's that the dead load has a significant influence on the stiffness of a suspension bridge. In the finite element analysis, this influence is included through the static analysis under dead loads before the live load or dynamic analysis is carried out. The objective of the static analysis process is intended to achieve the deformed equilibrium configuration of the bridge due to dead loads where the structural members are "pre-stressed". For a completed suspension bridge, the fact is that the initial position of the cable and bridge is unknown. Only the finial geometry of the bridge due to the dead load is known. The initial geometry of the ideal finite element model of a suspension bridge should be such that the geometry of a bridge does not change when a dead load is applied, since this is indeed the finial geometry of the bridge as it stands today. Also, no forces should be induced in the stiffening structure. In other words, the deformed configuration of the bridge under the self-weight dead load should be close to the initial geometry input. This can be approximately realized by manipulating the initial tension force in the main cables that is specified as an input quantity (pre-strain) in the cable elements. The initial tension in the cables is achieved by

trial until a value is found that leads to the minimum deflections and the minimum stresses in the stiffening structure due to dead load. In addition, the geometric nonlinear effect has been studied by including the stress stiffening and large deflection.

A suspension bridge is a highly pre-stressed structure. Starting from the deformed equilibrium configuration, the modal analysis is followed up. Consequently, the dead load effect to the stiffness can be included in the modal analysis. The modal analysis is therefore a "pre-stressed" modal analysis. All possible frequencies and mode shapes can be provided. A coupled mode can be included, which gives a comprehensive understanding of the dynamic behavior of suspension bridges. Parametric studies can also be performed. The parameters include self-weight of the deck, the stiffness of cables, the stiffness of suspenders, the stiffness of stiffening trusses and bending stiffness of floor beams and stringers.

Due to the deviation in the structure's original geometric or material properties, cracks, loose bolts, broken welds, corrosion, fatigue, etc., it is difficult to establish the finite element model for the structural evaluation initially. The original finite element model has to be updated or calibrated by the field testing in order to meet the current conditions of the bridge. The finite element model updating is carried out by the best matching the frequencies and modal shapes between the field tests and analytical finite element model. The updated finite element model will be served as the baseline for future load-carrying capacity evaluations of the bridge.

1.4 Bridge Capacity Evaluation

The objective of performing bridge load-carrying capacity evaluation is to determine the stiffness and strength of the bridge. The bridge load-carrying capacity evaluation aims at finding the deflected shape and member forces due to dead load and imposed live loads on the bridge. The finite element model of the Roebling suspension bridge, once calibrated by the dynamic testing on site, is capable to evaluate the global capacity. The considered live load patterns here are an extreme live loading (40% in addition to the dead load). The cable area is reduced by a certain percentage (10~40%) to simulate the deterioration and corrosion of the cables. The bridge safety is studied when the cable areas are reduced. The bridge capacity evaluation includes the maximum deflection, the capacity of the cables and the capacity of the stiffening trusses. It is demonstrated that the margin of safety in the main cables and the suspenders is fair under the extreme distributed live load condition and this is of great significance for the safety concerns of a suspension bridge. Assuming conservatively that the effective sectional area has been reduced by 40% for both primary and secondary cables, the safety factors of cables are still more than two. It is indicated that some truss members may be overstressed at an inventory loading. Therefore, it is suggested that some truss members should be rehabilitated in order to carry the increased loading.

1.5 Scopes of the Work

The primary aim of this investigation is to evaluate the load-carrying capacity and structural safety of the John A. Roebling suspension bridge subjected to current traffic loads governed by the AASHTO's Standard Load Specifications for Highway Bridges. The dynamics-based structural

evaluation method is used. To achieve the goal, the scope of work will be divided into the following four parts:

5) Finite element modeling and analysis;
6) On-site ambient vibration testing;
7) Finite element model calibration by the field testing;
8) Bridge capacity evaluation;

The outcome of this study can assist in the preservation of the Roebling suspension bridge, which is regarded by many as a "National Treasure."

2. THE JOHN A. ROEBLING SUSPENSION BRIDGE OVER THE OHIO RIVER

2.1 Gereral

The John A. Roebling suspension bridge (B48) as shown in Fig.2.1, formerly the Covington-Cincinnati suspension bridge, carries KY 17 over the Ohio River between Covington, Kentucky, and Cincinnati, Ohio. The 1,056 foot main span of the suspension bridge carries a two-lane 28 foot wide steel grid deck roadway (Fig. 2.2) with 8 foot and 6 inch wide sidewalks cantilevered from the trusses (Fig. 2.3). The towers are 240 feet in height and encompass 400,000 cubic feet of masonry. They are 82 feet long and 52 feet wide at their base. The towers bear on timber mat foundations which are 110 feet long, 75 feet wide, and 12 feet thick. The suspension bridge system is composed of two sets of suspension cables restrained by massive masonry anchorages. The primary cables (1865) are composed of iron wires and are 12 1/3 inches in diameter. The secondary cables (1897) are composed of steel wires and are 10 ½ inches in diameter. Stay cables radiate diagonally from the towers to the upper chords of the stiffening trusses. Deck loads are transferred from the stringers and floor beams to the suspenders, trusses, stay wires and then to the suspension cables and finally to the anchorages and towers. The approach span roadway varies from 20' to 24' wide and is composed of a concrete deck supported by riveted steel plate girders (Fig. 2.4). The plan view of the Roebling suspension bridge is as shown in Fig. 2.5.

The John A. Roebling suspension was the first permanent bridge to span over the Ohio River between Covington, Kentucky, and Cincinnati, Ohio. Completed in 1867, the Roebling suspension bridge still stands today, after 133 years of service. The bridge carries an average daily traffic of 21,843 vehicles per day according to 1985 traffic data supplied by the Kentucky Department of Highways, Division of Planning. In Ohio, the bridge intersects Second and Third Streets via one-way entrance and exit ramps. There are also bus ramps leading to the Dixie Terminal Building on Third Street. In Kentucky, KY 17 intersects Second Street approximately 150 feet from the south anchorage. The Ohio anchor span crosses over US52 (Riverside Parkway) and a single-track rail line owned by Norfolk Southern Railway. The bridge is currently posted at 15 tons for two-axle trucks and 22 tons for three, four and five-axle trucks.

As a tribute to the skill of its designer – John A Roebling, the bridge is a national Historic Civil Engineering Landmark, one in about 30 bridges honored nationwide by American Society of Civil Engineers. The Roebling suspension bridge was also listed on the National register of Historic Places in 1975 (Fig. 2.6).

Throughout its history, the John A. Roebling Bridge has proven its ability to accommodate new modes of transportation. Modifications have permitted the bridge to evolve from carrying pedestrian traffic and horse-drawn wagons to carrying trolleys and currently used by automobiles, buses, and trucks.

2.2 History Background of the Bridge

The need for a bridge spanning the Ohio River became apparent to the Legislative body of Kentucky due to increased commercial traffic between the north and south during the early 1800's.

The Covington and Cincinnati Bridge Company (CCBC) was incorporated in 1846 in hope of capitalizing on the construction of a bridge connecting the two cities. However, the Ohio Legislature, under pressure from the steamboat industry which was concerned that a bridge would interfere with river traffic, refused to grant a charter to the company until 1849.

The company, headed by local financier Amos Shinkle, consulted two prominent engineers, Charles Ellet and John A. Roebling, both of whom advocated the use of a suspension bridge which would minimize the effect on river traffic. In order to test the feasibility of a suspension bridge, the CCBC built a bridge spanning the Licking River between the cities of Covington and Newport, using local labor and engineers, at a cost of $80,000. Unfortunately, two weeks after its completion, a herd of cattle crossing the bridge caused enough vibration to collapse the bridge into the river.

Charles Ellet's Wheeling Suspension Bridge, which was constructed during the same time period over the Ohio River between Ohio and West Virginia, met with a similar fate during a violent storm four months later. These two failures, along with economic hardship and civil unrest, delayed further consideration of a bridge for several years.

In 1856, Amos Shinkle began a push forwards renewing the bridge project. Finally, he was awarded a contract to begin the construction of a suspension bridge between Covington and Cincinnati. The CCBC chosen John A. Roebling as Head Engineer. By the end of the 1858 construction season, a portion of both towers had been completed; however, construction was halted because of the lack of funds. Confederate invasions of Kentucky throughout the Civil War probably pointed out the strategic importance of a link in this area between Ohio and Kentucky. The difficulty of transporting troops and materials across the river during the Civil War emphasized the need for a bridge in the area. Additional funds were obtained, and construction resumed in 1863. The toll bridge was completed in December, 1866, with Roebling's son, Col. Washington A. Roebling, in the position of Assistant Engineer.

The bridge was opened to pedestrians on December 1, 1866, and was opened to vehicular traffic on January 1, 1867. At the time of its opening, the suspension bridge represented both the old and the new. Soaring masonry towers representative of construction methods to that date supported a state-of-the-art iron-wire cable technology. This monument to civil engineering of the 1800's represented the longest span in the world (1,056 feet) at the time of its opening. Today, the bridge remains the second longest span in Kentucky State. The U.S. 62 Suspension Bridge over the Ohio River at Maysville, Kentucky, constructed in 1931, has a main span length of 1,060 feet. It is truly remarkable that such a monumental work was achieved in an era of civil strife.

In the mid 1890's, the bridge was reconstructed. The primary cable ends in the anchorages were restored. A second set of suspension cables and anchorages was added. The stiffening trusses and floor system were replaced. The tower staircases were built. The sidewalks were replaced in 1934. A second major reconstruction occurred in the mid 1950's. Approximately 765 feet of the Ohio Approach were removed from Third Street to Front Street. New bus ramp bridges to the Dixie Terminal Building and a new bridge over Second Street were built. Abutment 1 was constructed. The remainder of the approach structure was replaced with earth fill. The open steel gird deck replaced a timber deck on the suspension spans.

The Suspension Bridge, as it was officially known for 117 years, was renamed "The John A. Roebling Bridge" by the Commonwealth of Kentucky in 1983 in order to honor its builder. The bridge was listed on the National Register of Historic Places in 1975. The Covington-Cincinnati suspension bridge served as a milestone in John A. Roebling's career which culminated in the design of his more famous Brooklyn Bridge. He died on July 22, 1869, after suffering an accident while working on the Brooklyn Bridge, of which the Roebling Bridge was a prototype.

The following summarizes the important events in the bridge history

- John A. Roebling was born in Germany on June 12, 1806, was educated at the Royal Polytechnic Institute in Berlin, emigrated to the United States in 1831, and began a career as a civil engineer.
- The Covington and Cincinnati Bridge Company (CCBC) was incorporated by the Legislature of Kentucky in 1846.
- The Covington and Cincinnati Bridge Company (CCBC) was incorporated by the Legislature of Ohio in 1849.
- Construction of John A. Roebling's railway suspension bridge over the Niagara Gorge was completed in 1856.
- Construction of the bridge over the Ohio River between Covington, Kentucky, and Cincinnati, Ohio, began in 1856 with John A. Roebling serving as Head Engineer.
- A portion of both towers had been completed by the end of the 1858 construction session. Construction was halted because of the lack of funds.
- The Civil War began on April 12, 1861.
- Additional bonds were sold, and construction resumed in 1863.
- The Civil War ended on April 9, 1865.
- The bridge was completed and opened to pedestrians on December 1, 1866. On December 2, at least 75,000 pedestrians crossed the bridge. The bridge was opened to vehicular traffic on January 1, 1867. Final project cost was $1,800,000. Its 1,056 foot main span was the largest in the world at that time and was the first to span the Ohio River between Kentucky and Ohio.
- John A. Roebling died on July 22, 1869, after suffering an accident while directing construction of the Brooklyn Bridge.
- The bridge was reconstructed in the mid 1890s in order to increase its capacity for modern highway loadings. The primary cable ends in the anchorages were reconstructed. A second set of suspension cables and anchorages was added. The stiffening trusses and floor system were replaced. Tower staircases were added.
- The sidewalks were replaced in 1934.
- The suspension bridge was the only bridge over the Ohio River between Steubenville, Ohio, and its confluence with the Mississippi River to remain open during the 1937 flood.
- The bridge was operated by the CCBC as a private toll facility until 1953, when it was purchased by the Commonwealth of Kentucky for $3.6 million.

❑ A second major reconstruction occurred in the mid 1950s. Approximately 765 feet of the Ohio Approach were removed from Third Street to Front Street. New bus ramp bridges to the Dixie Terminal Building and a new bridge over Second Street were built. Abutment 1 was reconstructed. The remainder of the approach structure was replaced with earth fill. An open steel grid deck replaced a timber deck on the suspension spans.

❑ Tolls were removed in 1963.

❑ The bridge was listed on the National Register of Historic Places in 1975.

❑ The Suspension Bridge was renamed the "John A. Roebling Bridge" by the Commonwealth of Kentucky in 1983.

The John A. Roebling suspension was the first permanent bridge to span over the Ohio River between Covington, Kentucky, and Cincinnati, Ohio. Throughout its history, the John A. Roebling Bridge has proven its ability to accommodate new modes of transportation. Modifications have permitted the bridge to evolve from carrying pedestrian traffic and horse-drawn wagons to carrying trolleys and its currently used by automobiles, buses, and trucks. The bridge has been playing an important role in local community since its opening. The importance of the Bridge to local community is summarized as follows:

❑ The John A. Roebling Bridge has been designed a National Historic Civil Engineering Landmark by the American Society of Civil Engineers.

❑ The bridge is one of four bridges providing local access to the Covington-Cincinnati street system. Two interstate bridges also link the urban areas of the two cities.

❑ The bridge carries an average daily traffic of 21,843 vehicles per day according to 1985 traffic data supplied by the Kentucky Department of Highways, Division of Planning.

❑ In Ohio, the bridge intersects Second and Third Streets via one-way entrance and exit ramps. There are also bus ramps leading to the Dixie Terminal Building on Third Street. In Kentucky, KY 17 intersects Second Street approximately 150 feet from the south anchorage. The Ohio approach spans Cincinnati's Riverfront Stadium parking lot.

❑ The bridge is currently posted at 15 tons for two axle trucks and 22 tons for three-, four-, and five-axle trucks.

❑ The bridge serves as an integral part of the Cincinnati riverfront development efforts.

2.3 Prior Inspections

The original design plans of the Roebling suspension bridge were unavailable. However, several sets of repair plans have been secured, one dating to the 1890's reconstruction. The seven (7) most recent inspection results are summarized below

1978	All anchorages leak causing cable corrosion; excessive pigeon waste in towers causing cable corrosion.
1979	All anchorages leak; concrete bearing pads at North abutment cracked, spalled.
1980	Unsafe tower stairways; swelling of cables in Kentucky secondary anchorages.
1981	Unsafe tower stairways; faulty expansion devices; deteriorating stiffening truss bearings.
1982	Unsafe tower stairways; faulty expansion devices; deteriorating stiffening truss bearings.
1983	Unsafe tower stairways; faulty expansion devices; deteriorating stiffening truss bearings.
1984	Wooden cable housings at top of tower in poor condition. Unsafe tower stairways; faulty expansion devices; deteriorating stiffening truss bearings.
1985	Heavy cracking and spalling of tower roofs.

As part of an effort to evaluate the present condition of the bridge after 121 years of service, the Kentucky Transportation Cabinet retained the consulting engineering firm of Parsons Brinckerhoff Quade & Douglas, Inc. in 1987 to perform an in-depth inspection of the bridge. The inspection was carried out in accordance with AASHTO's "Manual for Maintenance Inspection of Bridges" dated 1983. The following represents a brief summary of the major inspection findings and considerations for future rehabilitation of the bridge (Parsons Brinckerhoff Quade & Douglas Inc. 1988).

1987 Inspection Summary

❑ The Ohio Approach deck is in poor condition. There are numerous areas of leaking and corrosion of the steel floor. The suspension span's open steel grid deck are in good condition.

❑ The primary and secondary suspension cables are in fair condition. The areas of greatest deterioration are in the masonry anchorages. Twenty-one broken wires were counted in the south anchorage for the east secondary cable. Several strands are also bulging due to corrosion caused primarily by leakage of water through the roof. A report prepared by the Kentucky Department of Highways, Division of Maintenance, suggested that this cable has lost 35% of its ultimate strength. The paint system on the primary cable wrapping is in poor condition. The paint system on the secondary cable wrapping is in fair condition. There is also a heavy accumulation of pigeon waste on the cables in the towers.

❑ The suspension cable and stay cable saddles in the towers are in fair condition. They appear to be frozen due to heavy debris accumulation. This condition causes the towers to rock on their timber mat foundations.

❑ The suspenders and stays are in fair condition. Some of the suspenders to floor beam bearings in the main span have shifted laterally, shearing off the restraining angle. Some suspenders exhibit below average tension as compared with other suspenders on this bridge. The stays are embedded in heavy pigeon waste accumulation in the towers.

❑ The Ohio approach girders are in poor condition. Pack rust has developed between the bottom tension flange cover plates causing them to spread apart by ½" to 1". The diaphragms and cross frames are in poor condition at the ends of Spans 6 and 7 at the anchorages.

❑ The suspension span's stringers are in poor condition. There are many unseated stringers at expansion joint locations. This condition has caused cracks to develop in the webs of four stringers. Fifty percent (50%) localized pitting section loss of the top flanges is common. Pack rust has developed at the stringer to floor beam connections.

❑ The Ohio approach floor beams are in poor condition. The floor beams are mostly damaged beneath leaking expansion joints and the steel plate deck adjacent to Anchorage 1.

❑ The suspension span's floor beams are in fair condition. The floor beam to truss bearing connection angles are cracked in six of eight locations at the towers. The top flanges are heavily pitted. The top flanges of three floor beams are cracked. There are three cracks in the floor beam web at panel point L54.

❑ The stiffening trusses are in fair condition. The pins are loose and have moved 1/4" transverse to the bridge. There are two cracked pin nuts. Pins suffer from pitting corrosion. Most of the truss member corrosion is confined to the lower chord joints, where there is up to 50% section loss of diagonal eye bar heads. There are numerous locations of traffic impact damage to truss verticals.

❑ The north abutment is in poor condition. It has tilted, causing the girder bearing pads to spall severely.

❑ Anchorage 1 is in poor condition because of masonry deterioration, cracks, and open joints beneath the floor beams of the adjacent spans.

❑ Anchorages 2, 3 and 4 are in fair condition. There is heavy spalling of stones above the sidewalk and roadway elevations, which is hazardous to both pedestrians and vehicular traffic. There are large pieces of stones missing from Anchorage 2, causing a visually offensive appearance. Some of the foil roof material on the cable housing has peeled, allowing moisture to seep into the cable rooms cracks were observed inside the cable housing of Anchorages 3 and 4.

❑ The towers are in fair condition. The main problem with the domes and cable housings is that pigeons have penetrated through protective wires, depositing waste on the cables and floor to a depth of six inches. There are several areas of loose and missing joint material and bricks, with a hole through the wall of the east dome of the North Tower. The wooden cable housings are in fair condition. The most seriously problem discovered, in terms of immediate traffic safety, is

heavy layering and spalling of large blocks of stone above the roadway level. There is heavy joint material loss and vegetation growth in these areas.

1987 Recommendations and Future Considerations

Additional investigations should be carried out prior to the development of a comprehensive rehabilitation effort. These investigations will enable the engineers directing the rehabilitation effort to make informed decisions based on the better understanding of the condition and interaction of the various bridge components.

- Structural rating are needed which account for the existing condition and bus loadings, in order to better assess the course of action for current load limit posting of the bridge. However, a significant reduction of the posted weight limit in lieu of repairs would probably be the greatest contributing factor to the accelerated demise of this Historic Landmark.

- Wedge the east secondary cable in the Cincinnati anchorage. Locate and quantify section losses and compare with results obtained form the cable investigation in the Covington anchorage to obtain a more accurate appraisal of the cable's condition.

- Strain gages should be installed on the suspension cable eyebars in each anchorage to determine distribution of live loads as unit vehicles are driven across the bridge. This data base could also be used for future comparison.

- Surveying instrumentation/monumentation should be used to determine the possibility of excessive cable sag because of corrosion in anchorages.

- Unwrap portions of the suspension cables to determine the need for replacing the wrapping system. Install inspection ports at these locations for future inspection.

- Remove suspender cable bands at selected locations to ascertain the condition of the wrapping system and cable wires within.

- Remove suspenders at selected locations and perform tensile tests on the suspenders and sockets to determine the need for replacing suspenders.

- Surveying instrumentation/monumentation should be used to compare the current tilting of the towers with measurements taken in the 1950s.

- Core and examine samples from the timber mat foundations if live load capacity of the structure is upgraded.

Due to its redundant design, the John A. Roebling suspension bridge could probably remain in service for another five years using a minimal maintenance effort. However, once deterioration sets in, the rate of deterioration continues to increase exponentially to the point where repair and rehabilitation is not possible without enormous expenditures of money. Only with an ongoing

program of inspection, instrumentation, analysis, and repair the heritage of the John A. Roebling suspension bridge can be maintained until the time when new techniques and, materials are developed to aid preservation of the bridge indefinitely.

Fig. 2.1   The John A. Roebling Suspension Bridge

Fig. 2.2   View of Open Steel Grid Deck on Kentucky Anchor Span Looking North
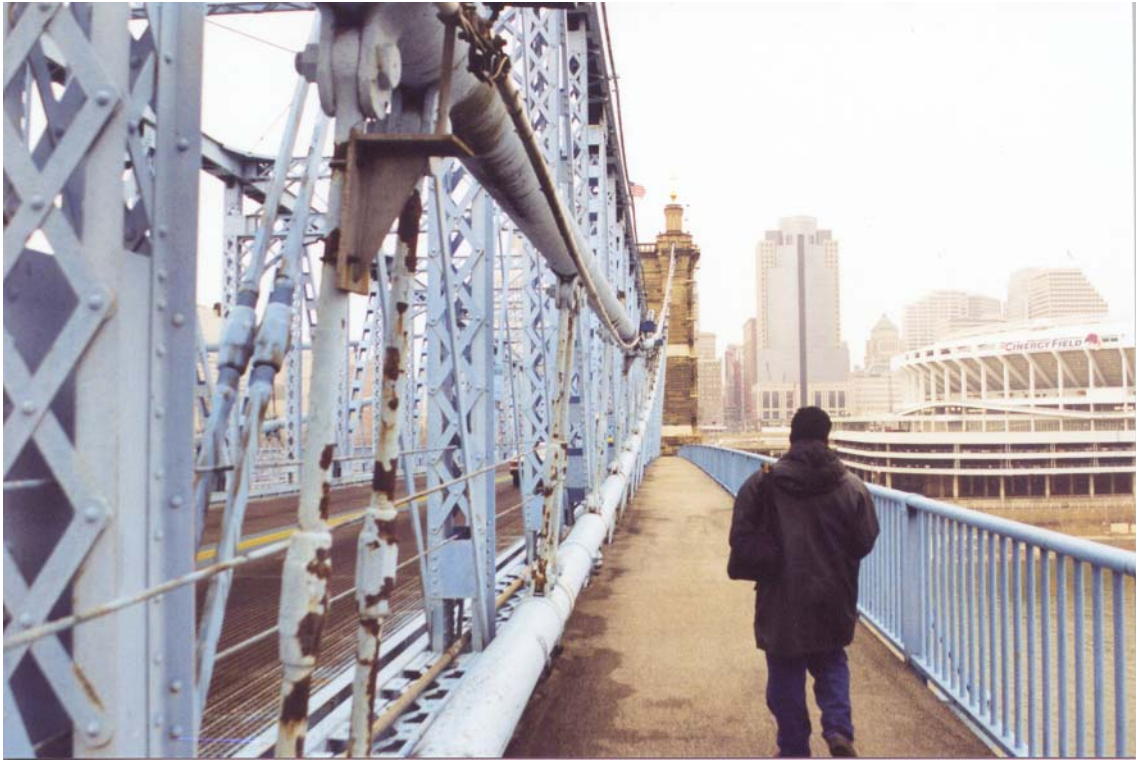
Fig. 2.3   One Side View of Sidewalks

Fig. 2.4   View of Approach Span Roadway

PLAN

TO CINCINNATI

TO COVINGTON

1937 HIGH WATER EL. 509.7

NORMAL POOL EL. 455.0

OHIO RIVER

ANCHORAGE 1

ANCHORAGE 2

NORTH TOWER

SOUTH TOWER

ANCHORAGE 3

ANCHORAGE 4

295'-0"

1056'-5"

921'-6"

ELEVATION
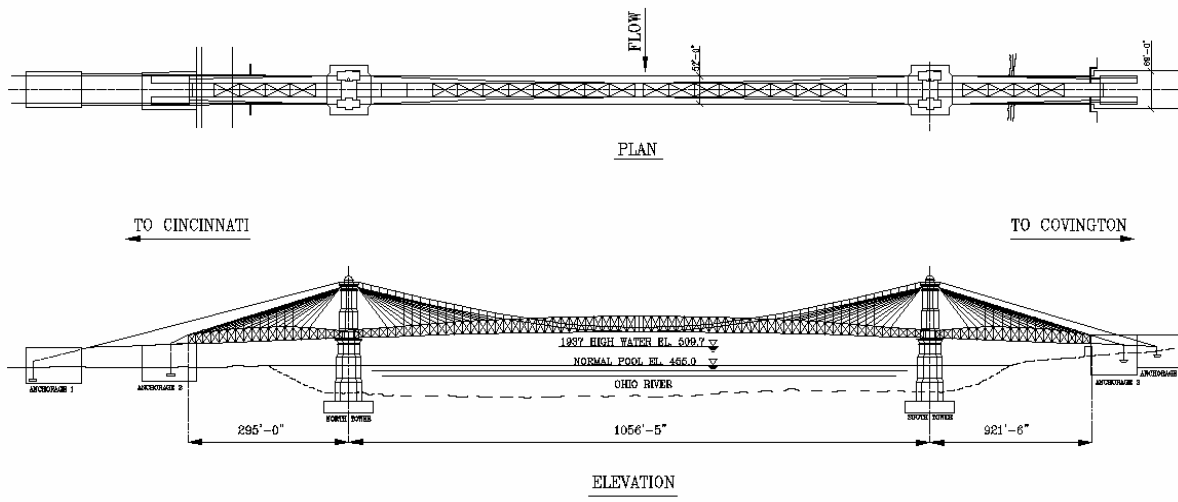
Fig. 2.5   Plan View of the Roebling Suspension Bridge
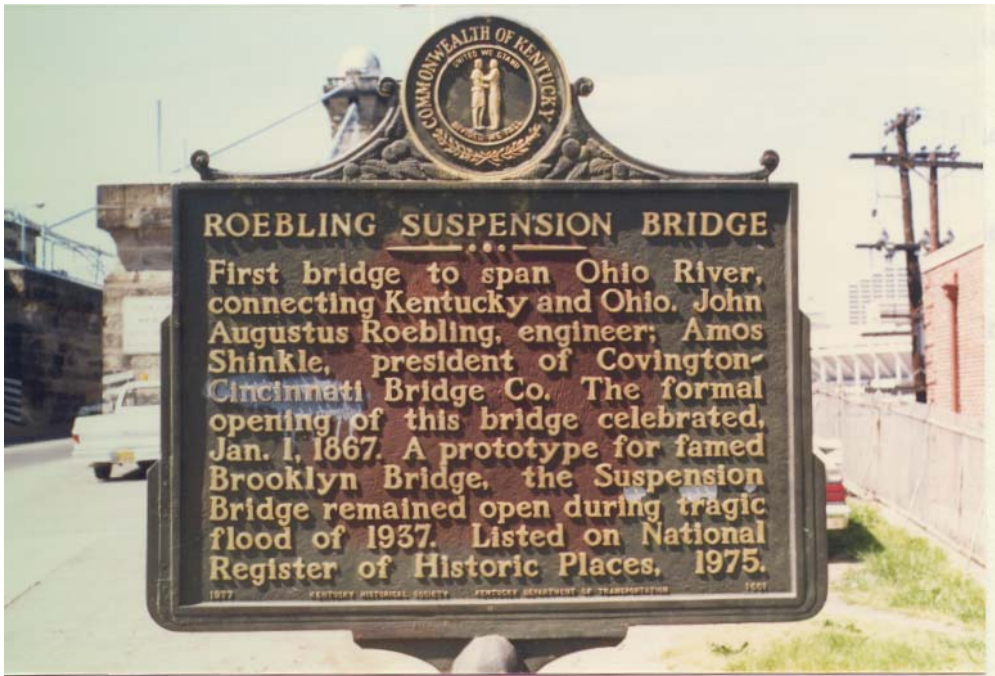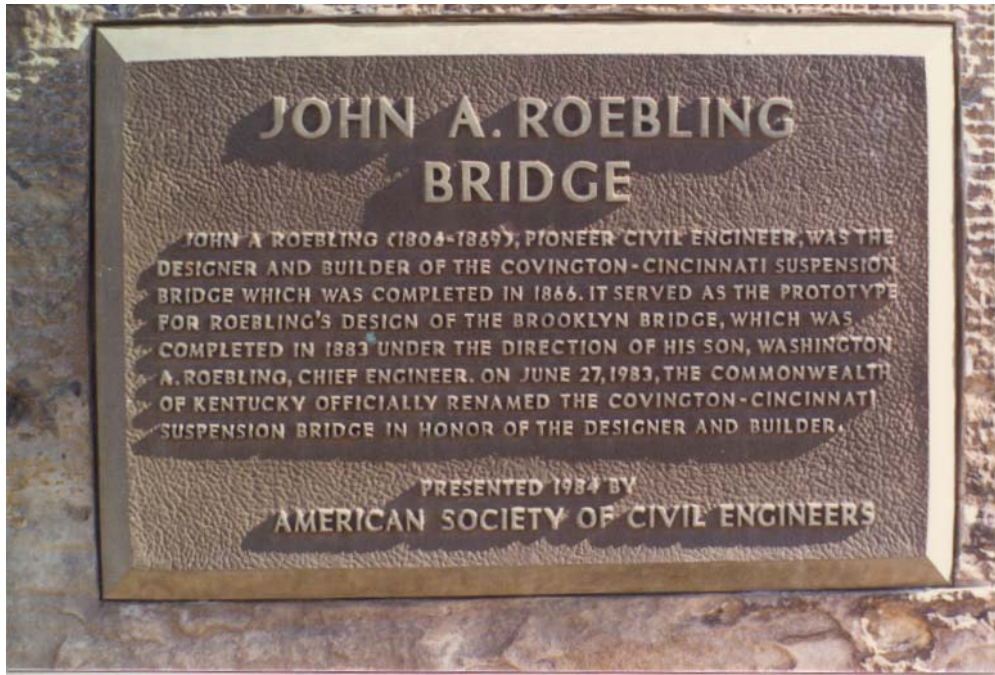
Fig. 2.6   The Historic Marker of the Bridge

3. FINITE ELEMENT MODELING AND MODAL ANALYSIS

3.1 General

The unique structural styles of suspension bridges make the span length longer and beautify the environment, but also add to the difficulties in accurate structural analysis. The commonly used classical theories for static analysis of suspension bridges are the elastic theory and the deflection theory (Steinman 1929; Bounopane and Billington 1993). The design of the oldest suspension bridges built as early as the first half of 19th century was based on the elastic theory of stress analysis. Indeed, it is the theory that was employed by J.A. Roebling to design this bridge (Roebling 1867).

The elastic theory is basically a linearized approximate theory, as it does not take into account the deformed configuration of the structure. Though the values of bending moment and shear yielded by the elastic theory are too high, it satisfies more safe design but not economy. This method is quite expeditious and convenient for preliminary designs and estimates. Basically, the elastic theory is sufficiently accurate for shorter spans or for designing relatively deep rigid stiffening systems that limit the deflections to small amounts. However, the elastic theory does not suite for designing the suspension bridges with long spans, shallow trusses, or high dead load. The deflection theory, on the contrast, is a more "exact" theory that took into account the deformed configuration of the structure and results in more economical and slender bridges. The deflection theory had dominated the suspension bridge design for many decades and ended with the dramatic failure of the Tacoma Narrows Bridge in 1940.

Nowadays, it is no longer a question to predict accurately both static and dynamic structural behavior of suspension bridges. The discreterized finite element method of structural continua provides a convenient and reliable idealization of the structure and is particularly effective in digital-computer analysis. The finite element type of idealization is applicable to structures of all types. Thanks to rapid computer developments and the accumulation matrix analysis studies on nonlinear problems, the finite deformation theory with a discrete finite element model has been the most powerful tool used in the nonlinear analysis of cable-supported bridges. The application of the finite deformation theory can include the effect of all nonlinear sources of suspension bridges such as cable sags, large deflections, axial force and bending moment interaction.

An important advantage of the finite element method is that structural complexities such as tower movements, side spans, hanger and cable extensibility, support conditions, etc. can be considered effectively. The finite element method can also analyze the effect of changes in different parameters, which allows the parameter design. Two- or three- dimensional finite element models with beam and truss elements are often used to model both the superstructure and the substructure of cable-supported bridges (Nazmy and Abdel-Ghaffar 1990; Wilson and Gravelle 1991; Lall 1992; Ren 1999a; Spyrakos et al. 1999). Another advantage of the finite element method lies in the capability of in-depth dynamic analysis. The dynamic characteristics of suspension bridges have been of particular interest since the collapse of the Tacoma Narrows Bridge in the State of Washington on November 7, 1940, as a result of wind action. A major effort in developing the finite element methodology for the analysis of the lateral vibrations (Abdel-Ghaffar 1978), torsional vibrations (Abdel-Ghaffar 1979) and vertical vibrations (Abdel-Ghaffar 1980) gives a comprehensive understanding of the dynamic behavior of suspension bridges. The parametric

frequencies and modes (West et al. 1984) using a finite element formulation demonstrate the variation of the modal parameters of stiffened suspension bridges. The finite element method has been a unique way to do the dynamic response analysis of cable-supported bridges under the loadings of winds, traffics and earthquakes (Boonyapinyo et al. 1999; Abdel-Ghaffar and Rubin 1982; Abdel-Ghaffar and Nazmy 1991; Ren and Obata 1999b).

This chapter describes the first step in the structural evaluation effort of the Roebling suspension bridge. Details of a three-dimensional finite element model are presented. The analytical model of the Roebling suspension bridge is conceived in the ANSYS, one of the most powerful engineering design and analysis software (ANSYS5.6 1999). The ANSYS is chosen because of the program's significant capability to account for the cable stress stiffening and the pre-stressed modal analysis capability. This model would be used for both static and dynamic analyses of the Roebling suspension bridge.

It was realized in the early 1850's that the dead load has a significant influence on the stiffness of a suspension bridge. In the finite element analysis, this influence is included through the static analysis under dead loads before the live load or dynamic analysis is carried out. The objective of the static analysis process is intended to achieve the deformed equilibrium configuration of the bridge due to dead loads where the structural members are "pre-stressed". A suspension bridge is indeed a highly pre-stressed structure. Starting from the deformed equilibrium configuration, the modal analysis is followed. Consequently, the dead load effect to the stiffness can be included in the modal analysis. The modal analysis is therefore a "pre-stressed" modal analysis.

Hence, the modal analysis of a suspension bridge must include two steps: static analysis due to dead load and "pre-stressed" modal analysis. For a completed suspension bridge, the initial position of the cable and bridge is unknown. Only the final geometry of the bridge due to the dead load is known. The initial geometry of the ideal finite element model of a suspension bridge should be such that the geometry of a bridge does not change when a dead load is applied, since this is indeed the final geometry of the bridge as it stands today. Besides, no forces should be induced in the stiffening structure. In other words, the deformed configuration of the bridge under the self-weight dead load should be close to the initial geometry input. This is approximately realized by manipulating the initial tension force in the main cables that is specified as an input quantity (pre-strain) in the cable elements. The initial tension in the cables is achieved by trial until a value is found that leads to the minimum deflections and the minimum stresses in the stiffening structure due to dead load. In addition, the geometric nonlinear effect has been studied by including the stress stiffening and large deflection. All possible frequencies and mode shapes can be provided performing the pre-stressed modal analysis. A coupled mode can be included to give a comprehensive understanding of the dynamic behavior of suspension bridges. Parametric studies are also performed. The parameters include self-weight of the deck, the stiffness of cables, the stiffness of suspenders, the stiffness of stiffening trusses and bending stiffness of floor beams and stringers. The results of the modal analysis will be compared later with in situ ambient vibration measurements to calibrate or update the initial finite element model.

3.2 Initial Finite Element Model

3.2.1 Primary Assumption

Due to the complexity and variations of such an old suspension bridge, there are too many uncertainties in both geometry and material. Some primary assumptions are made in establishing the initial finite element model of the Roebling suspension bridge:

❑ Towers: Only one section property is assumed for the full height, although the towers actually have 5 different sections along the height.

❑ Stiffening truss: Assumed that members in side spans are the same as those in the main span, i.e., there is only one section property for all diagonal members, one for all bottom chords, one for all top chords and one for all verticals. It appears that some of stiffening truss members have been replaced with different sections.

❑ Suspenders: all vertical suspenders are treated as same as steel ropes. Actually, three different types exist: latticed steel column, steel bars and steel ropes.

❑ Lateral bracing system at the top of stiffening truss and at the level of floor beams are not included in the model.

❑ Lateral cables: they are not included in the model because the condition of the lateral cables provided below the deck is not clear.

3.2.2 The Geometry of the Bridge

After selecting an appropriate modeling methodology, serious considerations must be given to proper representation of the bridge geometry. These geometric issues are directly related to the structural behavior. The consideration must include not only the global geometry of the bridge, but local geometric characteristics of individual bridge members. The geometry and member details are extracted from the drawings of the Roebling suspension bridge. These drawings include KY 17 Over Ohio River prepared by The Department of Highways, Commonwealth of Kentucky, the Rehabilitation of Cincinnati-Convington Suspension Bridge prepared by the Suspension Bridge Co. (1954) and the Bridge Inspection Report prepared by Parsons Brinckerhoff Quade & Douglas, Inc. (1988). Table 3.1 shows the member details extracted from drawings.

Table 3.1 Member Details Extracted from Drawings

Member	Reference
Tower	Elevation at side walk: Sheet 16; Plan at top: Sheet 3 (Drawing No 18429), Sheet 9,10,21 (Drawing No 22113), Inspection report
Primary cable	Sheet 4 (Drawing No 21972), Inspection report
Secondary cable	Sheet 4 (Drawing No 21972), Inspection report
Stay cables	Inspection report
Stiffening truss	Geometry: Drg. 15,16; Section & joint details: Drg. 17,18,19,20,21
Floor beams	Sheet 12 (Drawing No 23301)
Stringers	Sheet 4 (Drawing No 21972)
Cross beams	Sheet 14 (Drawing No 23301)
Suspenders	Sheet 1 (Drawing No 18926)
Tie rods	Sheet 4 (Drawing No 21972)
Lateral cables	Sheet 5,22 (Drawing No 21972): 2.25" dia. rope
Stabilizer cable	Sheet 24 (Drawing No 21972): 2.25" dia. rope
Lateral bracing	Sheet 16 (Drawing No 21925), Inspection report
Deck (steel grid)	Sheet 15 (Drawing No 23301), Inspection report

3.2.3 Element Types

A suspension bridge is a complex structural system. Each member of the bridge plays a different role. Different element types are therefore needed. In current FEM model, four types of finite elements are chosen for modeling the different structural members such as stiffening trusses, floor beams and stringers, main cables and suspenders, towers. They are 3-D elastic beam element (BEAM4), 3-D truss element (LINK8), 3-D tension-only truss element (LINK10) and membrane shell element (SHELL41). The theoretical background of each type of elements is briefly described below:

3.2.3.1 BEAM4 Element

BEAM4 is a uniaxial 3-D elastic beam element with tension, compression, torsion, and bending capabilities. The element has six degrees of freedom at each node: translations in the nodal x, y, and z directions and rotations about the nodal x, y, and z axes. BEAM4 3-D beam element is defined by two nodes, the cross-sectional geometrical properties, and the material properties. The geometry, node locations, and the coordinate system for this element are shown in Fig.3.1. The stiffness matrix of BEAM4 in element (local) coordinates is

$$[k_l] = \begin{bmatrix}
\frac{EA}{L} \\
0 & \frac{12EI_z}{L^3(1+\phi_y)} \\
0 & 0 & \frac{12EI_y}{L^3(1+\phi_z)} \\
0 & 0 & 0 & \frac{GJ_k}{L} \\
0 & 0 & -\frac{6EI_y}{L^2(1+\phi_z)} & 0 & \frac{(4+\phi_z)EI_y}{L(1+\phi_z)} \\
0 & \frac{6EI_z}{L^2(1+\phi_y)} & 0 & 0 & 0 & \frac{(4+\phi_y)EI_z}{L(1+\phi_y)} \\
-\frac{EA}{L} & 0 & 0 & 0 & 0 & 0 & \frac{EA}{L} \\
0 & -\frac{12EI_z}{L^3(1+\phi_y)} & 0 & 0 & 0 & -\frac{6EI_z}{L^2(1+\phi_y)} & 0 & \frac{12EI_z}{L^3(1+\phi_y)} \\
0 & 0 & -\frac{12EI_y}{L^3(1+\phi_z)} & 0 & \frac{6EI_y}{L^2(1+\phi_z)} & 0 & 0 & 0 & \frac{12EI_y}{L^3(1+\phi_z)} \\
0 & 0 & 0 & -\frac{GJ_k}{L} & 0 & 0 & 0 & 0 & 0 & \frac{GJ_k}{L} \\
0 & 0 & -\frac{6EI_y}{L^2(1+\phi_z)} & 0 & \frac{(2-\phi_z)EI_y}{L(1+\phi_z)} & 0 & 0 & 0 & \frac{6EI_y}{L^2(1+\phi_z)} & 0 & \frac{(4+\phi_z)EI_y}{L(1+\phi_z)} \\
0 & \frac{6EI_z}{L^2(1+\phi_y)} & 0 & 0 & 0 & \frac{(2-\phi_y)EI_z}{L(1+\phi_y)} & 0 & -\frac{6EI_z}{L^2(1+\phi_y)} & 0 & 0 & 0 & \frac{(4+\phi_y)EI_z}{L(1+\phi_y)}
\end{bmatrix}$$

where:

A = cross-section area

E = Young's modulus

L = element length

G = shear modulus

I_i = moment of inertia normal to direction i

J_k = torsional moment of inertia

$$\phi_y = \frac{12EI_z}{GA_Z L^2}$$

$$\phi_z = \frac{12EI_y}{GA_y L^2}$$

A_i = shear area normal to direction i

The consistent mass matrix of BEAM4 element in element coordinates with the effect of rotary inertia but without the effect of shear deformation is

$$[m_l] = \rho AL \begin{bmatrix}
\frac{1}{3} \\
0 & \frac{13}{35}+\frac{6I_z}{5AL^2} \\
0 & 0 & \frac{13}{35}+\frac{6I_y}{5AL^2} \\
0 & 0 & 0 & \frac{J_k}{3A} & & & & & symmetric \\
0 & 0 & -\frac{11L}{210}-\frac{I_y}{10AL} & 0 & \frac{L^2}{105}+\frac{2I_y}{15A} \\
0 & \frac{11L}{210}+\frac{I_z}{10AL} & 0 & 0 & 0 & \frac{L^2}{105}+\frac{2I_z}{15A} \\
\frac{1}{6} & 0 & 0 & 0 & 0 & 0 & \frac{1}{3} \\
0 & \frac{9}{70}-\frac{6I_z}{5AL^2} & 0 & 0 & 0 & \frac{13L}{420}-\frac{I_z}{10AL} & 0 & \frac{13}{35}+\frac{6I_z}{5AL^2} \\
0 & 0 & \frac{9}{70}-\frac{6I_y}{5AL^2} & 0 & -\frac{13L}{420}+\frac{I_y}{10AL} & 0 & 0 & 0 & \frac{13}{35}+\frac{6I_y}{5AL^2} \\
0 & 0 & 0 & \frac{J_k}{6A} & 0 & 0 & 0 & 0 & 0 & \frac{J_k}{3A} \\
0 & 0 & \frac{13L}{420}-\frac{I_y}{10AL} & 0 & -\frac{L^2}{140}-\frac{I_y}{30A} & 0 & 0 & 0 & \frac{11L}{210}+\frac{I_y}{10AL} & 0 & \frac{L^2}{105}+\frac{2I_y}{15A} \\
0 & -\frac{13L}{420}+\frac{I_z}{10AL} & 0 & 0 & 0 & -\frac{L^2}{140}-\frac{I_z}{30A} & 0 & -\frac{11L}{210}-\frac{I_z}{10AL} & 0 & 0 & 0 & \frac{L^2}{105}+\frac{2I_z}{15A}
\end{bmatrix}$$

where: $\rho =$ density

Fig. 3.1   BEAM4 3-D Elastic Beam Element

3.2.3.2 LINK8 Element

LINK8 is a uniaxial 3-D elastic truss element with both tension and compression capabilities. The element has three degrees of freedom at each node: translations in the nodal x, y, and z directions. As in a pin-jointed structure, no bending of the element is considered. LINK8 3-D truss element is defined by two nodes, the cross-sectional area, an initial strain, and the material properties. The LINK8 element may be thought of as truss element, a cable element, a link element, a spring element, etc., and then may be used in a variety of engineering applications. The geometry, node locations, and the coordinate system for this element are shown in Fig.3.2.
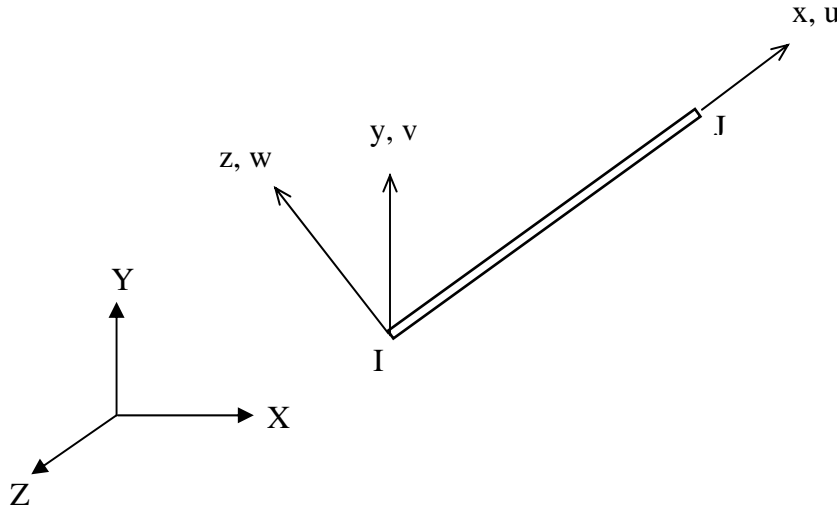
Fig. 3.2   3-D Truss Element

The stiffness matrix of LINK8 element in the element (local) coordinate system is:

$$[k_l] = \frac{AE}{L}\begin{bmatrix} 1 & 0 & 0 & -1 & 0 & 0 \\ 0 & 0 & 0 & 0 & 0 & 0 \\ 0 & 0 & 0 & 0 & 0 & 0 \\ -1 & 0 & 0 & 1 & 0 & 0 \\ 0 & 0 & 0 & 0 & 0 & 0 \\ 0 & 0 & 0 & 0 & 0 & 0 \end{bmatrix}$$

where:

A = element cross-sectional area
E = Young's modulus
L = element length

The consistent mass matrix of LINK8 element in the element coordinate system is:

$$[m_l] = \frac{\rho AL(1-\varepsilon^{in})}{6} \begin{bmatrix} 2 & 0 & 0 & 1 & 0 & 0 \\ 0 & 2 & 0 & 0 & 1 & 0 \\ 0 & 0 & 2 & 0 & 0 & 1 \\ 1 & 0 & 0 & 2 & 0 & 0 \\ 0 & 1 & 0 & 1 & 2 & 0 \\ 0 & 0 & 1 & 0 & 0 & 2 \end{bmatrix}$$

where:

$$\rho = \text{density}$$
$$\varepsilon^{in} = \text{initial strain (as an input)}$$

3.2.3.3   LINK10 Element

LINK10 element is a uniaxial 3-D elastic truss element with tension-only (or compression-only) capability. With the tension-only option used here, the stiffness is removed if the element goes into compression (simulating a slack cable or slack chain condition). The feature is unique in modeling the cables, stay cables and suspenders of the Roebling suspension bridge. The element has three degrees of freedom at each node: translations in the nodal x, y, and z directions. The same as LINK8 element, no bending of the element is considered. LINK10 3-D truss element is also defined by two nodes, the cross-sectional area, an initial strain, and the material properties. The mass matrix has the same formulas as LINK8 element. The stiffness matrix of tension-only truss element in the element coordinate system is:

$$[k_l] = \frac{AE}{L} \begin{bmatrix} C_1 & 0 & 0 & -C_1 & 0 & 0 \\ 0 & 0 & 0 & 0 & 0 & 0 \\ 0 & 0 & 0 & 0 & 0 & 0 \\ -C_1 & 0 & 0 & C_1 & 0 & 0 \\ 0 & 0 & 0 & 0 & 0 & 0 \\ 0 & 0 & 0 & 0 & 0 & 0 \end{bmatrix}$$

where:

A = element cross-sectional area
E = Young's modulus
L = element length
$C_1 = 1.0$ when tension; 1.0×10^6 when compression

An important input property of the LINK10 elements that are aimed at modeling cable behavior is the initial strain. The initial strain is used for calculating the stress stiffness matrix for the first cumulative iteration. Stress stiffening should always be used for sagging cable problems to provide numerical stability. The initial strain in the element is given by δ / L, where δ is the difference between the element length L and the zero strain length L_0.

3.2.3.4   SHELL41 Element

SHELL41 element is a 3-D shell element having membrane (in-plane) stiffness but no bending (out-of-plane) stiffness. It is intended for shell structures where bending of the elements is of secondary importance. The element has three degrees of freedom at each node: translations in the nodal x, y, and z directions. SHELL41 3-D membrane shell element is defined by three or four nodes, four thickness, and the material properties. The geometry, node locations, and the coordinate system for 3-D 4-node quadrilateral shell element are shown in Fig.3.3. The implicit expressions of shape function, stiffness matrix and mass matrix can be found in the standard book of finite element method (Bathe 1982; etc.)
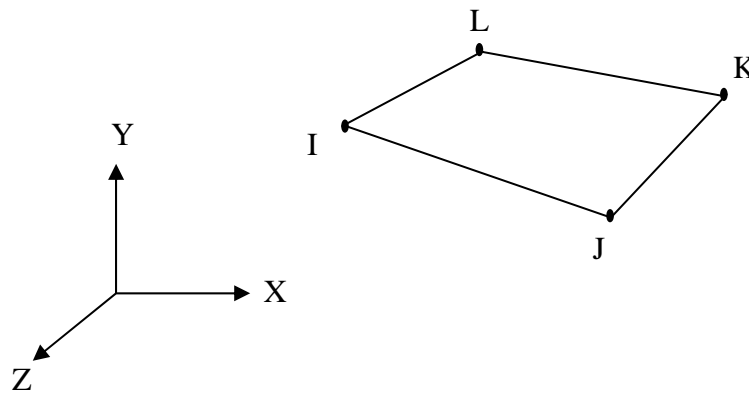
Fig. 3.3   SHELL41 4-Node Quadrilateral Shell Element

3.2.4 Material Properties and Real Constants

The basic materials used in the Roebling suspension bridge are structural steel, masonry towers and cables. The material constants used in current finite element model are shown in Table 3.2. They follow the typical values of ASMT standards. It has been noted that the mass density of floor beams and stringers includes the contribution from the bridge deck weight and sidewalks, as well as the contribution from the lateral bracing system.

Table 3.2 Material Properties

Group No.	Young's modulus MPa (lb/ft^2)	Poisson's ratio	Mass density kg/m^3 (lb/ft^3)	Structural member
1	2.1×10^5 (4.386×10^9)	0.3	7849 (490)	**Stiffening trusses**
2	2.0×10^5 (4.177×10^9)	0.3	7849 (490)	**Cables**
3	2.0×10^5 (4.177×10^9)	0.3	7849 (490)	**Suspenders**
4	2.0×10^5 (4.177×10^9)	0.3	7849 (490)	**Stay wires and tie rods**
5	2.0×10^4 (4.177×10^8)	0.15	2500 (156)	**Tower**
6	2.1×10^5 (4.386×10^9)	0.3	19575 (1222)	**Floor beams and stringers**

The real constants consist of all necessary geometric properties of the cross-section and initial strain if necessary. Depending on the element type, different real constants are considered as input. For the purpose of latter parametric study and model calibration through in-situ dynamic testing, these real constants are divided into 16 types to reflect effectively the properties of individual structural members. All types of real constants used in the current model are summarized in Table 3.3. Real constants are based on the following facts of the main structural members.

Stiffening Truss

The stiffening trusses are of the continuous type with an expansion bearing at each end, two fixed bearings at each tower, and a telescopic truss joint for expansion in the center of the span. The top chord is a built-up member with a solid cover plate while the bottom chord is a built-up member with top and bottom lacing bars. The top and bottom chords have riveted joints, but employ pin connections at each panel point for the verticals, which are latticed columns, the diagonals, and steel eyebars. The top chords are vertically curved, giving the anchor spans a maximum depth of 24′-6″ at their centers and the main span a maximum depth of 28′-0″ at its center. Each panel of the stiffening trusses is 15 feet wide and has pairs of crossing diagonals, one of which is equipped with screw sleeves for adjusting tension.

Primary Cables

The primary cables are composed of seven strands, each containing 740 No.9 gage cold blast charcoal iron wires, for a total of 5,180 wires. These wires are parallel to each other and form a cable which is 12 1/3 inches in diameter and has an effective area of 86.67 sq.in (0.602 sq.ft). The cable erection began on November 1, 1865 and ended on June 23, 1886. Once the cables were in place, they were coated with linseed oil and varnish and continuously wrapped with No.10 gage iron wire. The iron wire was manufactured by Richard Johnson & Nephew at Manchester, England. The total cable wire used, including the wrapping wire, was 1,050,183 lbs. The design ultimate strength of one wire is 1,620 lbs, therefore, the design ultimate strength per primary cable is 8,391,600 lbs ($5,180\times1,620$).

Secondary Cables

The secondary cables are composed of 21 strands, including 7 which contain 134 wires each and 14 which contain 92 wires each, for a total of 2,226 wires. The wires are No.6 gage ungalvanized steel wires, manufactured by John A. Roebling's Sons Company of Trenton, New Jersey. These wires are parallel to each other and form a cable which is 10 ½ inches in diameter, has an effective area of 66.78 sq.in (0.464 sq.ft). The design ultimate strength of one wire is approximately 5,400 lbs, therefore, the design ultimate strength per cable is 12,020,400 lbs (180,000 psi). These cables were erected in 1896-97 and were continuously wrapped with ungalvanized steel wire. The secondary cable is parallel to the primary cables in the main span and is approximately six feet above it. It rests independently on a saddle constructed above the primary cable saddle. The primary cables and secondary cables are connected together by the tie rods in the main span. The secondary cable supports its own weight plus a portion of the dead and live loads of the main span.

Suspenders

The suspension span's floor system is supported by means of suspenders connected to bearing plates beneath the floorbeam bottom flanges. These suspenders are of three types. The most predominant type is a system of three helical wire ropes. The outer pair of wrought iron wire rope is 1 1/2″ in diameter and is part of the original construction. The original truss and floor system were supported by these pairs of ropes at a five-foot spacing. In 1897, a third rope 2 1/4″ in diameter was added, and these three ropes are spaced at 15-foot intervals. The ultimate strength of the 1987 ropes is 386,000 lbs, while the ultimate strength of the original suspender ropes is 180,000 lbs. The combined ultimate strength is 566,000 lbs.

Stay Wires

A series of inclined stays emanate from the tops of the towers to the top chords of the stiffening trusses. The use of stays was the most economical and efficient means of providing stiffness to long span bridges. These stays are 2 1/4″ diameter, helical iron wire ropes, with an ultimate strength of 1800,000 lbs. each. Eighteen stay cables are attached to the truss at panel points. They continue over the tower where they rest on saddles which allow them to move independently of the main cable, and stretch out diagonally towards the center of the main span between panel points. This arrangement is repeated on each side of the bridge at both towers making a total of 72 stay cables. In addition, eight stay wires, or stabilizers, connect the primary cable to the tower below the lower cornice. Their function is just to prevent severe oscillations of the primary cables during periods of high wind, but serve no purpose under normal conditions.

Floor Beams and Stringers

In the suspension spans, the 5″ open steel grid deck is supported by C10×20 crossbeams spaced at 3′-9″ resting on six stringers spaced at approximately 5′-3″. The four outmost stringers are 15″ I 50 lbs. sections and the two center stringers are 20″ I 65 lbs. sections. These stringers frame into the

Floor beams spaced at each truss panel point. These floor beams are riveted, built-up steel sections. The web plate is 36″ deep with four flange angles riveted to it. Four horizontal angles provide additional bending strength near the center of the floor beams. The web is spliced at the centerline of bridge. The top flanges are riveted to the truss bottom chords. The suspenders have bearing plates supporting the base of the floor beams, allowing the sidewalks to be cantilevered from each end of the floor beams.

Table 3.3   Real Constants

Type	Cross-section area: m^2 (ft^2)	Inertia moment: m^4 (ft^4)		Initial strain or thickness	Structural member
		I_{zz}	I_{yy}		
1	0.02 (0.217)	3.194×10^{-4} (0.037)	9.667×10^{-4} (0.112)	-	Bottom chords
2	0.0318 (0.342)	1.079×10^{-3} (0.125)	1.510×10^{-3} (0.175)	-	Top chord
3	0.00594 (0.0639)	1.033×10^{-4} (0.01197)	1.726×10^{-4} (0.02)	-	Verticals
4	0.00759 (0.0817)	-	-	-	Diagonals
5	0.0559 (0.602)	-	-	0.8×10^{-3}	Primary cable
6	0.00485 (0.0522)	-	-	-	Suspender
7	0.0431 (0.464)	-	-	0.8×10^{-3}	Secondary cable
8	0.00384 (0.0413)	-	-		Tie rods
9	107.777 (1160.1)	2057.19 (238350)	459.25 (53209)	-	Columns
10	0.00256 (0.0276)	-	-	0.0	Stay wire
11	0.00256 (0.0276)	-	-	-	Stabilizer cable
12	0.00948 (0.102)	2.020×10^{-4} (0.0234)	4.993×10^{-5} (0.005785)	-	Outer stringer
13	0.0125 (0.135)	4.954×10^{-4} (0.0574)	7.492×10^{-5} (0.00868)	-	Inner Stringer
14	0.0314 (0.338)	4.100×10^{-3} (0.475)	5.757×10^{-4} (0.0667)	-	Floor beam
15	-	-	-	6.096 (20)	Web wall above deck
16	-	-	-	3.962 (13)	Web wall below deck

3.2.5 Details of the Model

A detailed element-level 3-D finite element model of the structure is developed. This model would be used for both static and dynamic analysis of the bridge. The main structural members of the Roebling suspension bridge are the stiffening truss, cables, suspenders, and towers that are discreterizd by different finite elements. The finite elements used for modeling the bridge are described below.

Modeling of the cable is possible in ANSYS by employing the tension-only truss elements and utilizing its stress stiffening capability. The element is nonlinear and requires an iteration solution. All cable members of the Roebling suspension bridge such as primary cables, secondary cables, suspenders, stay cables and stabilizer cables are designed to sustain the tension force only and hence modeled by 3-D tension-only truss elements (LINK10) but the section properties are different. The main cable between two suspenders and the secondary cable between two tie rods are modeled as a single finite element. The stiffness is removed with this element if the element goes into compression. And thus the element can simulate a slack cable. Both stress stiffening and large displacement capability are available. The stress stiffening capability is needed for analysis of structures with a low or non-existing bending stiffness as is the case with cables. Hence, an important feature input for this element is the initial strain in the element. This initial strain is used in calculating the stress stiffness matrix for the first cumulative iteration. The cable sagging effect can be considered with the stress stiffening capability.

The columns of towers are model as 3-D elastic beam elements (BEAM4), whereas the web walls of towers above and below the deck are modeled as 3-node quadrilateral membrane shell elements (SHELL41) as the bending of these walls is of secondary importance. Another function of these shell elements is to model the composite action of towers on each side of the span. Large deflection capability is available.

The stiffening truss is modeled as a 3-D truss made up of beam and truss elements. The top chords and bottom chords of the truss are modeled as 3-D elastic beam elements (BEAM4) because of their continuous natural across many panels. The verticals of the truss are also modeled as 3-D elastic beam elements (BEAM4) to provide some bending stiffness, whereas the inclined diagonals of the truss are modeled as 3-D truss elements (LINK8) because they are pinned and probably do not provide much bending stiffness. The truss is modeled as it exists in reality rather than the more usual practice of modeling the truss as bending element with a moment of inertia obtained by considering equivalent section of the truss.

The deck is simplified as stringer beams and floor beams in the model. In other words, the principal load bearing structural elements of the deck here are recognized to be the stringer and floor beams. These stringer beams and floor beams are all the structural members possibly subjected to tension, compression, bending and torsion, and then they are modeled as 3-D elastic beam elements (BEAM4). The member between each stringer beam and floor beam is modeled as a single beam element.

In addition, the tie rods that connect the primary and secondary cables, are modeled as 3-D truss elements (LINK8) because they act as the rods with both tension and compression capability.

The finite element model of the Roebling suspension bridge totally consists of 1756 nodes and 3482 finite elements that include 2186 BEAM4 elements, 560 LINK8 elements, 692 LINK10 elements, and 44 SHELL41elements. As a result, the number of active degree of freedom (DOF) is 7515. The details of the model such as element types, material type and real constant type are summarized in Table 3.4 for individual structural members. The detailed 3-D finite element models are shown in Fig. 3.4, Fig.3.5 and Fig.3.6.

Table 3.4   Details of the Model

Member		Element Type	Material Type	Real Constant Type
Stiffening truss	Bottom chord	BEAM4	1	1
	Top chord	BEAM4	1	2
	Verticals	BEAM4	1	3
	Diagonals	LINK8	1	4
Cable	Primary	LINK10	2	5
	Secondary	LINK10	2	7
Tower	Columns	BEAM4	3	9
	Web walls above deck	SHELL41	3	15
	Web walls below deck	SHELL41	3	16
Stringer beam	Outer	BEAM4	4	12
	Inner	BEAM4	4	13
Floor beam		BEAM4	4	14
Vertical suspender		LINK10	2	6
Tie rod (connecting primary & second cable)		LINK8	2	8
Stay wire		LINK10	2	10
Stabilizer cable		LINK10	2	11

Full Elevation
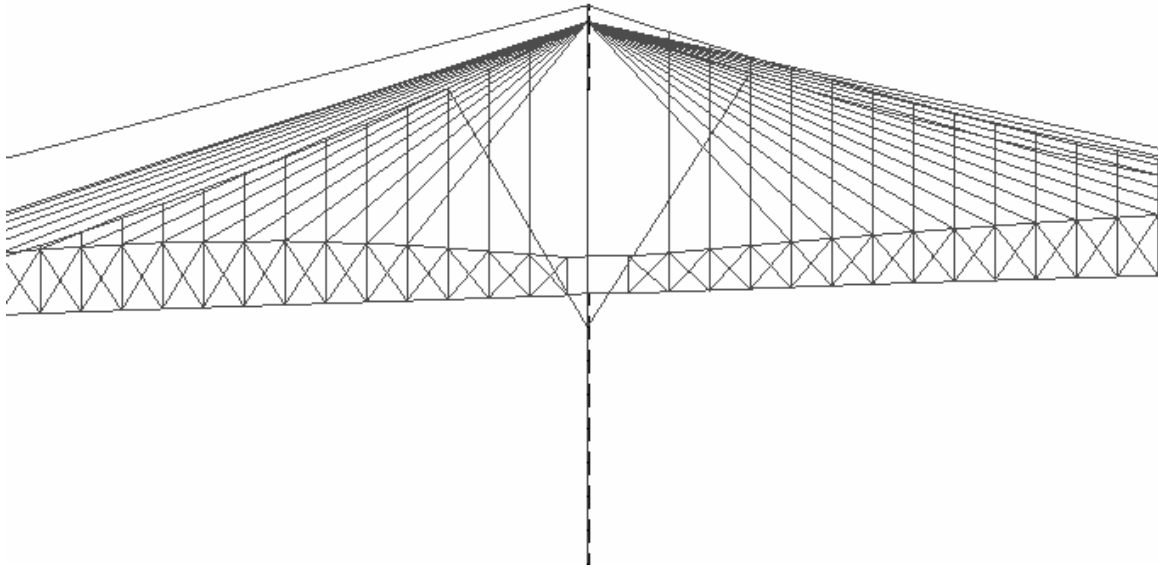
Part Elevation – Tower and Cables
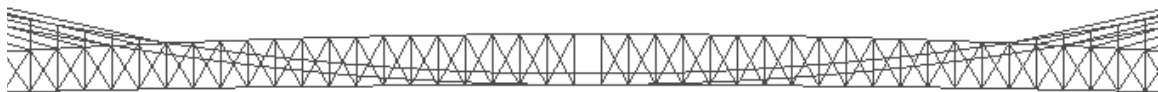
Part Elevation – Central Span and stiffening Truss

Fig. 3.4   Elevation of Finite Element Model

Full Plan

Part Plan – Tower and Floor Beams
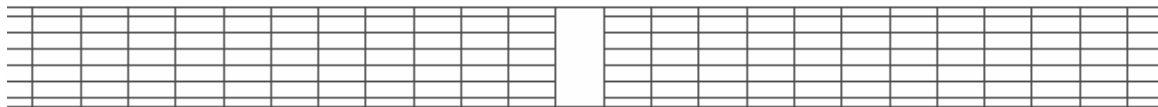
Part Plan – Central Span and Floor Beams

Fig. 3.5   Plan of Finite Element Model
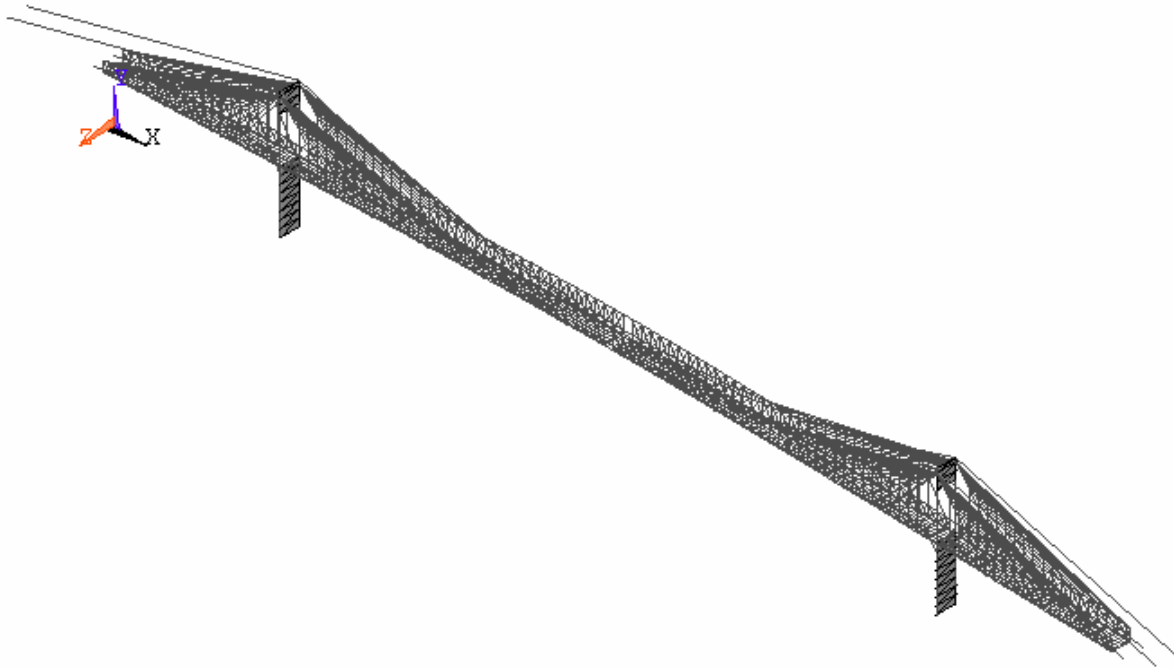
Fig. 3.6a   Full Elevation – Isotropic
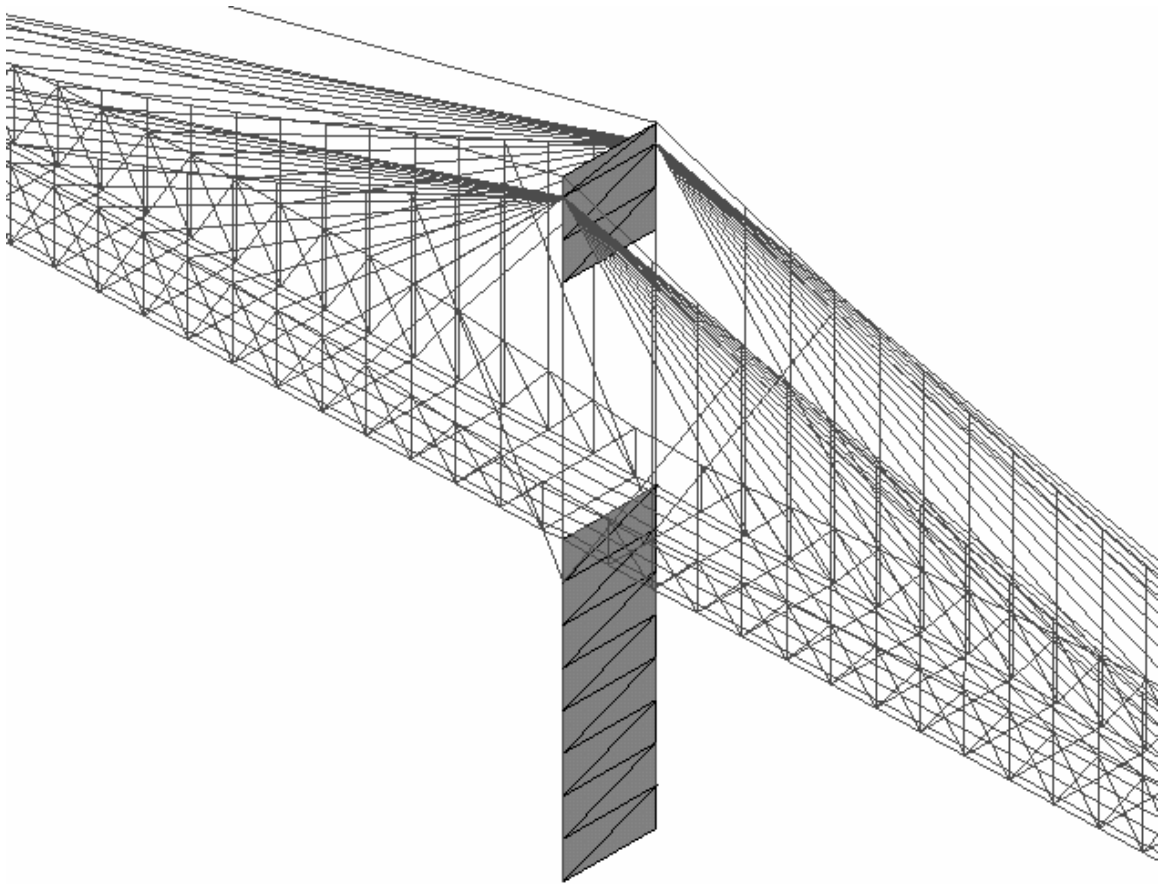
Fig. 3.6b   Part Elevation – Tower and Cables
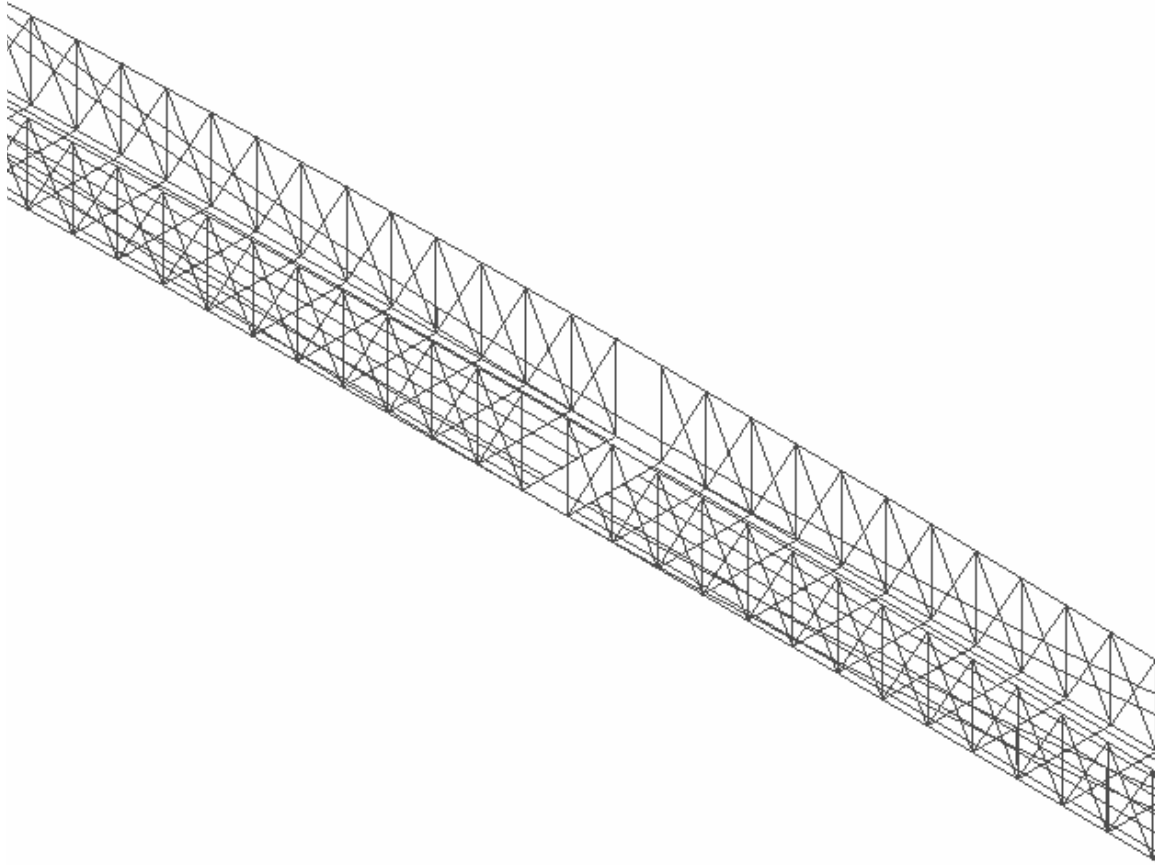
Fig. 3.6c   Part Elevation – Central Span and Stiffening Truss

Fig. 3.6   Isotropic Elevation of Finite Element Model

3.2.6 Boundary Conditions

The boundary conditions of an actual bridge are always complex and they are often idealized as fixes, hinges and rollers in the analytical model. In current model, the towers of the Roebling suspension bridge are modeled as fixed at the bases. The cable (both primary and secondary) ends are modeled as fixed at the anchorages. The stiffness truss and stringer beams are assumed to have a hinge support at the left and right masonry support, whereas they are continuous at the towers to simulate the real structure.

In addition, the stiffening truss for the Roebling suspension bridge is an uncommon one-hinge design. This hinge was designed in the center of the span to provide for temperature expansion. The hinge was modeled by defining separately coincident nodes in the top as well as the bottom chords at the mid- span, i.e., one node is connected to the truss member on the right, while the other is connected to the same member on the left. Coupling the vertical and transverse displacements of these nodes while allowing them to move independently in the horizontal direction simulates the expansion hinge effect. However, this model leads to a discontinuity of slope at the hinge in the deflected structure. To remedy this, the rotations of the two points immediately to the left and right of the hinge location have been coupled. This results in a smooth curve deflection of the truss while allowing independent horizontal translation of the left and right half of the bridge at the hinge location.

3.3 Static Analysis under Dead Load

In the design of suspension bridges, the dead load often contributes most of bridge loads. It was realized as early as the 1850's that the dead load has a significant influence on the stiffness of a suspension bridge. In the finite element analysis, this influence can be included through the static analysis under dead loads before the live load or dynamic analysis is carried out. The objective of the static analysis process is intended to achieve the deformed equilibrium configuration of the bridge due to dead loads where the structural members are "pre-stressed". Started from the deformed equilibrium configuration, the real analysis is followed. Consequently, the dead load effect to the stiffness is included in the analysis.

For the static analysis of the Roebling suspension bridge under dead load, the value of the deck dead load is chosen as 2,500 lbs./ft (36.49 kN/m). This dead load is taken from the report by Hazelat and Erdel (1953). Actually, the deck loads are transferred from the stringers and floorbeams to the suspenders, stiffening trusses and stays and then to the suspension cables. Thus in the finite element analysis, the dead load is applied directly on each node of both inner stringers (corresponding to each panel point of bottom chords in the stiffening truss). The distribution load value of 2,500 lbs./ft is equivalent to $2,500 \times 15 = 37,500$ lbs. (166.81 kN) point load applied on each node of the inner stringers.

The capabilities of the static analysis procedure in ANSYS include large deflections (geometrically nonlinear analysis) and stress stiffening. As the structure involves nonlinearity, an iterative solution associated with the Newton-Raphson solution procedure is required.

3.3.1 Initial Tension in the Cables

A cable-supported bridge directly derives its stiffness from cable tensions. For a completed suspension bridge, the fact is that the initial position of the cable and bridge is unknown. Only the final geometry of the bridge due to the dead load is known. The initial geometry of the bridge that we have modeled is really the dead load deflected shape of the bridge. Actually, the bridge deck was suspended piece-by piece from the cable. And thus the cable stretched and deflected down until almost all of the deck was suspended from the cables, resting on each end on the towers. When the bridge is erected the truss is initially unstressed. The dead load is borne completed by the cables. This is, in fact, a key assumption of both the Classical Theory as well as the Deflection Theory.

It turns out that the ideal finite element model of a suspension bridge should be such that on application of the dead load, the geometry of the bridge does not change, since this is indeed the finial geometry of the bridge as it stands today. Besides, no forces should be induced in the stiffening structure. In other words, the deformed configuration of the bridge under the self-weight dead load should be as close to the initial geometry input. This can be approximately realized by manipulating the initial tension force in the main (primary and secondary) cables that is specified as an input quantity (pre-strain) in the cable elements. Hence, the bridge can be modeled in the finial geometry with a pre-tension force in the cables. In such a way, the initial tension force in the cables plays an important role. The initial tension in the cables can be achieved by trial until a value is found that leads to

- Minimum deflections of the deck due to dead load;
- Minimum stresses in the stiffening structure due to dead load.

The variations of maximum forces and deflections with different pre-strains in the cables are summarized in Table 3.5. The deck deflected shapes for varying pre-strains in the cables are plotted in Fig.3.7. It is clearly shown that the deck deflection and the forces in the stiffening truss are reduced while the forces in the cables and suspenders are increased with the increasing in the cable pre-strains. It is observed that the smaller pre-strains in the cables (below 0.1×10^{-3}) have almost no effect on the deflection and forces of the bridge.

The major interest herein as mentioned previously is only a pre-strain that would give minimum deck deflections and forces in the stiffening members for dead load. It is evident that for a pre-strain of 0.8×10^{-3} in both primary and secondary cables the deflections of the deck are quite nominal. In the computer model, the deflection of the deck can not be reduced anymore by increasing the pre-strain without causing an upward deflection of the deck at other points. Although the maximum deflection at the deck center with this pre-strain is about 0.39 feet, it is considered as an adequate simulation of the dead load deflected shape of the real bridge. Even though this leads to initial stresses in the stiffening truss, the magnitude of the stresses is reduced to a minimum as most of the dead load is taken by the cables as evident from the forces in the suspenders. The presence of some initial stresses in the stiffening truss is not entirely avoidable in practical construction and considerable uncertainty exists regarding the condition of the truss at the time of construction. The presence of initial stresses in the truss model is conservative in any case as far as estimating the capacity of the truss is concerned.

With the cable pre-strain of 0.8×10^{-3}, the force in the suspenders of the main span due to dead load alone is typically 33,000 pounds. This means that the force of 37,500 pound applied at each panel point along the bridge deck, 33,000 pounds are transferred to the main cable. Thus the use of the pre-strain of 0.8×10^{-3} in the primary and secondary cables is about 90% efficient in keeping the truss stress-free under the action of gravity loads

The total (primary plus secondary) cable tension of 3863,900 pounds determined by the computer analysis with the cable pre-strain 0.8×10^{-3} is very close to the horizontal component of cable tension calculated from the formula:

$$H = wL^2 / 8d = 2.5 \times 1065^2 / (8 \times 89) = 3982,500 \ \text{pounds}$$

where d is the sag of the main cable. The main span length of the Robeling bridge is 1065 feet and thus the sag to span ratio is taken as 1/12. In addition, the total cable tension force due to dead load reported in the rating analysis of the Roebling suspension bridge by Hazelet and Erdal (1953) is about 3500,000 pounds that is remarkably close to the current analysis.

Therefore, both the requirements of minimum deck deflections and deck forces are considered to be met with an initial pre-strain of 0.8×10^{-3}, and model with this initial strain in the cable elements is considered the correct analytical model. The optimization of initial tension forces in the cables is out of the topic.

Another interesting feature of the Roebling suspension bridge is the inclined stays. In the original design, Roebling felt that the use of stays was the most economical and efficient means of providing stiffness to long span bridges. These stays also carry approximately 10% of the total bridge load (Hazelet and Erdal 1953). The comparison of the deck deflection for the model with and without inclined stays, as shown in Table 3.6 and Fig.3.8, demonstrates that the stay wires do improve the deck deflection. The stay wires contribute much more to the side spans than to the main span. Numerical results show that the stay wires reduce the central deck deflection by about 55% in the side spans but only by 10% in the main span. The results also show that enough amount of initial strain in the stay wires contribute slightly to the deck deflection so the pre-strain in the elements of inclined stays is neglected in the analytical model.

An inspection of the axial forces induced in the bottom chords and top chords of the stiffening truss shows that the force pattern changes along the bridge deck under dead load. As shown in Table 3.5, the axial compression in the bottom chords of the main span is changed into the axial tension from the tower to the span center, while the axial tension in the top chords is changed into the axial compression. This force pattern change is due to the continuity of the stiffening truss through towers, the inclined stays connected at the top chords of the stiffening truss and the hinge in the center of the stiffening truss. With the introduction of the central hinge in the stiffening truss, the force in the chords drops to zero towards the center of the truss where the hinge is located. At the main span, the presence of the inclined stays adds significantly the axial compression in the bottom chords and the axial tension in the top chords by the same action of holding up the side span.

Table 3.5 Variation of maximum forces and deflection with cable pre-strain

Pre-strain	Bottom chord (pound)		Top chord (pound)		Cable members (pound)			Deflection (foot)
	Panel 30	Panel 55	Panel 40	Panel 55	Primary cable	Secondary cable	Suspender	
0.0	-398,150	161,970	636,410	-8,425	1572,100	1125,200	22,831	-3.172
0.1×10^{-5}	-397,700	161,820	635,700	-8,416	1573,000	1125,580	22,843	-3.168
0.1×10^{-4}	-386,250	160,430	629,280	-8,335	1580,200	1131,600	22,957	-3.136
0.1×10^{-3}	-354,080	146,420	565,210	-7,520	1652,700	1189,900	24,095	-2.818
0.5×10^{-3}	-178,660	82,565	283,160	-3.794	1972,500	1450,700	29,165	-1.414
0.6×10^{-3}	-135,030	66,500	213,850	-2,825	2052,800	1516,500	30,440	-1.066
0.7×10^{-3}	-91,459	50,487	145,200	-1,837	2133,500	1583,700	31,719	-0.724
0.8×10^{-3}	-48,061	34,537	77,275	-829	2214,600	1649,300	33,003	-0.387

Table 3.6 Variation of maximum forces and deflection with stays

Stays	Bottom chord (pound)		Top chord (pound)		Cable members (pound)			Deflection (foot)	
	Panel 30	Panel 55	Panel 40	Panel 40	Primary cable	Secondary cable	Suspender	Side span	Main span
Without stays	-17,556	8,332	4,322	663	2275,300	1705,400	34,066	-0.083	-0.426
With stays	-48,061	34,537	77,275	-829	2214,600	1649,300	33,003	-0.038	-0.387
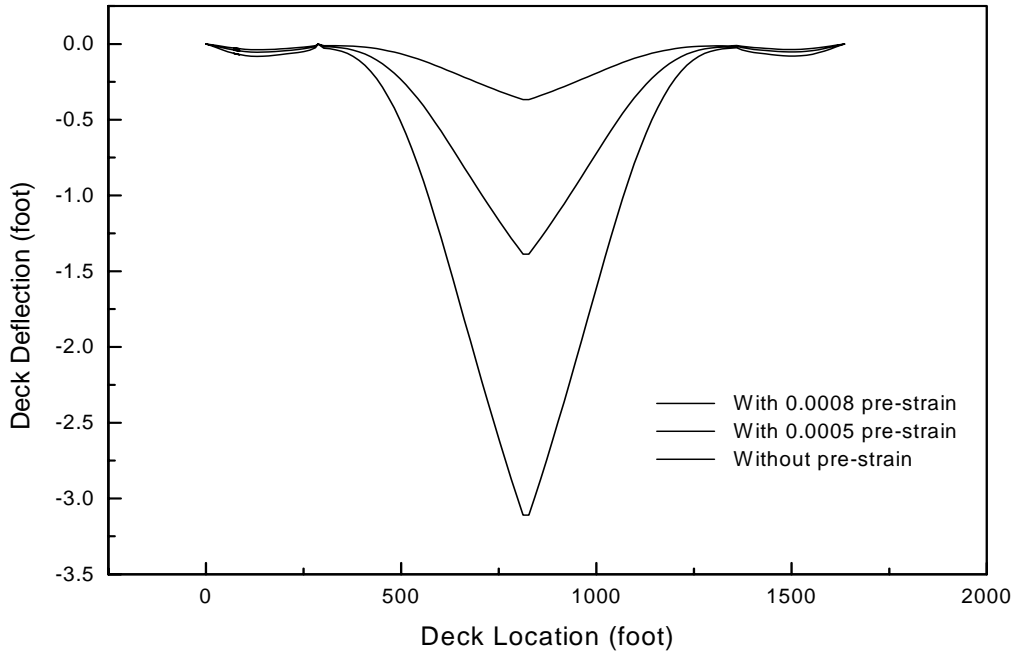
Fig. 3.7   Deck Deflection for Varying Initial Strain in the Cable
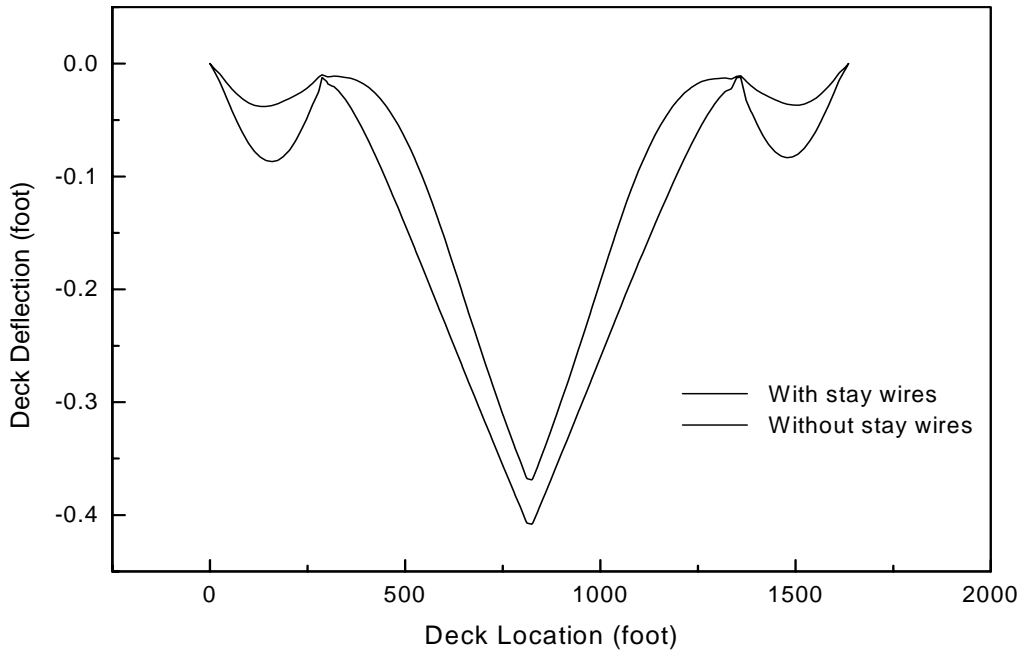
Fig. 3.8   Deck Deflection with and without Stay Wires

3.3.2 Geometric Nonlinearity

For the static analysis, it is well known that a long span cable-supported bridge exhibits geometrically nonlinear characteristics that are reflected in the nonlinear load-deflection behavior under loadings. These geometrically nonlinear sources may come from

❑ The large deflection effect due to changes in geometry;
❑ The combined axial load and bending moment interaction effect.
❑ The sag effect due to changes in cable tension load levels;

In the structural analysis of small deflection, the geometry change of the structure is always assumed to be small and neglected so that all quantities such as force and deformation are determined by the original configuration of the structure. In such a case, the overall stiffness of the structure in the deformed configuration is assumed equally to the stiffness of the undeformed configuration, making the analysis simpler. However, a large deflection solution is required whenever the displacements are large enough so that the structural stiffness matrix based on the initial geometry does not characterize the deformed structure. Since suspension bridges are highly flexible structural system, the displacements under normal working loads are deemed sufficiently large to warrant a nonlinear analysis that accounts for the rigid body motion of the structure. The geometric change can be no longer neglected. In this case the bridge stiffness must be always updated in the simultaneous deformed configuration. Due to this simultaneous deformed configuration is also unknown, the iteration techniques should be used.

In ANSYS, the large deflection capability is available for most of the structural element types. The large deflection is accounted for by reorienting the stiffness into its new configuration through updating the nodal locations. In the geometrically nonlinear analysis, the deformations are characterized by large displacements, large rotations but small strains. This is consistent with the fact that most of structures behave. The total Lagrange (T.L.) formulation is employed where the basic working variable is the total displacement vector rather than the incremental displacement vector as the updated Lagrange (U.L.) formulation does.

The main girder or tower of a suspension bridge is often the structural members subjected to both axial force and bending moment. In the linear structural analysis, the axial stiffness and flexural stiffness is considered to be uncoupled. However, if the deformations are no longer small, these structural members are subjected to an interaction between axial force (tension or compression) and bending moment. Additional bending moment would be caused by a simultaneously applied axial force due to the lateral deformation of a bending member and altering the flexural stiffness of the member. As a result, the effective bending stiffness of the member will decrease for a compressive axial force and increase for a tensile axial force. On the other hand, the presence of bending moments will affect the axial stiffness of the member due to an apparent shortening of the member caused by bending deformations. For the case of suspension bridges, the large deformation may occur. The interaction between axial force and bending moment might be significant and should be included. This effect can be included in the geometric stiffness matrix through geometrically nonlinear analysis.

For a cable, supported at its ends and subjected to its own weight and an externally applied axial force, it sags into the shape of a catenary. The axial stiffness of the cable varies nonlinearly as

a function of cable tension force, which in turn changes with the displacement of cable ends. For conventional truss members the sag due to self weight can be ignored but for cable members this sag should be considered for accurate analysis. Indeed, the sag phenomenon of individual cables results in geometrically nonlinear behavior of cable-supported bridges. The sagging cable problem needs an explicit stress stiffness matrix included in the mathematical formulation to provide numerical stability. Basically, the cable sag effect can be included by introducing axial strains in the cables and then running a static stress-stiffening analysis to determine an equilibrium configuration where the cables are "pre-stressed".

The cable sag can be accounted for in the ANSYS by employing the tension-only truss element and utilizing its stress-stiffening capability in conjunction with a large deflection analysis. Stress stiffening is an effect that causes a stiffness change in the element due to the loading or stress within the element. The stress-stiffening capability is needed for analysis of structures with a low or non-existent bending stiffness as is the case with cables. Physically, the stress-stiffening represents the coupling between the in-plane and transverse deflections within the structure. This coupling is the mechanism used by thin flexible structures to carry the lateral loads. As the in-plane tensile force increases, the capacity to carry the lateral loads increases. In other words, the transverse stiffness increases as the tensile stress increases. More details can be found in the ANSYS (1999).

The finite element model described previously is used here to reveal the large deflection effect on the structural behavior of the Roebling suspension bridge due to dead load. Table 3.7 lists the comparison of the forces in typical members and the maximum deck deflection at the span center between small deflection analysis and large deflection analysis. The stress-stiffening capability is always present to ensure the convergent solution. It is clearly shown that the large deflection has almost no effect on the member forces and deck deflection due to dead load alone. This is consistent with the observation that the maximum deck deflection of the bridge is very limited (about 0.38 feet) due to introducing enough amount of pre-strain 0.8×10^{-3} in the cables where the bridge becomes quite stiffening. Further comparison between small deflection analysis and large deflection analysis without introducing the cable pre-strain, as shown in Table 3.8, has demonstrated that the large deflection does not change the member forces and deck deflection significantly even though the maximum deck deflection of the bridge is about 3.1 feet. Therefore, the large deflection analysis is not necessary in determining the initial equilibrium configuration of the bridge due to dead load and the small deflection analysis is enough in the current finite element model. But the stress-stiffening must be always included in the static analysis of cable-supported bridges and hence the static analysis of a suspension bridge is always geometrically nonlinear.

Table 3.7   Comparison of maximum forces and deflection with cable pre-strain

Analysis type	Bottom chord (pound)		Top chord (pound)		Cable members (pound)			Deflection (foot)
	Panel 30	Panel 55	Panel 40	Panel 55	Primary cable	Secondary cable	Suspender	
Small deformation	-48,061	34,537	77,275	-829	2214,600	1649,300	33,003	-0.387
Large deformation	-47,717	35,906	77,360	-843	2217,600	1649,400	33.007	-0.386

Table 3.8   Comparison of maximum forces and deflection without cable pre-strain

Analysis type	Bottom chord (pound)		Top chord (pound)		Cable members (pound)			Deflection (foot)
	Panel 30	Panel 55	Panel 40	Panel 55	Primary cable	Secondary cable	Suspender	
Small deformation	-398,150	161,970	636,410	-8,425	1572,100	1125,200	22,831	-3.172
Large deformation	-377,580	178,780	642,160	-8,032	1592,500	1135,300	23,041	-3.100

The three-dimension nonlinear simulation of the suspension bridge with both the lower as well as the upper cables has proved to be difficult. The smaller discretization would be computationally very large and inefficient. Convergence of such a large number of nonlinear elements is not always guaranteed. In the finite element model developed by Lall (1992), for simplicity, both primary cable and secondary cable were modeled as a single cable that combined the section properties of the two independent cables.

In the finite element modeling of a suspension bridge, it is quite natural to discretize the cable between two suspenders into a single tension-only truss element (cable element). But two node cable elements, as we know, are relatively weak elements. One node needs at least three constraints to maintain the stability. The suspenders and tie rods connecting the primary and secondary cables, also as the truss elements, can not provide sufficient constraints at each node of cable elements in the transverse (Z-) direction. Consequently, the global stiffness of the bridge encounters the zero or very small pivot at each node of cable elements in the transverse direction. This results in the model that is unconstrained or unstable and nonlinear static analysis or modal analysis can not be carried out. The problem is solved here by coupling the transverse displacement of each cable node with the transverse displacement of corresponding node at the bottom chord of the stiffening truss. In such a way, the transverse displacement constrain is forced to each cable node and is mandatory equal to the transverse displacement of each corresponding node at the bottom chord of the stiffening truss. This is quite acceptable when the overall structural behavior instead of local cable behavior is concerned. Furthermore, when above the cable elements are replaced by the beam elements, everything is all right. The general beam element or the beam element even with small bending stiffness, however, can not represent the main feature of suspended cables, even thought most of investigators have done in that way.

Another key feature in the nonlinear structural analysis is the choice of convergence criterion to control the iteration procedure. The defaulted force convergence criterion in the ANSYS can not provide an efficient iteration solution in the large deflection analysis of the Roebling bridge. Sometimes the force convergence criterion results in the divergence especially when the structural deflection reaches slightly large. Instead, the displacement convergence criterion is very effective and always results in the convergent solution. In addition, as mentioned previously the stress stiffening plays an important role in the static analysis of suspension bridges. The sagging of the cable requires the stress part in the stiffness matrix and results in the nonlinear analysis. Stress stiffening must be always used for sagging cable problem to provide numerical stability. Using a large deformation solution without the stress stiffening capability leads to an aborted run due to divergent oscillation.

3.4   Modal Analysis

Since the collapse of the Tacoma Narrows Bridge in 1940, considerable amount of research has been conducted to study the dynamic behavior of cable suspension bridges as a part of the design of wind and seismic resistance. The dynamic characteristics of a structure is effectively analyzed in terms of natural frequencies and mode shapes. Modal analysis is needed to determine the natural frequencies and mode shapes of the entire suspension bridge. The natural frequencies and mode shapes of the Roebling suspension bridge are studied using current finite element model. Since the established model is completed 3-D finite element model, a general modal analysis is capable to provide all possible modes of the bridge (transverse, vertical, torsional and coupled).

The modal analysis needs to solve the eigenvalue problem. The eigenvalue and eigenvector extraction technique used in the analysis is the Block Lanczos method. The Block Lanczos eigenvalue extraction method is available for large symmetric eigenvalue problems. Typically, this solver is applicable to the type of problems solved using the Subspace Eigenvalue method, however, at a faster convergence rate. The Block Lanczos algorithm is basically a variation of the classic Lanczos algorithm, where the Lanczos recursions are performed using a block of vectors as opposed to a single vector. Additional theoretical details on the classic Lanczos method can be found in any textbooks on eigenvalue extraction.

3.4.1   Effect of Initial Equilibrium Configuration

As mentioned previously, the modal analysis of a cable-supported bridge should include two steps: static analysis under dead load and followed by pre-stressed modal analysis. This kind of pre-stressed modal analysis is available in ANSYS. In order to investigate the effect of initial equilibrium configuration due to dead load and the pre-strain in the cables on the dynamic properties of the Roebling suspension bridge, the following three cases are computed:

- Case 1: the regular modal analysis without dead load effect where the modal analysis is starting from the undeformed configuration;

- Case 2: the pre-stressed modal analysis where the modal analysis follows a dead-load linear static analysis without the pre-strain in the cables;

- Case 3: the pre-stressed modal analysis where the modal analysis follows a dead-load linear static analysis with a pre-strain of 0.8×10^{-3} in the cables.

Table 3.9   Comparison of Frequencies (Hz)

Model order	Case 1	Case 2	Case 3
1	0.152	0.191	0.196
2	0.334	0.412	0.420
3	0.493	0.599	0.614
4	0.647	0.684	0.686
5	0.714	0.841	0.869
6	0.879	1.032	1.069
7	1.116	1.243	1.246
8	1.121	1.294	1.336
9	1.294	1.500	1.513
10	1.488	1.515	1.546
11	1.518	1.571	1.574
12	1.561	1.782	1.839
13	1.744	1.989	2.008
14	1.872	2.004	2.051
15	2.031	2.300	2.314
16	2.232	2.310	2.364

The comparison results of frequencies among above three cases are summarized in Table 3.9. It is clearly shown that the beneficial effect of self-weight is used in improving stiffness. The suspension bridge with sufficient amount of pre-strain in the cables is a highly pre-stressed structure. The lateral stiffness benefits much more than the vertical stiffness does. In the current case of the Roebling suspension bridge, the dead load effect will increase the lateral natural frequency by about 20% but increase the vertical natural frequency by about 5% due to the stiffening of the structure. Therefore, the regular modal analysis without a dead-load static analysis will result in the under-estimation of the cable-supported bridge capacity and consequently provides more safe evaluation of the bridge capacity.

Furthermore, compared with Case 2 and Case 3, the pre-strain in the cables slightly increases only the natural frequencies of the suspension bridge if the pre-stressed modal analysis is used. It implies that it is the self-weight not the initial equilibrium configuration starting the vibration contributes the stiffness improvement because the pre-strain in the cables only changes the initial equilibrium configuration and the distribution of the pre-stress due to dead load. But the initial equilibrium configuration to start the vibration is obviously essential to the dynamic responses under wind or seismic loadings.

3.4.2 Modal Analysis Results

To close to the real situation, the pre-stressed modal analysis starting from the dead-load deformed equilibrium configuration with a pre-strain of 0.8×10^{-3} in the cables is implemented here to evaluate the modal properties of the Roebling suspension bridge. The natural frequencies and modal participation factors are summarized in Table 3.10. The participation factor of particular mode demonstrates the importance of that mode. The participation factor table is available in the ANSYS to provide the list of participation factors, mode coefficients and mass distribution percentages for each mode extracted. The participation factors and mode coefficients are calculated based on an assumed unit displacement spectrum in each of the global Cartesian directions.

In general, several modes of vibration contribute to the total dynamic response of the structure. For the purpose of directional uncertainty and the simultaneous occurrence of forces in the three orthogonal directions, coupling effects within each mode of vibration should be considered. Coupling effects, however, make it difficult to categorized the modes into simple vertical, transverse, and torsional, thus making comparisons with experimental measurements difficult. Most of studies are aimed to analyze the modal behavior of suspension bridges in terms of pure vertical, transverse and torsional modes of vibration (Abdel-Ghaffar 1978; Abdel-Ghaffar 1979; Abdel-Ghaffar 1980; Lall 1992; West et al. 1984). Since the Roebling suspension bridge is modeled as a complete 3-D structure, all possible coupled modes can be obtained. It provides the full understanding of the dynamic behavior of the bridge.

The several dominated transverse mode shapes, vertical mode shapes and torsional/coupled mode shapes are shown in Fig. 3.9, Fig.3.10 and Fig.3.11 respectively. All mode shapes are normalized to unity instead of mass matrix in order to check with the corresponding mode shapes obtained from the ambient vibration tests later on. It can be observed that the main dominated natural vibration modes are in the transverse direction. This may be explained by the fact that the lateral system of the Roebling bridge is a single truss system unlike the lateral systems of modern bridges which have major lateral load resisting systems comprising of two lateral trusses. The lateral load resisting system of the Roebling bridge , however, comprises of a single truss in the plane of the bottom stiffening truss chords. The Guy wires in the horizontal plane of the lower chords that were meant to add lateral stability are also slack and ineffective. It can also be found that one dominated mode is always coupled with other modes. The vibration modes of the Roebling suspension bridge are complicated and coupled.

Table 3.10 Natural Frequencies (Hz) and Participation Factors

Frequency	Participation Factor						Dominated Mode
(Hz)	X	Y	Z	ROTX	ROTY	ROTZ	
0.196	-0.0126	0.0880	317.15	32456	260380	16.933	1st transverse
0.420	-0.0052	-0.3294	1.5853	160.37	85109	-44.081	2nd transverse
0.614	0.0206	0.2430	116.34	11272	-96576	193.25	3rd transverse
0.686	-0.1071	230.57	-0.0935	-3.5792	65.240	189170	1st vertical
0.869	0.0235	-0.1295	0.3947	23.356	-52797	-116.16	4th transverse
1.067	-0.0170	-0.1787	71.459	6688.0	-60134	-64.046	5th transverse
1.246	-35.108	2.3341	-0.2777	9.3106	362.94	70568	2nd vertical
1.336	0.1182	0.5354	3.7246	330.75	27165	237.78	6th transverse
1.513	-0.2083	-4.3911	-11.290	-3942.0	9586.4	-3400.4	1st torsional
1.546	-0.2723	-6.9722	47.374	3732.5	-41202	-5373.6	Coupled mode
1.574	-0.1476	-202.48	-1.3983	79.332	1304.1	167710	3rd vertical
1.839	0.1552	-0.3850	4.6048	442.84	17338	-496.37	7th transverse
2.008	-0.2750	2.6519	1.4672	230.45	520.58	2223.1	2nd torsional
2.051	-0.0547	0.2528	39.138	3630.4	-34519	296.81	8th transverse
2.314	0.6975	2.1473	-1.7940	-2844.7	2281.4	-60.115	2nd torsional
2.363	-0.2694	0.0674	5.4452	642.25	13944	444.16	9th transverse
2.429	-31.464	-0.0386	-0.3010	-140.29	225.27	56925	4th vertical

Elevation

Plan
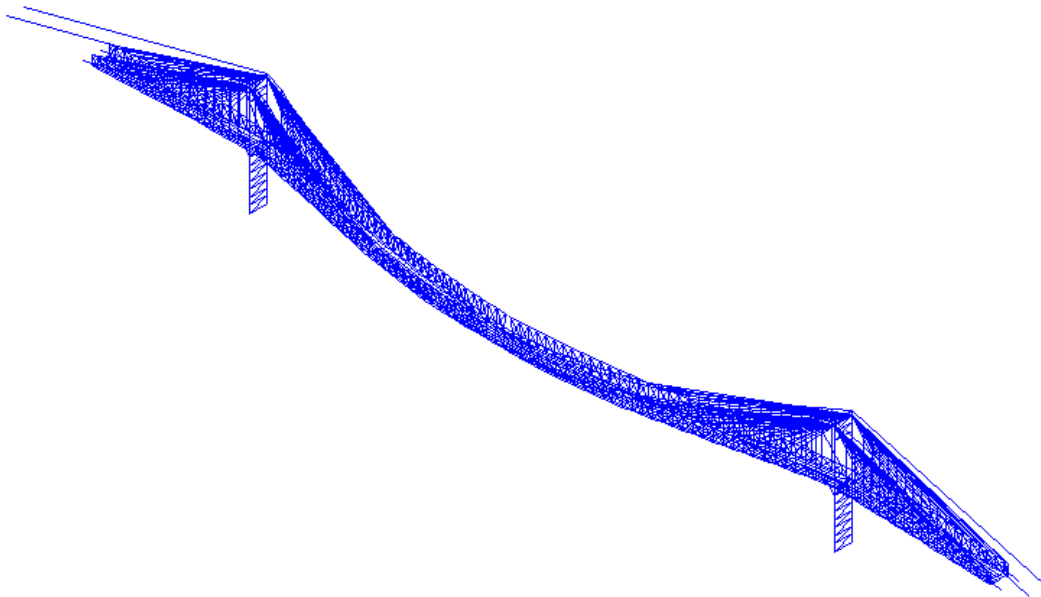
3-D View

Fig. 3.9(a)   1st Transverse Mode Shape (f=0.196Hz)

Elevation
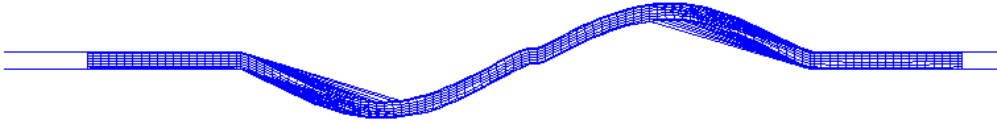
Plan
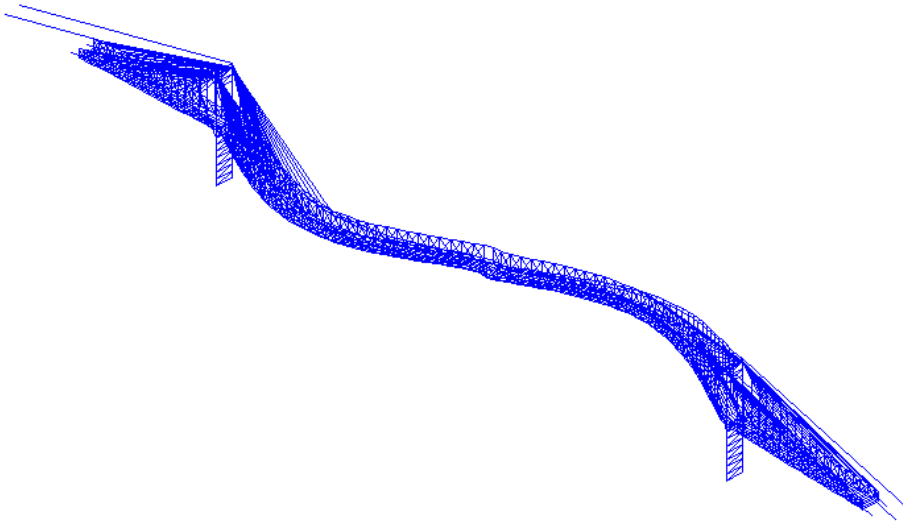
3-D View

Fig. 3.9(b)   2nd Transverse Mode Shape (f=0.420Hz)
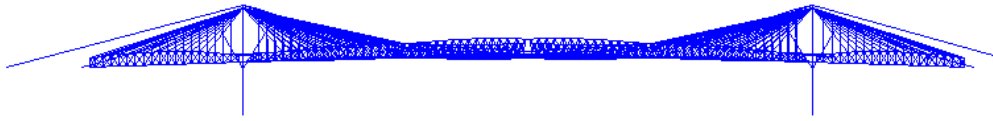
Elevation
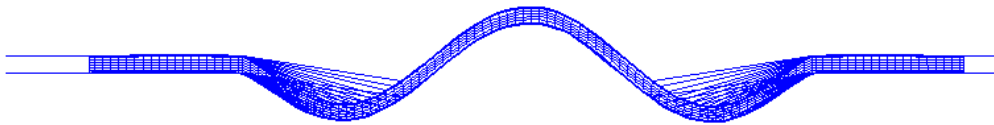
Plan
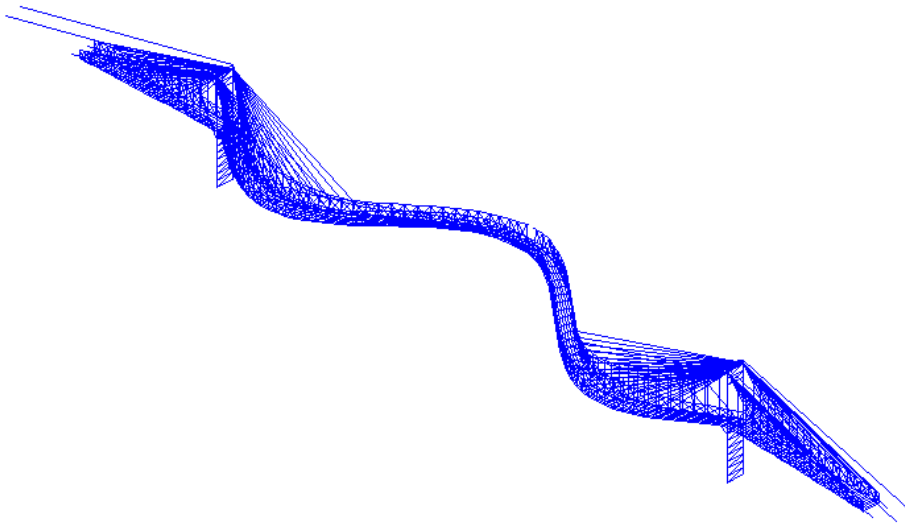
3-D View

Fig. 3.9(c)   3rd Transverse Mode Shape (f=0.614Hz)

Elevation
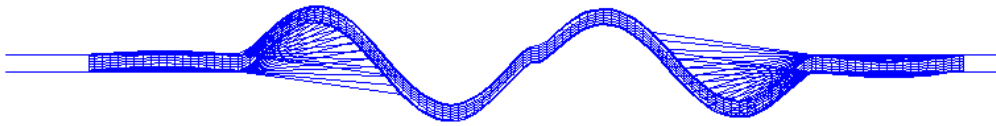
Plan
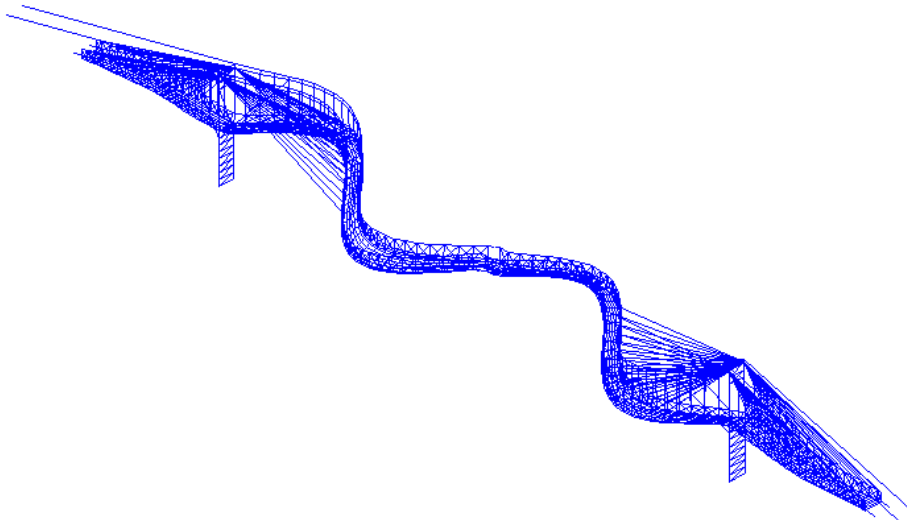
3-D View

Fig. 3.9(d)   4th Transverse Mode Shape (f=0.869Hz)
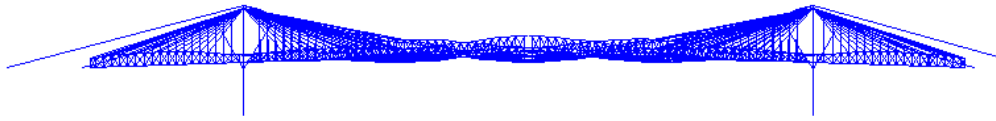
Elevation
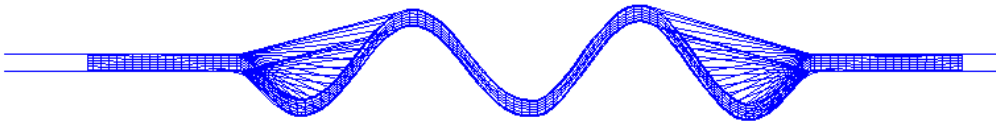
Plan
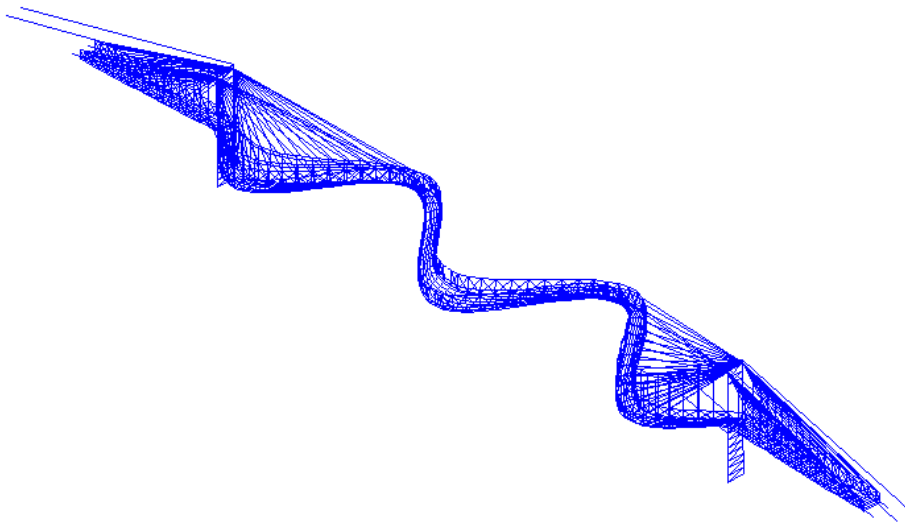
3-D View

Fig. 3.9(e)   5th Transverse Mode Shape (f=1.067Hz)
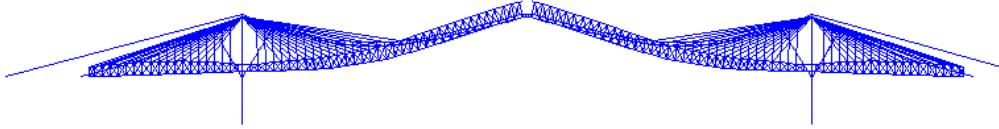
Elevation

Plan
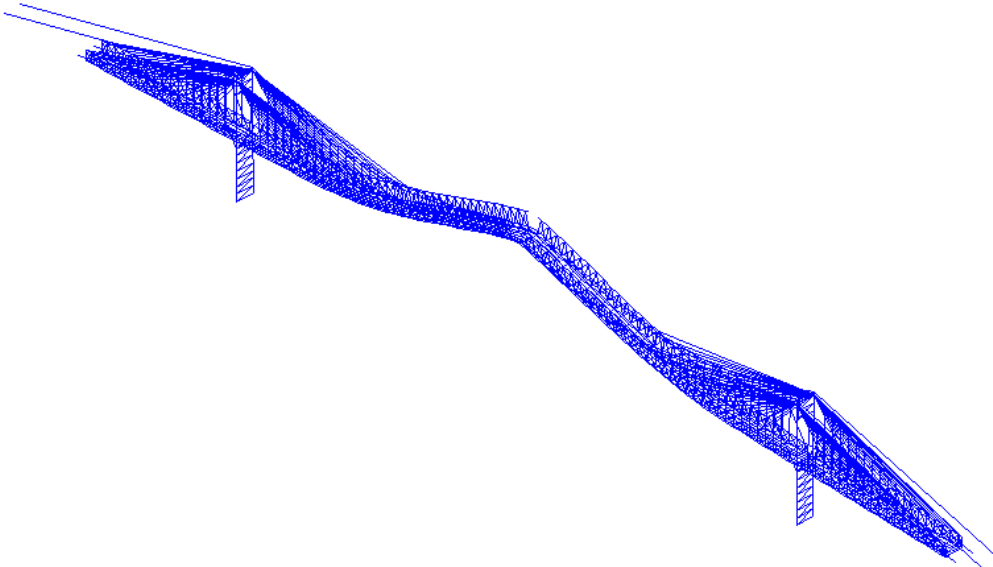
3-D View

Fig. 3.10(a)   1st Vertical Mode Shape (f=0.686Hz)
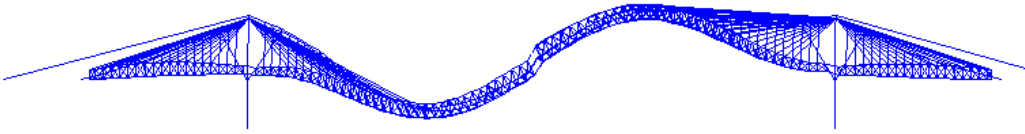
Elevation

Plan
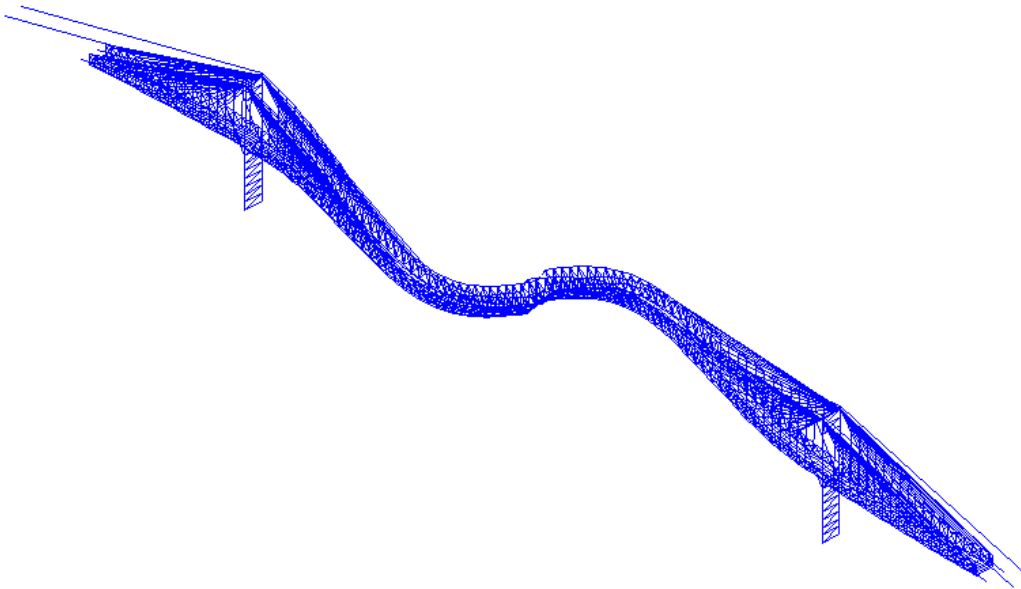
3-D View

Fig. 3.10(b) 2nd Vertical Mode Shape (f=1.246Hz)
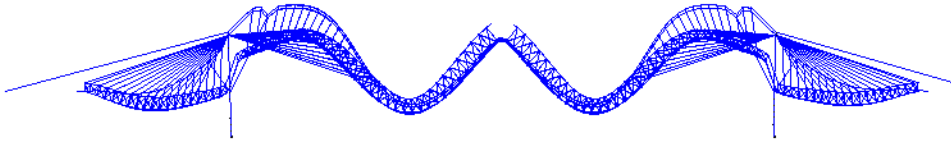
Elevation

Plan
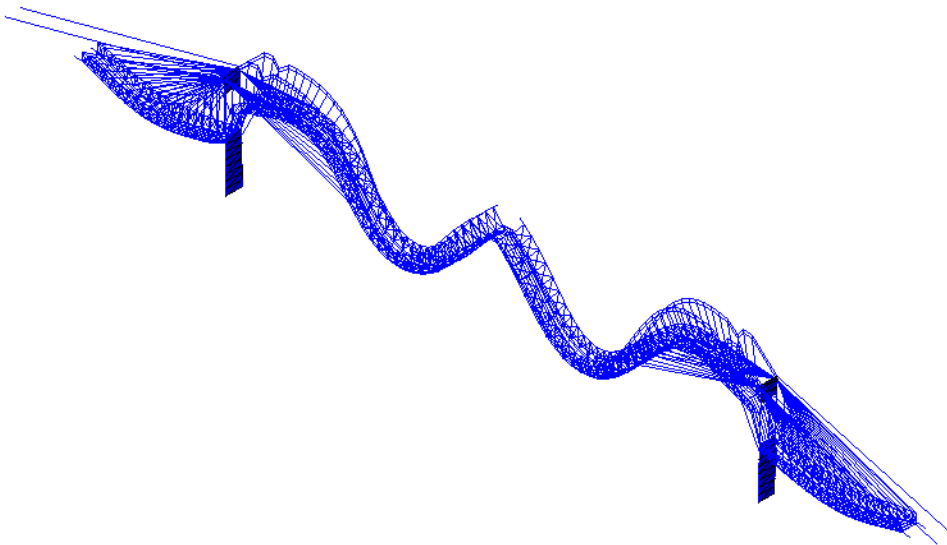
3-D View

Fig. 3.10(d) 3rd Vertical Mode Shape (f=1.574Hz)
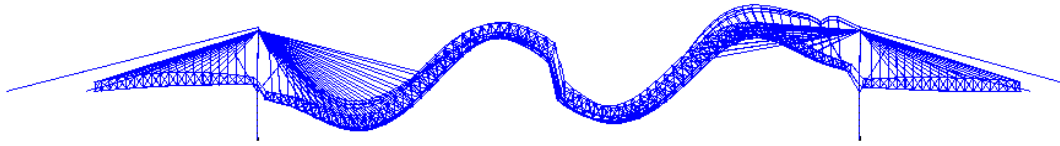
Elevation

Plan
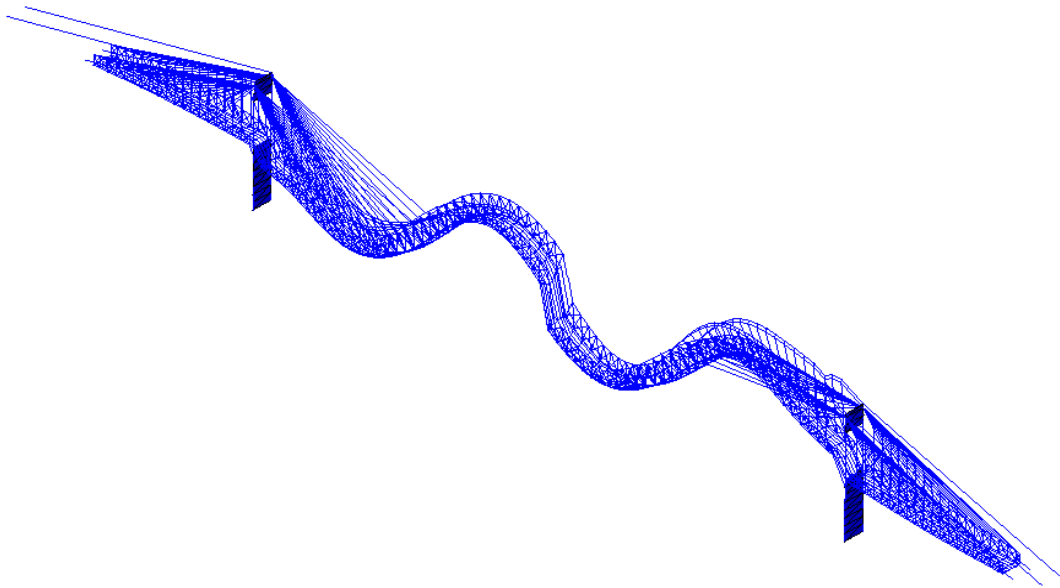
3-D View

Fig. 3.10(e)   4th Vertical Mode Shape (f=2.429Hz)
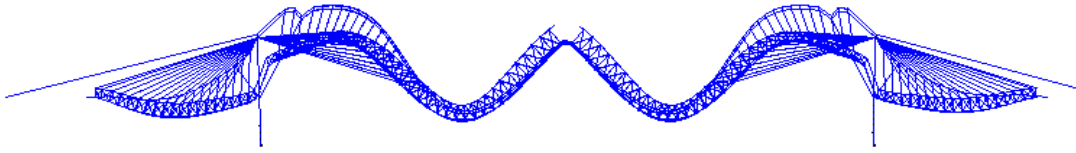
Elevation

Plan
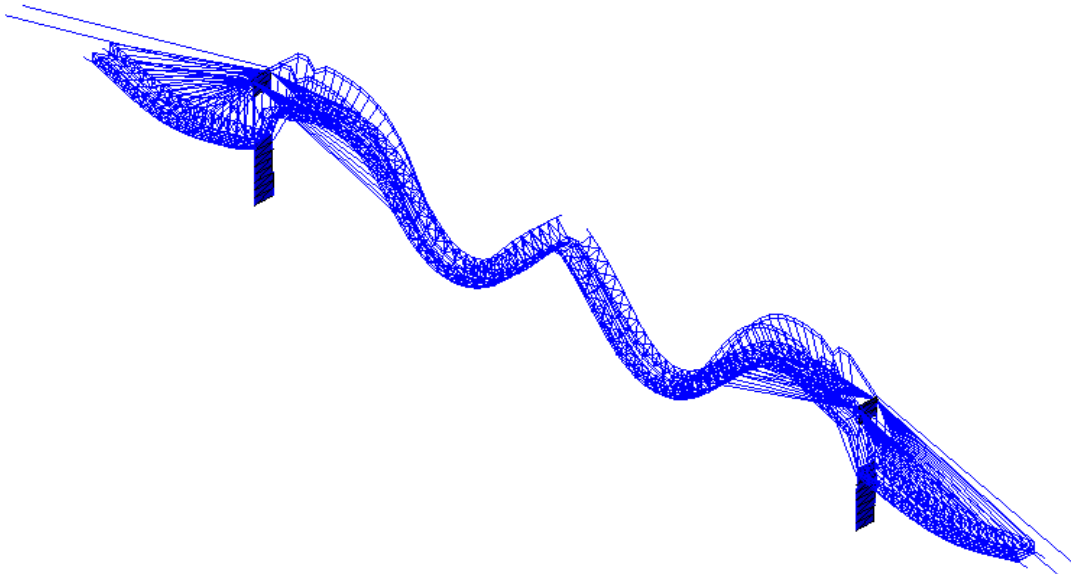
3-D View

Fig. 3.10(e) 5th Vertical Mode Shape (f=2.975Hz)
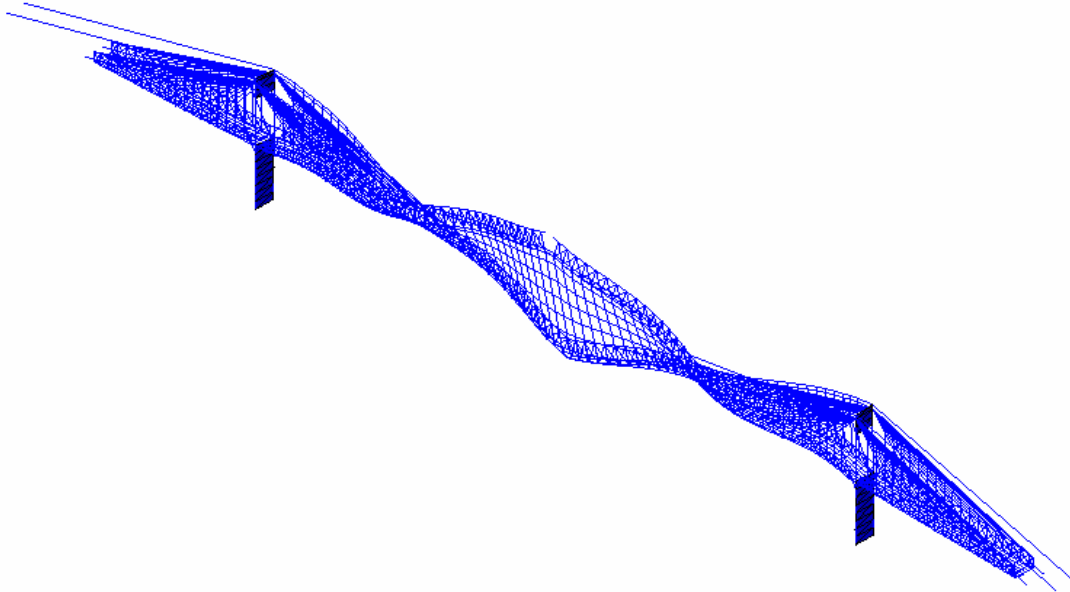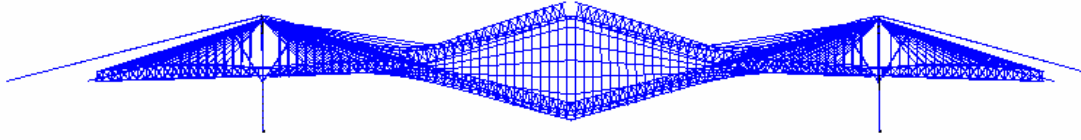
Fig. 3.11(a)   1st Torsional Mode Shape (f=1.513Hz)
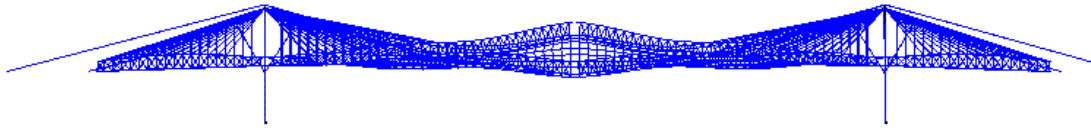
Elevation
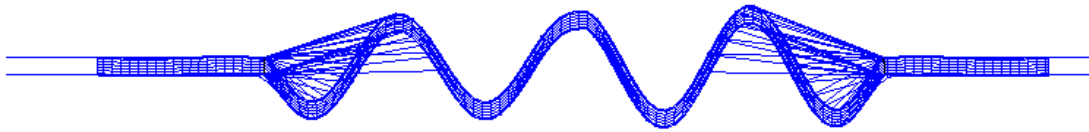
Plan
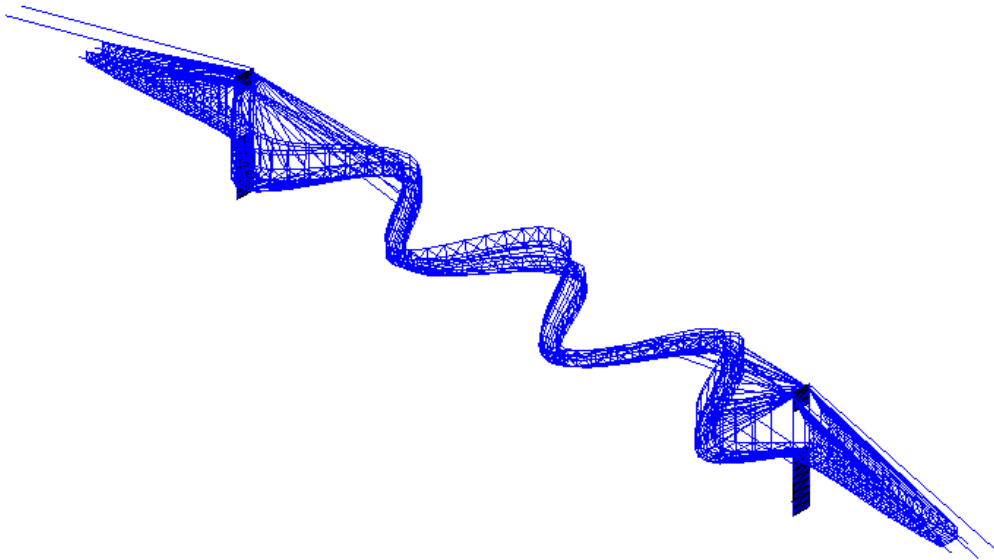
3-D View

Fig. 3.11(b)   Coupled Torsional and Transverse Mode Shape (f=1.546Hz)
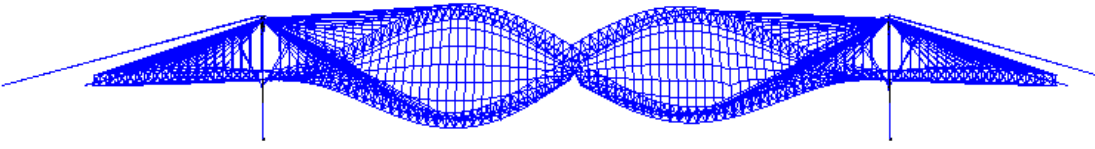
Elevation

Plan
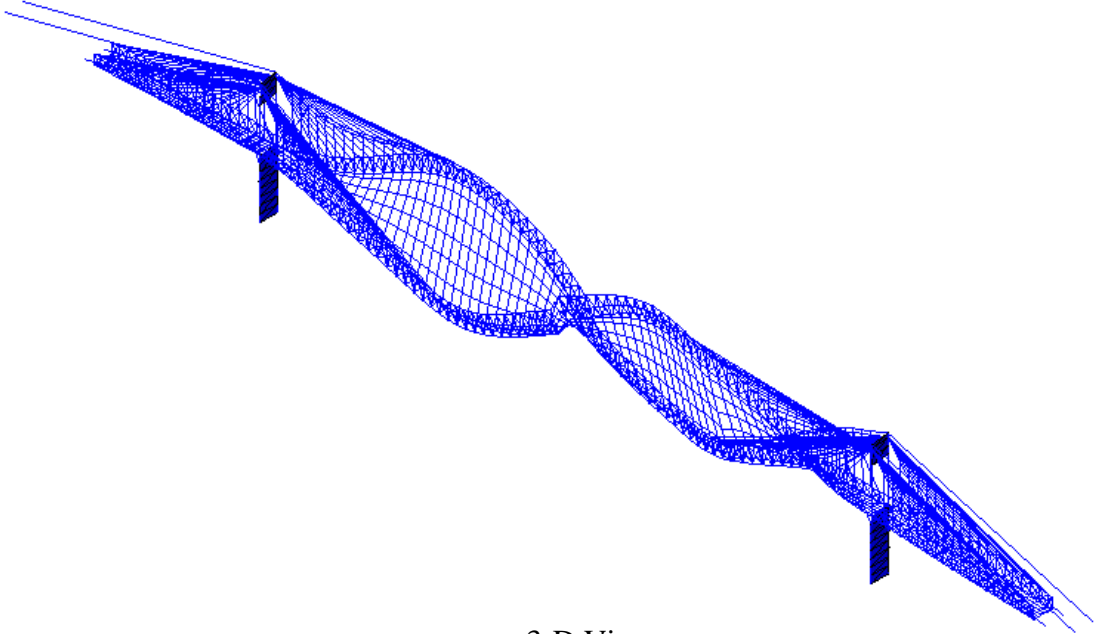
3-D View

Fig. 3.11(c)   2nd Torsional Mode Shape (f=2.008Hz)

3.5 Parametric Studies

In order to calibrate the FEM model of the Roebling suspension bridge with in situ ambient vibration measurements in the sense of modal parameters, the structural and material parameters that may largely affect the modal properties of the bridge are supposed to be identified. This can be realized by the parametric studies. As mentioned previously, one of the most advantages of finite element modeling and analysis is to make the parametric studies possible. The parametric studies can demonstrate the extent and nature of variation in modal properties that a variation in the input parameters can cause. The parametric studies reported here not only prove the efficiency of the finite element methodology, but also demonstrate the extent and nature of variation in modal properties that a variation in the input parameters can cause. The FEM model calibration can then be carried out by adjusting these parameters to match the frequencies and mode shapes best between testing and modeling.

There are several structural and material parameters that would affect the modal behavior of the Roebling suspension bridge, such as mass, cable tension stiffness, suspender tension stiffness, the stiffness of the stiffening trusses, vertical and transverse bending stiffness of the deck. The effects of these parameters on the modal properties of the bridge are studied as follows.

3.5.1 Deck Weight

The change of deck self weights is reflected by the relative mass density of floor beams and stringers that is defined by

$$\bar{\rho} = \frac{\rho}{\rho_0}$$

where ρ_0 is the standard mass density of stringers used in the current model. Frequencies for different deck mass density are summarized in Table 3.11 . The variation of the first two transverse and vertical frequencies with the relative mass density for the stringers is shown in Fig.3.12 It is clear that both transverse and vertical frequencies increase steadily with decreasing in the deck self weight.

Table 3.11   Frequencies (Hz) for different deck mass densities

Mode order	Relative mass density $\bar{\rho} = \dfrac{\rho}{\rho_0}$ for the deck					
	0.0	0.25	0.5	1.0	1.5	2.0
1	0.264	0.241	0.223	0.196	0.178	0.163
2	0.559	0.512	0.475	0.420	0.381	0.351
3	0.817	0.748	0.694	0.614	0.556	0.512
4	0.926	0.843	0.779	0.686	0.619	0.569
5	1.175	1.061	0.983	0.869	0.787	0.725
6	1.422	1.301	1.207	1.069	0.966	0.890
7	1.663	1.522	1.411	1.246	1.128	1.038
8	1.702	1.628	1.511	1.336	1.211	1.115
9	1.778	1.648	1.600	1.513	1.400	1.288
10	2.061	1.886	1.749	1.546	1.425	1.312
11	2.094	1.919	1.780	1.574	1.442	1.378
12	2.433	2.191	2.080	1.839	1.666	1.534
13	2.450	2.242	2.120	2.008	1.857	1.710
14	2.594	2.494	2.320	2.051	1.913	1.829
15	2.740	2.526	2.444	2.314	2.140	1.970
16	3.154	2.885	2.675	2.364	2.195	2.023

Frequency (Hz)

Relative deck mass density $\overline{\rho}$

(a)   First Two Transverse Frequencies *vs* Deck Mass Density
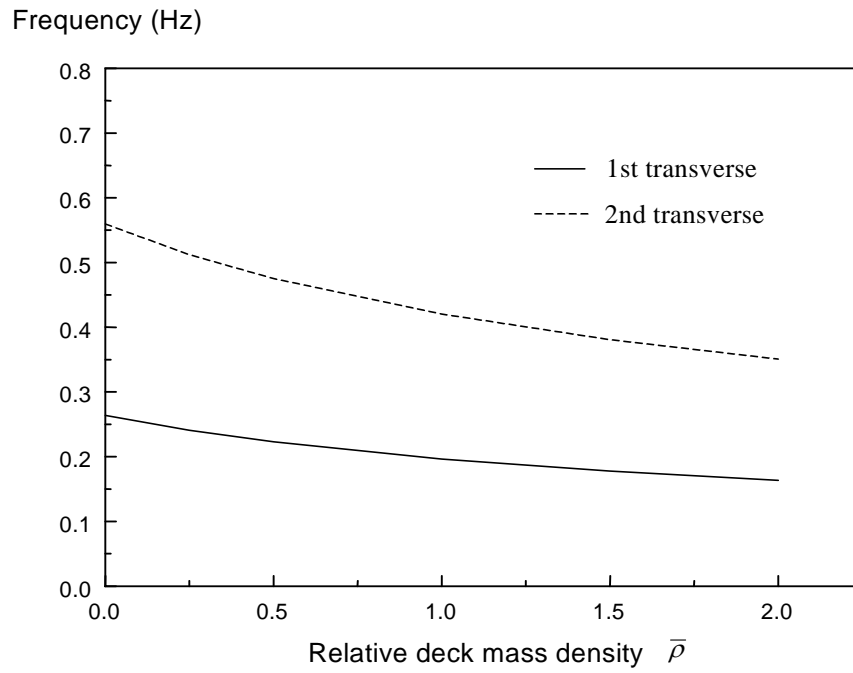
Frequency (Hz)

Relative deck mass density $\overline{\rho}$
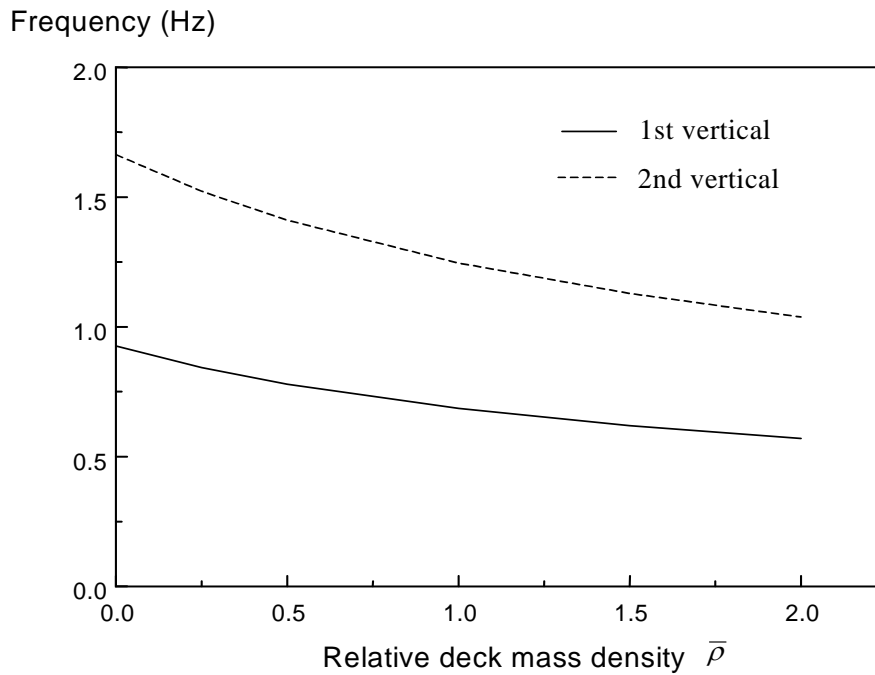
(b) First Two Vertical Frequencies *vs* Deck Mass Density

Fig. 3.12   Frequencies vs Deck Mass Density

3.5.2 Cable Stiffness

The tension stiffness of cables depends on the sectional area A and elastic modulus E. The effect of them on the modal properties of the bridge is studied separately in the following. Note that the cable of the Roebling suspension bridge is composed of both primary and secondary cables so the change of cable parameters means that both cables change by the same ratio.

3.5.2.1 The Sectional Area of Cables

The change of cable sectional areas is represented by the relative sectional area of cables that is defined by

$$\overline{A} = \frac{A}{A_0}$$

where A_0 is the standard sectional area of cables used in the current model. Frequencies for different cable area ratios are summarized in Table 3.12. The variation of the first two transverse and vertical frequencies with the relative cable area is shown in Fig.3.13. It has been found that the increment of cable sectional areas has a little effect on the value of both transverse and vertical frequencies. It is quite a truce that the increment of cable sectional areas implies the larger tension stiffness, which is supposed to increase the frequencies. But, at the same time, the weight of cables increases with increasing in the cable areas, which results in reducing the frequencies. The compensation of both makes the frequencies almost unchanged.

It should be noted that a variation in cable areas does cause a reordering of the dominated mode shapes as they relate to the sequential order of natural frequencies. The first symmetric vertical frequency, for instant, is the order 3 when $\overline{A} = 0.5$, while it becomes the order 4 when $\overline{A} = 0.75$ or 1.0.

3.5.2.2   The Elastic Modulus of Cables

The variation of cable elastic modulus is represented by the relative cable elastic modulus that is defined by

$$\overline{E} = \frac{E}{E_0}$$

where E_0 is the standard elastic modulus of cables used in the current model. Frequencies for different cable elastic modulus ratios are summarized in Table 3.13. The variation of the first two transverse and vertical frequencies with the relative cable elastic modulus is shown in Fig.3.14. It has been observed that a variation in cable elastic modulus (cable tension stiffness) causes a reordering of the dominated mode shapes as they relate to the sequential order of natural frequencies, especially for higher modes. Both transverse and vertical frequencies increase smoothly

as the elastic

modulus of cables increases in most cases. The exception is in the range of $\overline{A} = 1.0 \sim 1.5$ for the second vertical (the first asymmetric) mode. Similarly it happens for the third vertical (the second symmetric) mode. This is probably caused by a reordering of the mode shapes.

Table 3.12   Frequencies (Hz) for different cable areas

Mode order	Relative sectional area $\overline{A} = \dfrac{A}{A_0}$ for the cables					
	0.25	0.5	0.75	1.0	1.5	2.0
1	0.209	0.206	0.200	0.196	0.184	0.175
2	0.446	0.440	0.428	0.420	0.398	0.381
3	0.576	0.627	0.625	0.614	0.576	0.549
4	0.652	0.643	0.665	0.686	0.670	0.680
5	0.911	0.906	0.885	0.869	0.826	0.805
6	1.119	1.112	1.086	1.069	0.883	0.870
7	1.327	1.304	1.246	1.246	1.008	0.959
8	1.405	1.394	1.362	1.336	1.098	1.087
9	1.628	1.612	1.556	1.513	1.263	1.201
10	1.692	1.626	1.576	1.546	1.398	1.325
11	1.715	1.665	1.610	1.574	1.461	1.390
12	1.937	1.921	1.875	1.839	1.710	1.651
13	2.163	2.143	2.074	2.008	1.740	1.655
14	2.305	2.194	2.090	2.051	1.747	1.666
15	2.500	2.473	2.404	2.314	1.789	1.670
16	2.658	2.546	2.411	2.364	1.942	1.848

Table 3.13 Frequencies (Hz) for different cable stiffness

Mode order	Relative elastic modulus $\bar{E} = \dfrac{E}{E_0}$ for the cables						
	0.1	0.25	0.5	1.0	1.5	2.0	4.0
1	0.180	0.186	0.191	0.196	0.196	0.198	0.204
2	0.386	0.398	0.409	0.420	0.424	0.429	0.443
3	0.462	0.512	0.581	0.614	0.614	0.619	0.639
4	0.560	0.581	0.598	0.686	0.715	0.770	0.873
5	0.776	0.812	0.841	0.869	0.873	0.879	0.903
6	0.954	0.998	1.034	1.069	0.942	0.984	1.062
7	1.157	1.182	1.211	1.246	1.074	1.082	1.114
8	1.203	1.254	1.296	1.336	1.170	1.226	1.389
9	1.388	1.414	1.451	1.513	1.346	1.355	1.444
10	1.396	1.452	1.501	1.546	1.532	1.564	1.609
11	1.514	1.530	1.548	1.574	1.557	1.573	1.654
12	1.662	1.729	1.785	1.839	1.747	1.784	1.857
13	1.859	1.931	1.966	2.008	1.854	1.866	1.881
14	1.899	1.935	1.993	2.051	1.865	1.867	1.912
15	2.154	2.233	2.287	2.314	1.952	1.999	2.132
16	2.252	2.269	2.301	2.364	2.070	2.083	2.195
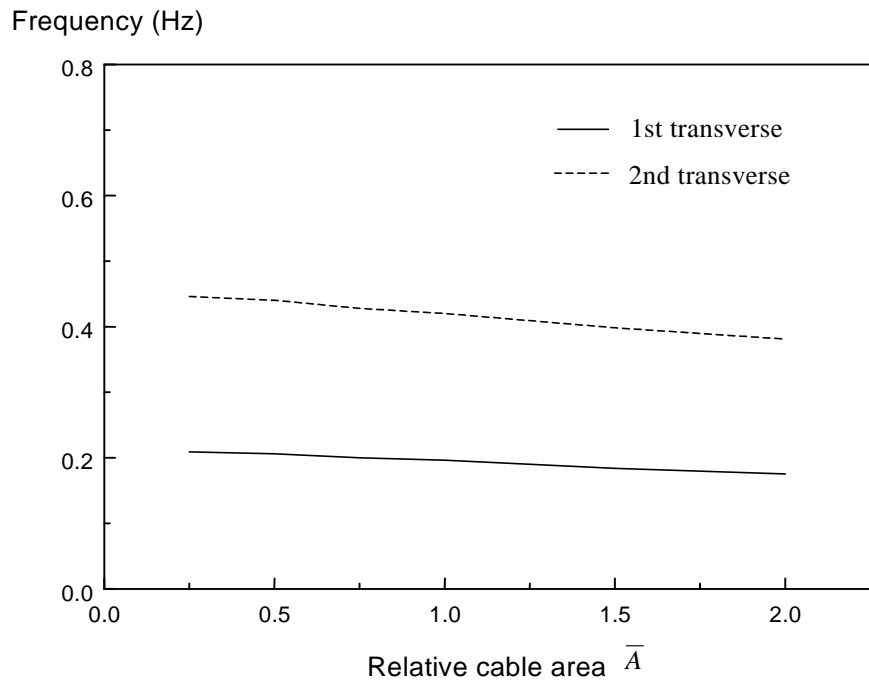
Frequency (Hz)

(a) **First Two Transverse Frequencies *vs* Cable Section Area**
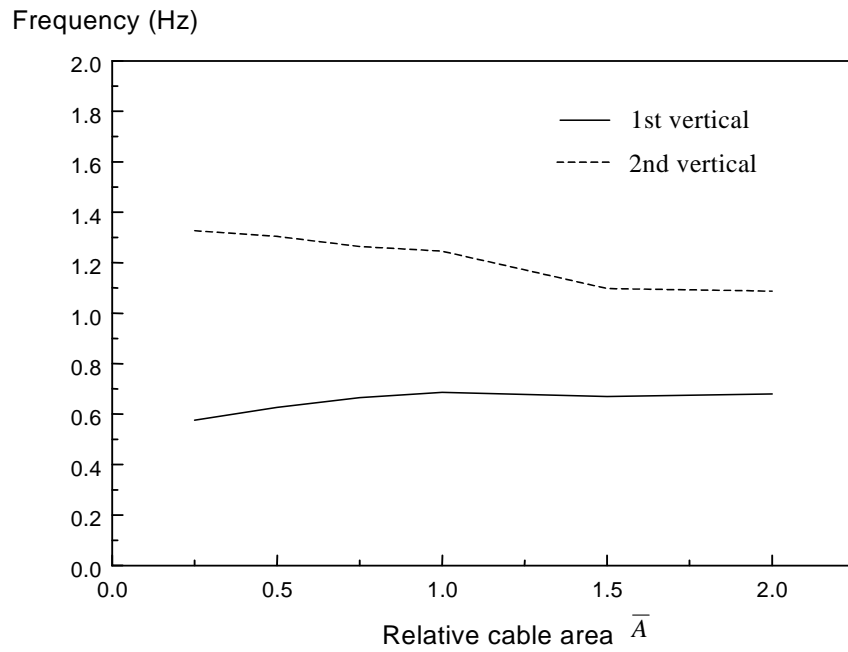
Frequency (Hz)

(b) **First Two Vertical Frequencies *vs* Cable Section Area**

Fig. 3.13 **Frequencies vs Cable Section Area**
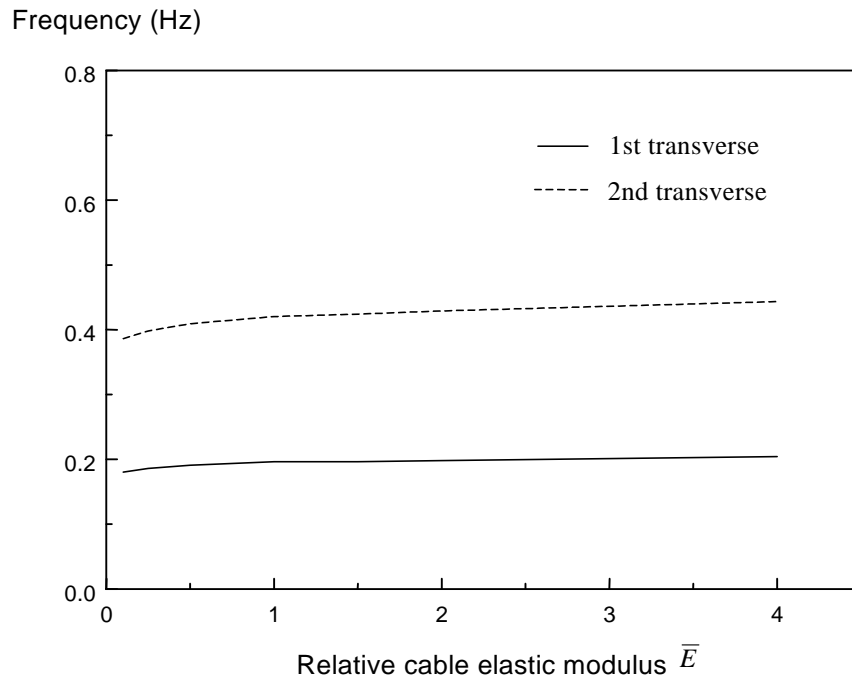
Frequency (Hz)

(a) First Two Transverse Frequencies *vs* Cable Elastic Modulus
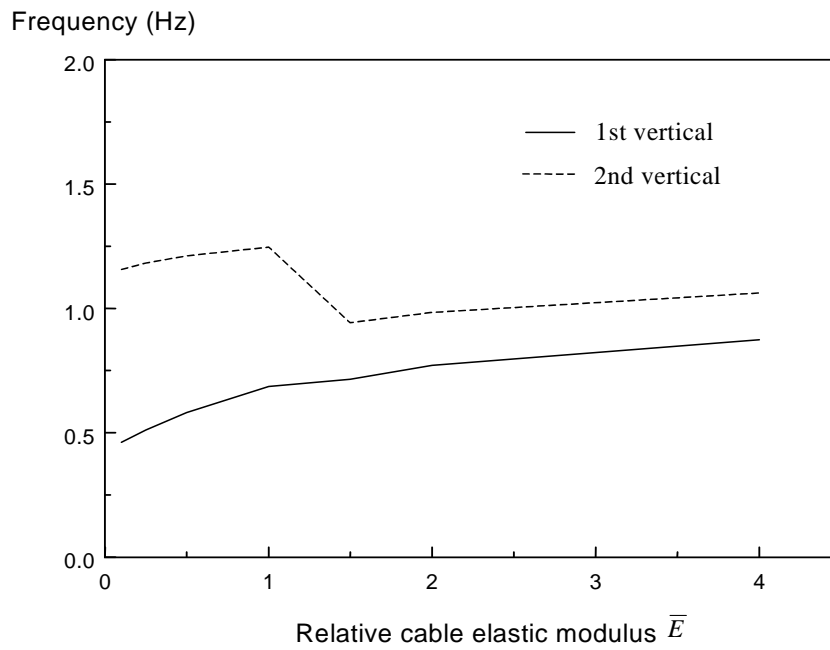
Frequency (Hz)

(b) First Two Vertical Frequencies *vs* Cable Elastic Modulus

Fig. 3.14   Frequencies vs Cable Elastic Modulus

3.5.3 Suspender Stiffness

Similarly, a variation in the tension stiffness of suspenders is represented by the relative elastic modulus of suspenders that is defined by $\overline{\overline{E}} = \dfrac{E}{E_0}$, where E_0 is the standard elastic modulus of suspenders used in the current model. Frequencies for different suspender tension stiffness are summarized in Table 3.14. The variation of the first two transverse and vertical frequencies with the relative elastic modulus of suspenders is shown in Fig. 3.15. It is clearly shown that the vertical frequencies increase smoothly when the suspender stiffness increases. Almost no variation in the transverse frequencies can be found. The results are consistent with the observation that the suspenders of a suspension bridge provide the stiffness in their own plane.

Table 3.14   Frequencies (Hz) for different suspender stiffness

Mode order	Relative elastic modulus $\overline{\overline{E}} = \dfrac{E}{E_0}$ for the suspenders					
	0.1	0.5	1.0	1.5	2.0	4.0
1	0.195	0.196	0.196	0.197	0.197	0.197
2	0.420	0.420	0.420	0.420	0.421	0.421
3	0.611	0.613	0.614	0.614	0.615	0.615
4	0.635	0.662	0.686	0.704	0.718	0.758
5	0.868	0.867	0.869	0.869	0.869	0.869
6	0.967	1.067	1.069	1.066	1.066	1.065
7	1.068	1.150	1.246	1.303	1.335	1.335
8	1.179	1.336	1.336	1.336	1.341	1.423
9	1.338	1.430	1.513	1.523	1.531	1.359
10	1.481	1.499	1.546	1.547	1.549	1.568
11	1.547	1.546	1.574	1.658	1.715	1.835
12	1.761	1.840	1.839	1.838	1.837	1.840
13	1.842	1.916	2.008	2.049	2.049	2.047
14	1.864	2.051	2.051	2.066	2.108	2.205
15	1.953	2.178	2.314	2.362	2.361	2.359
16	2.056	2.197	2.364	2.399	2.458	2.589

77
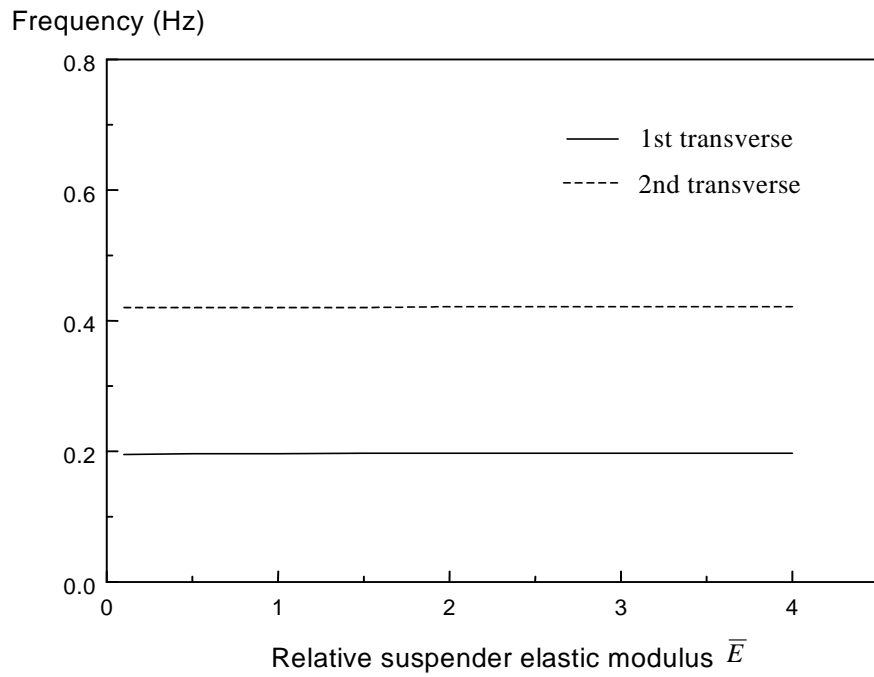
Frequency (Hz)

(a) First Two Transverse Frequencies *vs* Suspender Elastic Modulus
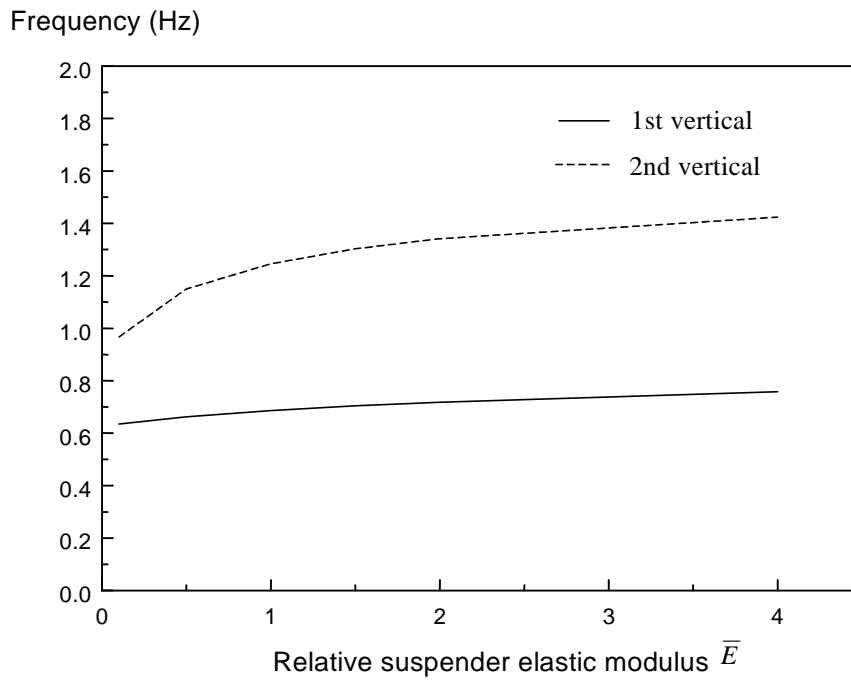
Frequency (Hz)

(b) First Two Vertical Frequencies *vs* Suspender Elastic Modulus

Fig. 3.15 Frequencies vs Suspender Tensional Stiffness

3.5.4 The Stiffness of Stiffening Truss

For the stiffness trusses, the stiffness of bottom chords, top chords, verticals as beam elements and diagonals as truss elements all depend on the elastic modulus. A variation in the stiffness of stiffening trusses is therefore represented by the relative elastic modulus of trusses that is defined by $\bar{E} = \dfrac{E}{E_0}$, where E_0 is the standard elastic modulus of stiffening truss used in the current model. Frequencies for different truss stiffness are summarized in Table 3.15. The variation of the first two transverse and vertical frequencies with the relative elastic modulus of stiffening trusses is shown in Fig.3.16. It is clearly shown that both transverse and vertical frequencies are increased with the increment in the stiffness of stiffening trusses, especially for the higher modes. The reduction of truss stiffness leads to modal reordering. The higher truss stiffness results in the delay of torsion modes and higher vertical modes.

Table 3.15　Frequencies (Hz) for different truss stiffness

Mode order	Relative stiffness $\bar{E} = \dfrac{E}{E_0}$ for the stiffening truss					
	0.1	0.25	0.5	1.0	1.5	2.0
1	0.166	0.175	0.185	0.196	0.203	0.208
2	0.353	0.375	0.397	0.420	0.434	0.444
3	0.519	0.549	0.580	0.614	0.633	0.646
4	0.579	0.617	0.650	0.686	0.708	0.725
5	0.729	0.774	0.819	0.869	0.899	0.921
6	0.763	0.911	1.006	1.069	1.102	1.127
7	0.799	0.943	1.059	1.246	1.375	1.425
8	0.904	0.989	1.195	1.336	1.386	1.474
9	1.033	1.179	1.252	1.513	1.602	1.644
10	1.073	1.194	1.356	1.546	1.733	1.862
11	1.113	1.348	1.420	1.574	1.764	1.870
12	1.289	1.370	1.627	1.839	1.918	1.979
13	1.361	1.608	1.715	2.008	2.139	2.206
14	1.365	1.615	1.900	2.051	2.296	2.533
15	1.508	1.711	1.918	2.314	2.479	2.571
16	1.681	1.795	2.040	2.364	2.627	2.824
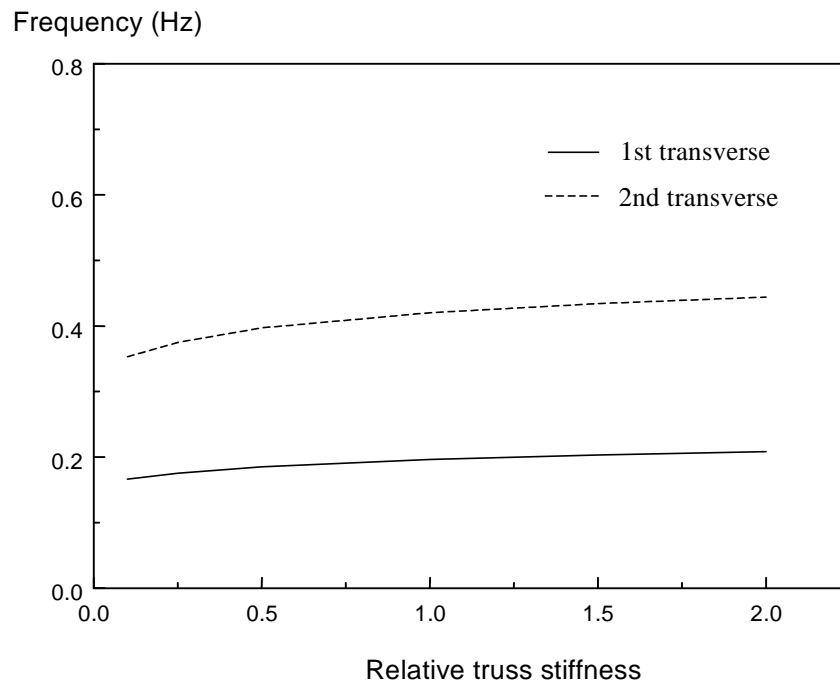
(b)   First Two Transverse Frequencies *vs* Truss Stiffness
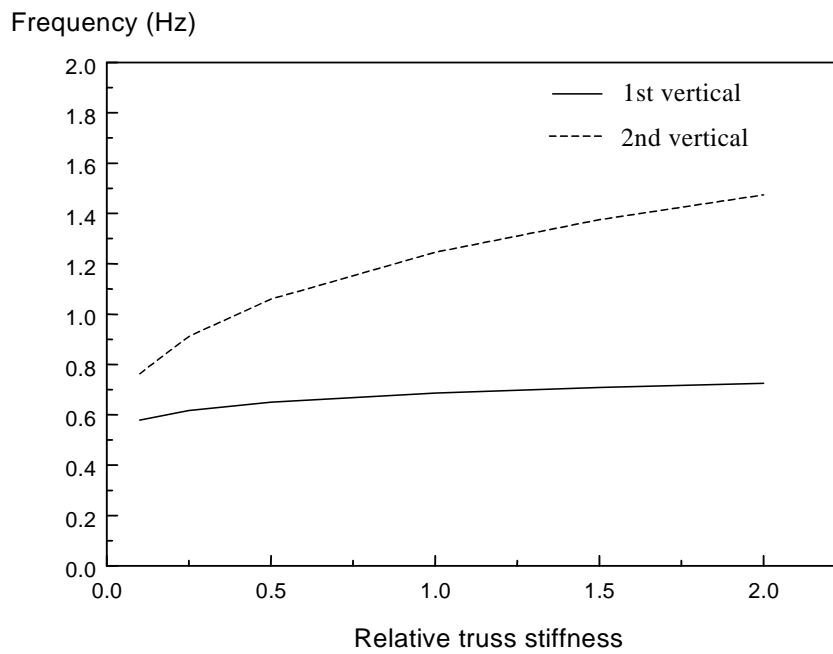
(b)   First Two Vertical Frequencies *vs* Truss Stiffness

Fig. 3.16   Frequencies vs Truss Stiffness

3.5.5 The Bending Stiffness of Deck

The deck system of the Roebling suspension bridge is modeled by floor beams and stringers. A variation in the bending stiffness of deck is then represented by the relative moment of inertia of floor beams and stringers. They are changed by the same ratio. The vertical bending stiffness and lateral bending stiffness of floor beams and stringers are studied separately.

3.5.5.1 The Vertical Bending Stiffness of Deck

The variation in the vertical bending stiffness of deck is represented by the relative vertical moment of inertia of floor beams and stringers that is defined by

$$\bar{I}_z = \frac{I_z}{I_{z0}}$$

where I_{z0} is the standard vertical moment of inertia of floor beams and stringers used in the current model. Frequencies for different vertical bending stiffness of deck are summarized in Table3.16. The variation of the first two transverse and vertical frequencies with the relative vertical bending stiffness of deck is shown in Fig.3.17. The results demonstrate that the vertical bending stiffness of deck does not contribute to both transverse and vertical frequencies, even though the vertical bending stiffness of deck is increased by five times. It is consistent with the fact that the deck as it was designed does not provide vertical bending stiffness to the whole bridge.

3.5.5.2 The Lateral Bending Stiffness of Deck

The variation in the lateral bending stiffness of deck is represented by the relative lateral moment of inertia of floor beams and stringers that is defined by

$$\bar{I}_y = \frac{I_y}{I_{y0}}$$

where I_{y0} is the standard lateral moment of inertia of floor beams and stringers used in the current model. Frequencies for different lateral bending stiffness of deck are summarized in Table 3.17. The variation of the first two transverse and vertical frequencies with the relative lateral bending stiffness of deck is shown in Fig.3.18. It is demonstrated that the increment in the lateral bending stiffness of deck does increase the transverse frequencies but does not contribute to vertical frequencies as we anticipated. It has been noted that a variation in the lateral bending stiffness of the deck causes a reordering of the dominated mode shapes as they relate to the sequential order of natural frequencies in Table. The first vertical symmetric bending mode, for example, occurs at order 5 when $\bar{I}_y = 0.1$ or 0.5, while it becomes the third order when $\bar{I}_y = 2.0$.

Throughout the parametric studies, it is found that the key parameters affecting the vertical modal properties are the mass, cable elastic modulus and stiffening truss stiffness. The key parameters affecting the transverse modal properties are the mass, cable elastic modulus, stiffening truss stiffness and the transverse bending stiffness of deck system.

Table 3.16   Frequencies (Hz) for different vertical deck stiffness

Mode order	Relative vertical bending stiffness $\bar{I}_z = \dfrac{I_z}{I_{z0}}$ for the deck				
	0.1	0.5	1.0	2.0	5.0
1	0.196	0.196	0.196	0.196	0.197
2	0.420	0.420	0.420	0.420	0.420
3	0.613	0.614	0.614	0.614	0.614
4	0.682	0.685	0.686	0.687	0.691
5	0.868	0.869	0.869	0.869	0.869
6	1.065	1.067	1.069	1.067	1.067
7	1.231	1.242	1.246	1.251	1.258
8	1.335	1.336	1.336	1.336	1.336
9	1.408	1.450	1.513	1.518	1.519
10	1.544	1.546	1.546	1.546	1.546
11	1.552	1.569	1.574	1.578	1.586
12	1.838	1.839	1.839	1.839	1.838
13	1.901	1.992	2.008	2.017	2.045
14	2.049	2.050	2.051	2.051	2.050
15	2.209	2.300	2.314	2.323	2.330
16	2.324	2.363	2.364	2.363	2.363

Frequency (Hz)

(a) First Two Transverse Frequencies *vs* Deck Vertical Bending Stiffness
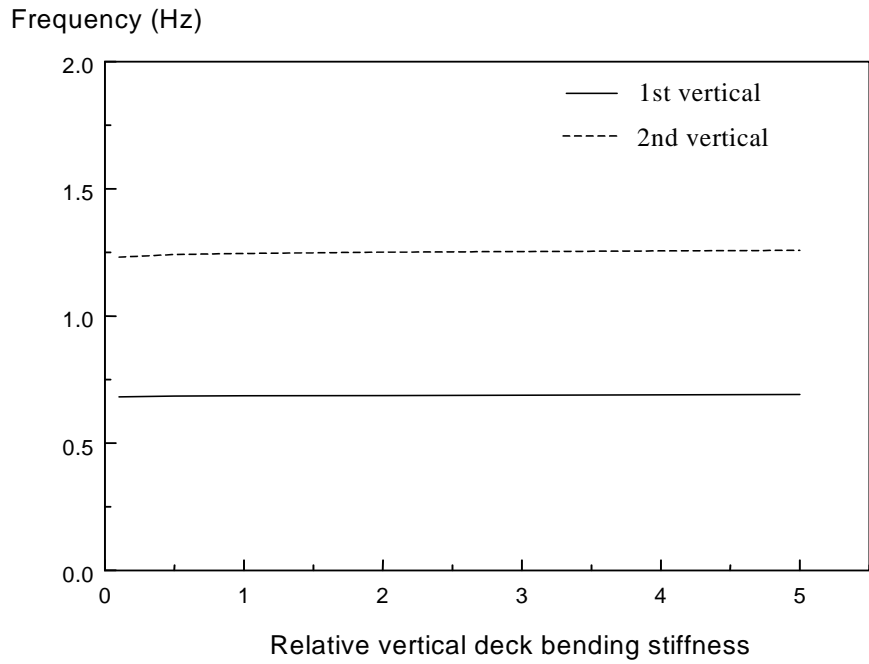
Frequency (Hz)

(b) First Two Vertical Frequencies *vs* Deck Vertical Bending Stiffness

Fig. 3.17   Frequencies vs Deck Vertical Bending Stiffness

Table 3.17   Frequencies (Hz) for different lateral deck stiffness

Mode order	Relative lateral bending stiffness $\bar{I}_y = \dfrac{I_y}{I_{y0}}$ for the deck					
	0.1	0.25	0.5	1.0	1.5	2.0
1	0.138	0.153	0.172	0.196	0.213	0.224
2	0.287	0.320	0.361	0.420	0.463	0.496
3	0.417	0.456	0.526	0.614	0.677	0.687
4	0.589	0.656	0.684	0.686	0.687	0.727
5	0.681	0.683	0.742	0.869	0.964	1.038
6	0.717	0.801	0.908	1.069	1.186	1.253
7	0.905	1.009	1.141	1.246	1.251	1.283
8	1.042	1.163	1.237	1.336	1.484	1.520
9	1.211	1.226	1.450	1.513	1.517	1.585
10	1.255	1.396	1.510	1.546	1.581	1.606
11	1.396	1.507	1.560	1.574	1.721	1.866
12	1.505	1.545	1.574	1.839	2.033	2.054
13	1.526	1.555	1.734	2.008	2.043	2.213
14	1.628	1.808	1.972	2.051	2.277	2.365
15	1.703	1.947	2.032	2.314	2.346	2.444
16	1.738	1.974	2.230	2.364	2.438	2.476
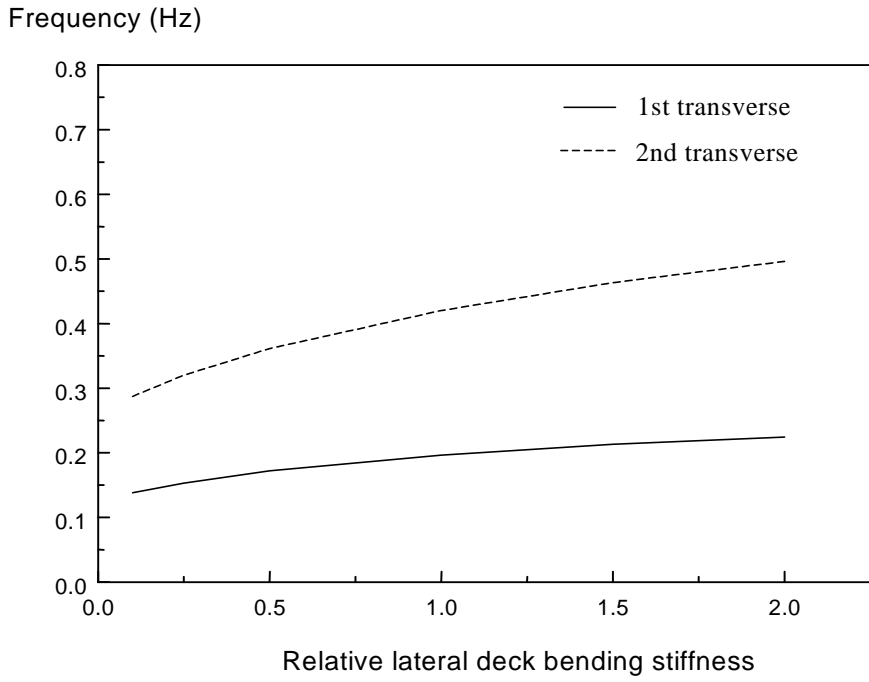
(a) First Two Transverse Frequencies *vs* Deck Lateral Bending Stiffness
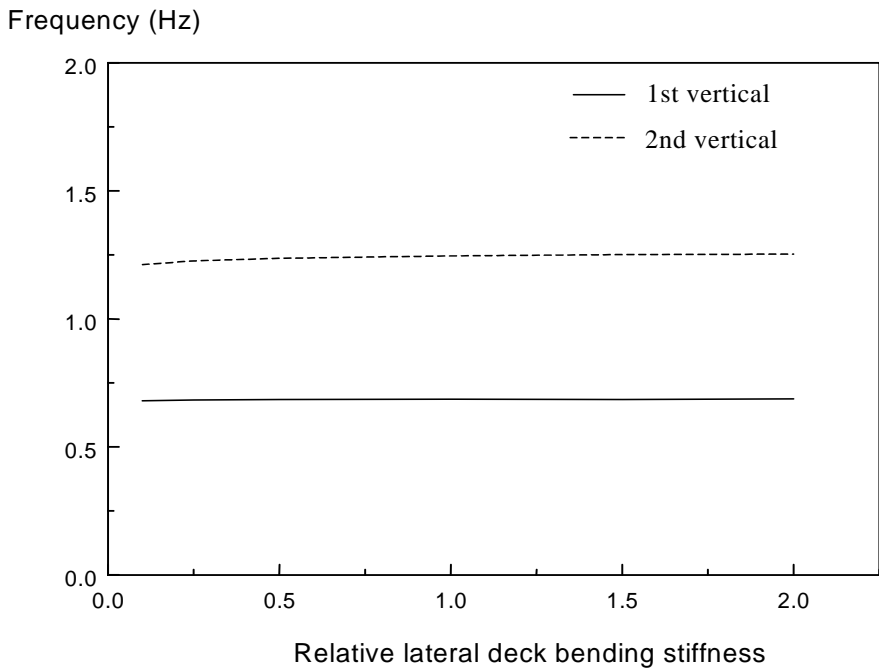
(b) First Two Vertical Frequencies *vs* Deck Lateral Bending Stiffness

Fig.3.18 Frequencies vs Deck Lateral Bending Stiffness

3.6 Observations and Remarks

A detailed 3-D finite element model has been developed for the J.A. Roebling suspension bridge in order to make a start toward the evaluation of this historic structure. From the static analysis due to dead loads, followed by pre-stressed modal analysis and parametric studies, the following observations and comments can be made:

1. It is quite natural to discretize the cable between two suspenders into a single tension-only truss element (cable element). Two node cable elements, however, are relatively weak elements. The suspenders or tie rods connecting the primary or secondary cable cannot provide sufficient constraints at each cable node in the transverse (Z-) direction. Consequently, the global stiffness matrix of the bridge meets the zero or relatively small pivots. This results in the model that is unconstrained or unstable. Hence the nonlinear static analysis and modal analysis can not be carried out. The extra restraints should be provided at each cable node in the transverse direction to obtain the stable solution.

2. The complete 3-D nonlinear modeling of a suspension bridge has proved to be difficult. The smaller discretization would be computationally very large and inefficient. Convergence of such a large number of nonlinear elements is not always guaranteed. The choice of convergent criterion to control the iteration procedure becomes essential. The common force convergent criterion defaulted in the ANSYS is not so effective in the nonlinear analysis of a suspension bridge. Instead, the displacement convergence criterion has proved to be effective and often results in the convergent solution.

3. Due to the cable sagging, the static analysis of a suspension bridge is always a geometric nonlinear. The stress stiffening of cable elements (cable sagging effect) plays an important role in both the static and dynamic analysis of a suspension bridge. Nonlinear static analysis without the stress stiffening effect will leads to an aborted run due to the divergent oscillation even though the displacement convergence criterion is used.

4. Large deflection has demonstrated the limited effect on the member forces and deck deflection of the bridge under dead loads. After introducing enough amount of initial strain in the cables, the static analysis of the Roebling suspension bridge due to dead loads can be elastic and small deflection. The stress stiffening effect, however, is always required to ensure the convergent solution.

5. The initial strain in the cables is the key factor to control the initial equilibrium configuration under dead loading. For a completed bridge, the common fact is that the initial position of the cable and bridge is unknown. The initial geometry of the bridge that we have modeled is really the dead load deflected shape of the bridge. The initial equilibrium configuration of the bridge due to dead loads can be approximately achieved by manipulating the initial tension forces in the cables until a value is estimated that leads to the minimum deck deflection and minimum stresses in the stiffening structure.

6. It is demonstrated that a suspension bridge is a highly pre-stressed structure. The modal or any dynamic analysis must start from the initial equilibrium configuration due to dead loads. This

initial equilibrium configuration can be a small deflection static analysis because the large deflection can be ignored. In other words, the modal analysis of a suspension bridge should include two steps: small deflection static analysis under dead loading and followed by pre-stressed modal analysis, so that the dead load effect to the stiffness can be included. In other words, the modal analysis of a suspension bridge must be a pre-stressed modal analysis.

7. It is clearly shown that the self-weight effect can improve the stiffness of a suspension bridge. In the case of the Roebling suspension bridge, the lateral stiffness benefits much more than the vertical stiffness. The dead load effect increases the transverse natural frequency by about 20% but increases the vertical natural frequency by 5% only. Therefore, the regular modal analysis without a dead-load static analysis will under estimate the stiffness of the suspension bridge and consequently provide the more safe evaluation of the bridge.

8. It is observed that one dominated mode is always coupled with other modes. The dominated mode shapes of the Roebling suspension bridge in the low-frequency (0~1.0 Hz) range are transverse direction. This reveals the fact that the lateral stiffness of the bridge is relatively weak because the lateral system of the Roebling bridge is a single truss system unlike the lateral systems of modern bridges which have major lateral load resisting systems comprising of two lateral trusses.

9. Throughout the parametric studies, the key parameters affecting the vertical modal properties of the Roebling suspension bridge are the mass, cable elastic modulus and stiffening truss stiffness. The key parameters affecting the transverse modal properties are the mass, cable elastic modulus, stiffening truss stiffness and the transverse bending stiffness of deck system.

10. It is observed that the effect of decreasing the truss stiffness by 50% does not lead to an decrease in the bridge frequencies as significant as a reduction of 50% in the cable stiffness. This fact once again points to the importance of the cable in governing the stiffness of the suspension bridge.

4. FIELD DYNAMIC TESTING AND MODEL CALIBRATION

4.1 General

On-site dynamic testing of a bridge provides an accurate and reliable description of its real dynamic characteristics. There are two main types of dynamic bridge testing:

❑   Forced Vibration Test
❑   Ambient Vibration Test

In the first method, the structure is excited by artificial means such as shakers or drop weights. By suddenly dropping a load on the structure, a condition of free vibration is induced. The disadvantage of this method is that traffic has to be shut down for a rather long time, especially for large structures, e.g. long-span bridges with many test setups. It is clear that this can be a serious problem for intensively used bridges. In contrast, ambient vibration testing does not affect the traffic on the bridge because it uses the traffics and winds as natural excitation. This method is obviously cheaper than forced vibration testing since no extra equipment is needed to excite the structure. However, relatively long records of response measurements are required and the measurement data are highly stochastic. Consequently, the system identification results are not always that good.

For the Roebling suspension bridge, on-site dynamic testing has been performed in the way of ambient vibration tests. The Roebling suspension bridge consists of 1000' main span and 300' side span. The bridge has 28' width roadway and 9' sidewalks. Since the bridge is symmetric, ambient vibration measurements are carried out on only one-half of the bridge (one-half main span and one side span). The measured data are the acceleration-time histories. The equipment used to measure the acceleration-time histories consists of bi-axial accelerometers in conjunction with its own data acquisition system. The system identification is performed by rather simple peak picking method.

As mentioned previously, the original finite element model has to be updated or calibrated by the field testing in order to meet the current conditions of the bridge. It is anticipated that a realistic computer model, calibrated with the help of on-site experimental measurements, can be an in valuable tool in the efforts to reserve the historic bridges. The finite element model updating is carried out by the best matching the frequencies and modal shapes between the ambient vibration measurements and analytical finite element model. The updated finite element model will be the basis for future load-carrying capacity evaluations of the bridge.

4.2 Instrumentation and Data Record

The instrumentation scheme is shown in Fig. 4.1. The main features are as follows:

❑   Seven locations will be instrumented with bi-axial accelerometers (one for transverse direction and one for vertical direction).

❑   Four bi-axial accelerometers will be placed on one-half (500' length) of the main span at an interval of 125'.

- ❑ One bi-axial accelerometer will be placed on the deck at the tower location.

- ❑ Remaining two bi-axial accelerometers will be placed on the side span at 125' interval.

- ❑ Measurements at all stations will be made at the same time.

- ❑   Only one side of the deck is planned to be instrumented in this scheme. So the torsional mode can not be measured.

All accelerometers (total 14) are placed at the floor beam, lower chord interactions of upstream stiffening truss. All transverse accelerometers are oriented in the direction of rive flow. The more detailed measurement instrumentation is shown in Fig.4.2. The ambient vibration measurements of the Roebling suspension bridge have been repeated three times. The attempt is to make sure other data are available in case one set is wrong or lost. There are therefore three sets of test data named Test1, Test2 and Test3. For each test data set, there are 14 channels that are consistent with above sensor lay-out: seven stations and two directions for each station (one for transverse direction, one for vertical direction and no longitudinal direction data recorded).

For each channel the ambient vibration measurement data are recorded 1024 seconds with interval 0.078 second, which results in total 131,072 data points. Consequently, the sampling frequency is 128Hz.

4.3   Data Processing

Figs. 4.3 and 4.4 show the raw measurement data of the first (vertical) and second (transverse) channels at Station 1 of Test1. Fig.4.3a and Fig.4.4a are the raw acceleration-time history measurements visualized in the time domain, while Fig.4.3b and Fig.4.4b are the corresponding Power Spectral Density (PSD) visualized in the frequency domain.

The sampling frequency on site was chosen to be 128Hz to capture the transient signals of ambient vibration. For most bridges, however, the frequency range of interest lies between 0 and 10 Hz, containing at least the first ten eigen frequencies. So the resampling of the raw measurement data is necessary. It is important to proceed with this now, because afterwards other preprocessing steps will go much faster due to the reduced amount of data. A resampling and filter from 128 Hz to 8 Hz is the same as decimating (=low-pass filtering and resampling at a lower rate) 8 times. The decimating 8 times of raw data results in 131072/8=16384 data points and an excellent frequency range from 0 till 8 Hz. A smaller interval would reduce the number of points too much. Fig.4.5 and Fig.4.6 give the resampled vertical and transverse acceleration time data and corresponding Power Spectral Density at the Station 1 of Test1.

After resampling, the PSD still doesn't look so good. The reason is that, at this moment, the DPS is computed as the Fourier transform of all available ambient vibration data points (16384 points). A much nicer spectrum can be obtained by adjusting the PSD parameters. We select 1024 data points as "window-length". In this manner the PDS will be taken for all 1024 succeeding points. Afterwards the 16 (=16384/1024) different PDS's are averaged. This results in a noise-free signal as shown in Fig. 4.7 and Fig.4.8. Now, the data are ready for the system identification to extract the eigen frequencies and eigen mode shapes.

4.4 System Identification

System identification is originally a topic of control engineering (Juang 1994; Ljung 1987). However, it has received a world-wide attention recently for various types of applications. In the context of civil engineering, structures such as bridges or buildings are considered system and identification means the extraction of modal parameters (eigen-frequencies, damping ratios and mode shapes) from dynamic measurements. These modal parameters will serve as basis or input to the finite element model updating, to the damage identification algorithms in detecting and locating the possible damage in structures, and to the safety evaluation after the structure suffered from heavy damages such as earthquakes. These modal parameters will also be essential in the monitoring of structures on service and the controlling of structures.

Over the past decades, the system identification of civil engineering structures has developed very fast. Techniques such as modal testing and modal analysis have become available and widely used (Ewins 1986; Maia et al. 1997). Basically, the system identification procedure is carried out according to both input and output measurement data through the frequency response functions (FRFs) in the frequency domain or impulse response functions (IRFs) in the time domain. For civil engineering structures there is normally no difficulty to obtain the output measurements (dynamic responses). The structural dynamic responses are the direct records of the sensors that are installed at several locations of the structure. However, the input or excitation of the real structure in the operational condition often hardly realizes. It is extremely difficult to measure the input dynamic forces acting on a large-scale structure. Although forced excitations (such as heavy shakers and drop weights) and correlated input-output measurements are sometimes available, testing or structural complexity and achievable data quality restrict these approaches to dedicated applications.

On the other hand, ambient excitations such as traffic, wave, wind, earthquake and their combination are environmental or natural excitations. The ambient vibration has the advantage of being inexpensive since no equipment is needed to excite the structure. Also the service state of the structure does not have to be interrupted by using this technique. The ambient vibration measurements have been successfully applied to many large structures, for instance, the Golden Gate Bridge (Abdel-Ghaffer and Scanlan 1985) and the Brent-Spence Bridge (Harik et al. 1997) to evaluate the seismic safety.

Therefore, the system identification techniques through ambient vibration measurements have become a very attractive topic in the area of civil engineering structures. Ambient excitation does not lend itself to FRFs or IRFs calculations because the input force can not be measured. In this case only response data of ambient vibrations are measurable while actual loading conditions are unknown. A system identification procedure will therefore need to base itself on output-only data. System identification using ambient vibration measurements presents a challenge requiring the use of special identification techniques, which can deal with very small magnitudes of ambient vibration contaminated by noise without the knowledge of input forces. There have been several ambient vibration system identification techniques available that were developed by different investigators or for different uses such as:

❑ Peak-picking from the power spectral densities (PSDs) (Bendat and Piersol 1993);

❑ Auto Regressive-Moving Average (ARMA) model based on discrete-time data (Andersen et al. 1996);

- ❑   Natural excitation technique (NExT) (James et al. 1995);

- ❑   Stochastic subspace methods (Van Overschee and De Moor 1996);

- ❑   Maximum likelihood frequency domain methods (Hermans et al. 1998; Ren et al. 2000c), etc;

An extensive literature review on system identification techniques using ambient vibration measurements can be found in Van der Auweraer et al. (1999) and De Roeck et al. (2000). In fact, the mathematical background for many of these methods is often very similar, differing only from implementation aspects (data reduction, type of equation solvers, sequence of matrix operations, etc.).

The rather simple peak picking (PP) method is used here to identify the basic dynamic characteristics of the Roebling suspension bridge in the sense of ambient vibration measurements. The peak picking method is initially based on the fact that the FRF goes through an extremum around the natural frequencies. The peak picking method is therefore a kind of frequency domain based technique. The frequency at which this extremum occurs is a good estimate for the eigenfrequency. In the context of ambient vibration measurements only the FRF is replaced by the auto spectra of the ambient outputs (Bendat and Piersol 1993). In this way the natural frequencies are simply determined from the observation of the peaks on the graphs of the average normalised power spectral densities (ANPSDs). The ANPSDs are basically obtained by converting the measured accelerations to the frequency domain by a discrete Fourier transform (DFT). The coherence function computed for two simultaneously recorded output signals has values close to one at the natural frequency. This fact also helps to decide which frequencies can be considered as natural. The data processing and system identification are carried out by both MACEC, modal analysis for civil engineering construction (De Roeck and Peeter 1999) and DADiSP, data analysis and display software (DADiSP 1995).

The vertical and transverse average normalized power spectral densities (ANPSDs) are as shown in Fig.4.9, Fig.4.10 and Fig.4.11 for Test1, Test2 and Test3 respectively. The peak points are clearly shown and then the eigen frequencies can be picked up. It has been noted that the figures have been zoomed to focus on the frequency range of interest.

The identified vertical and transverse frequencies in Table 4.1 and Table 4.2 come out of the peak picking. It can be observed that the identified eigen frequencies from three separate ambient vibration measurements are quite stable. The first vertical vibration frequency of the Roebling suspension bridge is about 0.56Hz, while the first transverse vibration frequency of the Roebling suspension bridge is about 0.18Hz. The first four transverse frequencies are located within 1Hz.

Table 4.1   The Identified Vertical Frequencies (Hz)

Order	f1	f2	f3	f4	f5
Test1	0.57143	0.90365	1.2093	1.9269	2.3123
Test2	0.55814	0.90365	1.2093	1.9269	2.2990
Test3	0.55814	0.90365	1.2359	1.9402	2.3123
Average	0.56257	0.90363	1.2182	1.9313	2.3079

Table 4.2 The Identified Transverse Frequencies (Hz)

Order	f1	f2	f3	f4	f5
Test1	0.18605	0.45183	0.61130	0.97010	1.24920
Test2	0.17276	0.45183	0.58472	0.90023	1.24920
Test3	0.19834	0.43854	0.61130	0.94352	1.26250
Average	0.18571	0.44740	0.60244	0.93793	1.25363

The components of the mode shapes are normally determined by the values of the transfer functions at the natural frequencies. It is important to note that in the context of ambient testing, transfer function does not mean the ratio of response over force, but rather the ratio of response measured by a roving sensor over response measured by a reference sensor. So every transfer function yields a mode shape component relative to the reference sensor.

Fig. 4.1.   Instrumentation Scheme: Seven Stations
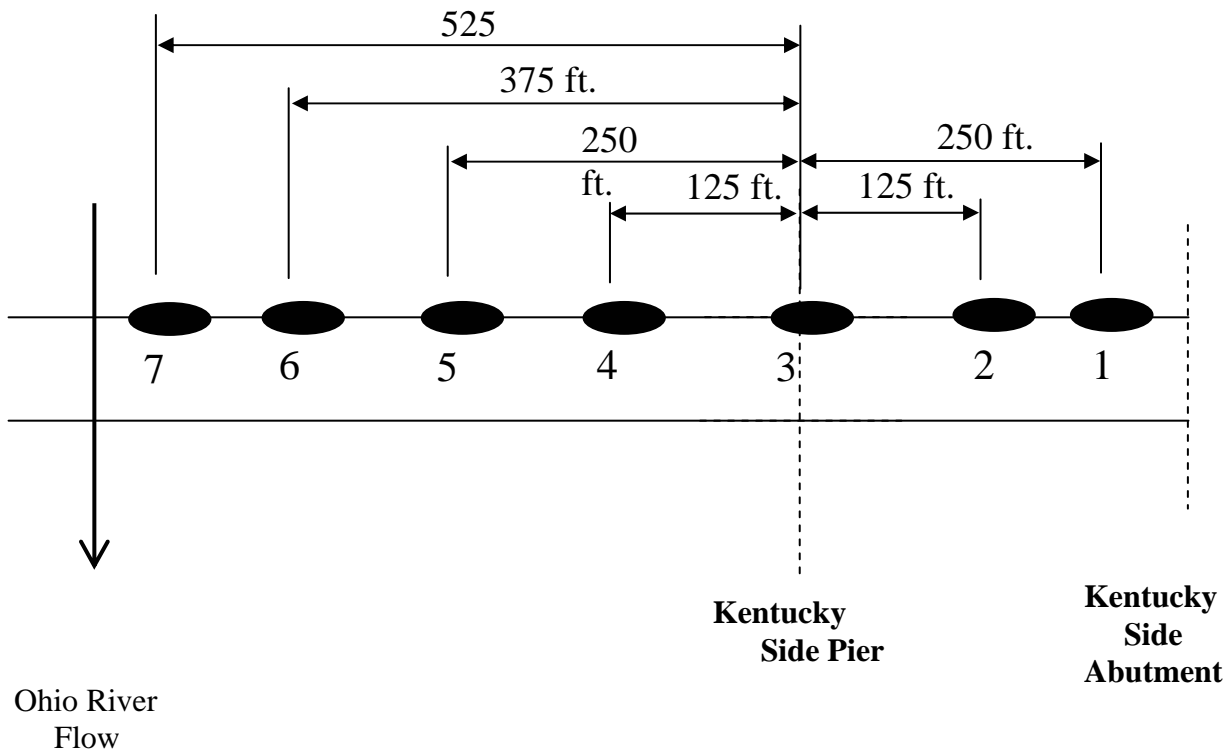
At Station 1 :   Channel 1   - Vertical
                  Channel 2   - Transverse

At Station 2 :   Channel 3   - Vertical
                  Channel 4   - Transverse

At Station 3 :   Channel 5   - Vertical
                  Channel 6   - Transverse

At Station 4 :   Channel 7   - Vertical
                  Channel 8   - Transverse

At Station 5 :   Channel 9   - Vertical
                  Channel 10 - Transverse

At Station 6 :   Channel 11 - Vertical
                  Channel 12 - Transverse

At Station 7:   Channel 13 - Vertical
                  Channel 14 - Transverse

All transverse accelerometers are oriented in direction of river flow.
All accelerometers positioned at floorbeam, lower chord intersections
of upstream stiffening truss.

Fig. 4.2   The Detailed Instrumentation

93
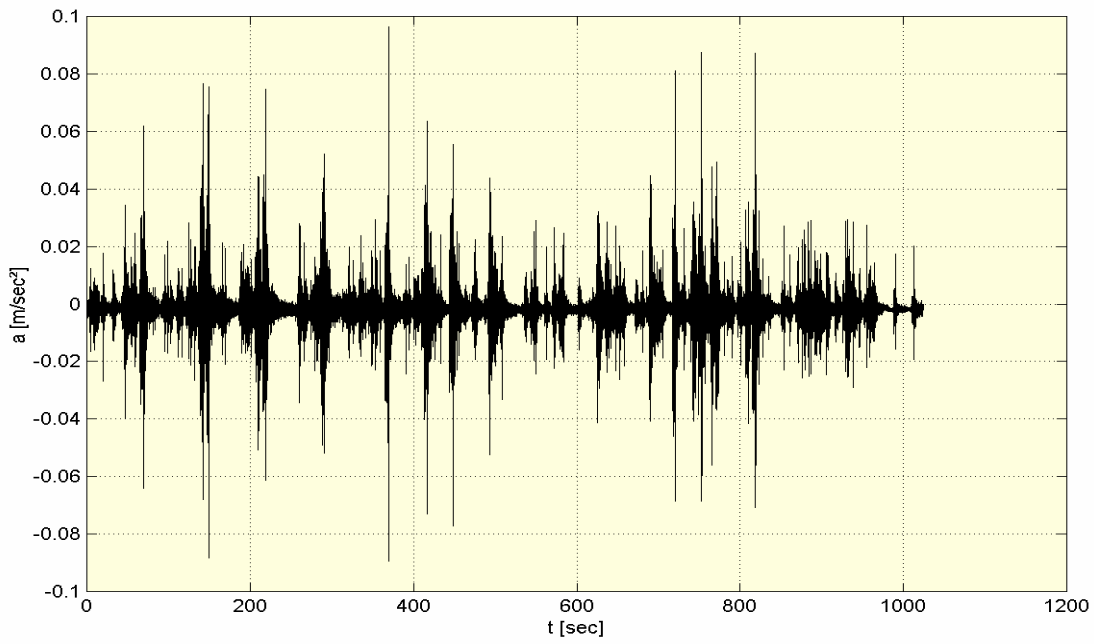
Fig. 4.3a Vertical Raw Acceleration-Time Measurement at Station 1 (Test1)
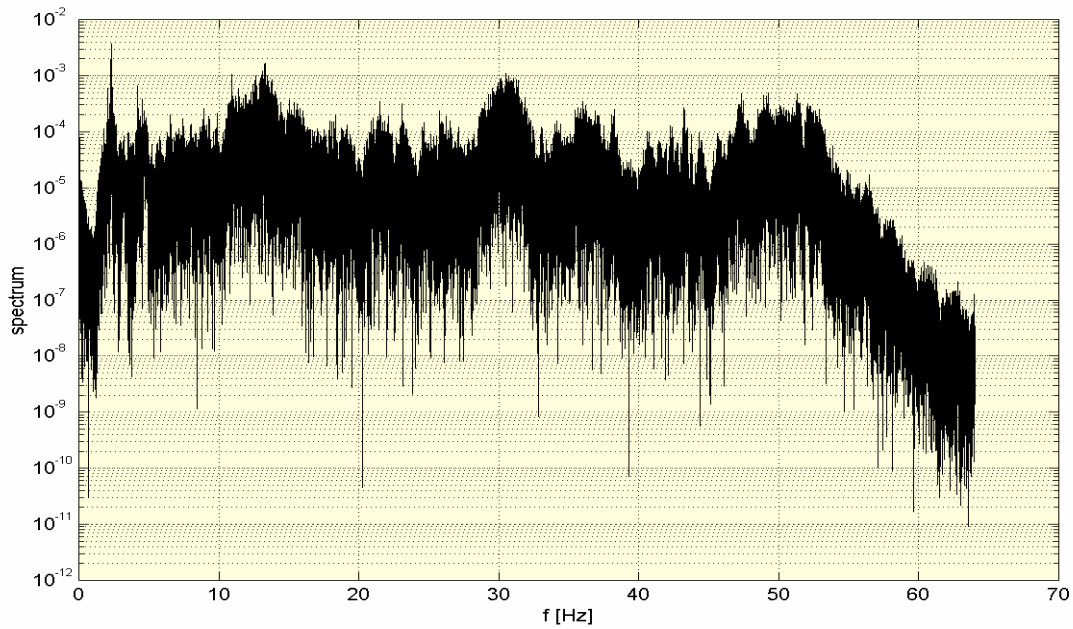
Fig. 4.3b   Vertical Power Spectral Density at Station 1 (Test1)
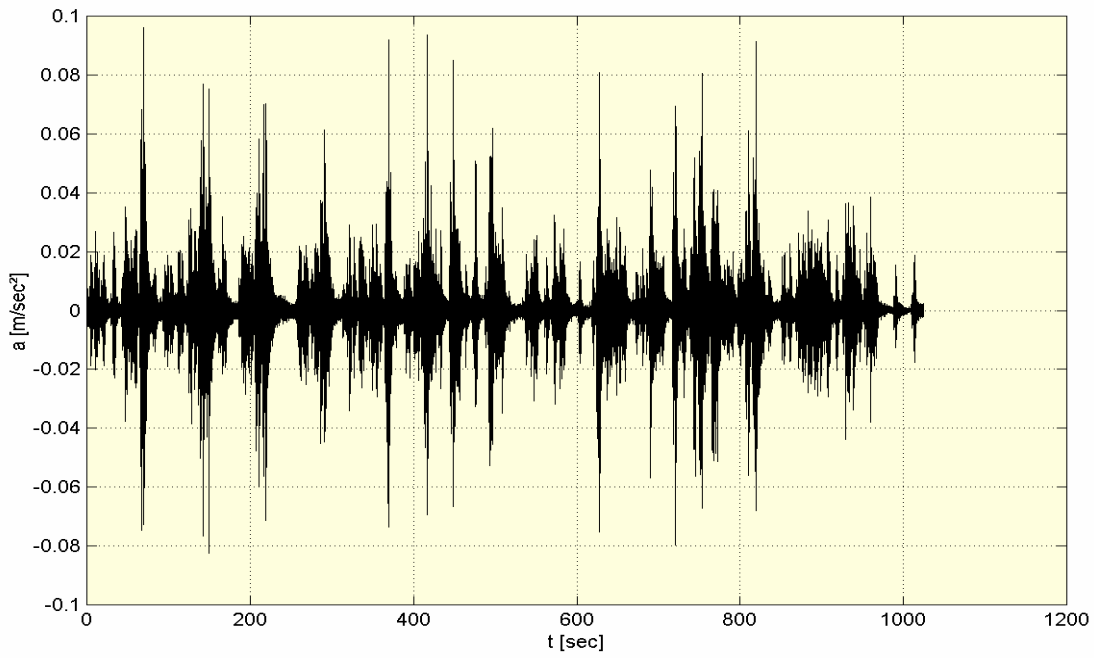
Fig. 4.4a   Transverse Raw Acceleration-Time Measurement at Station 1 (Test1)
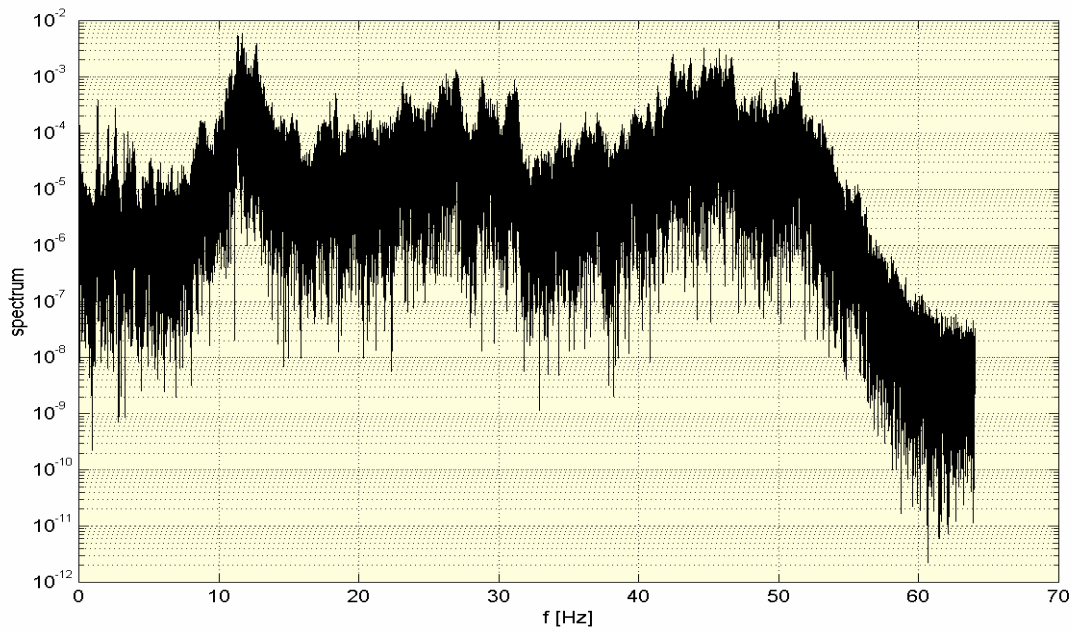
Fig. 4.4b   Transverse Power Spectral Density at Station 1 (Test1)
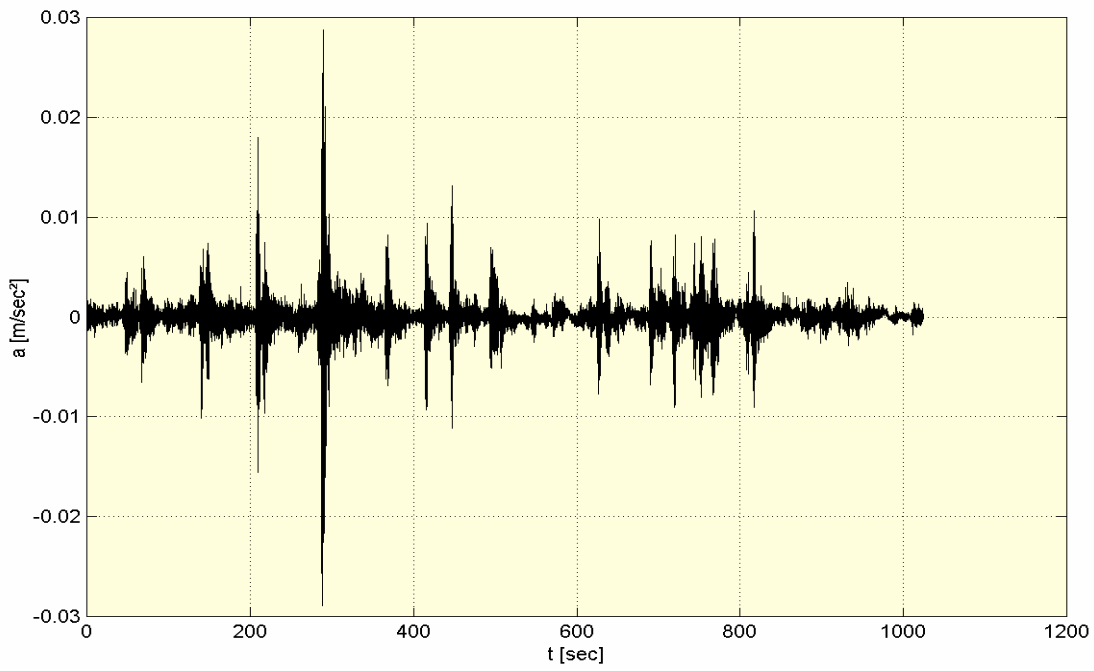
Fig. 4.5a   Resampled Vertical Acceleration-Time Measurement at Station 1 (Test1)
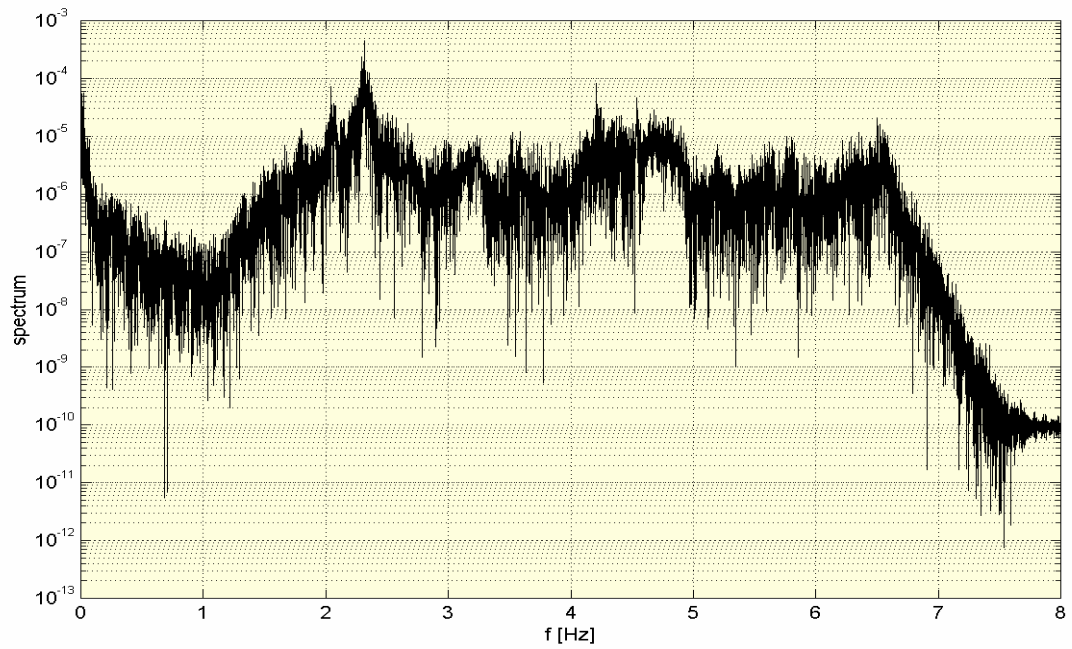
Fig. 4. 5b   Resampled Vertical Power Spectral Density at Station 1 (Test1)
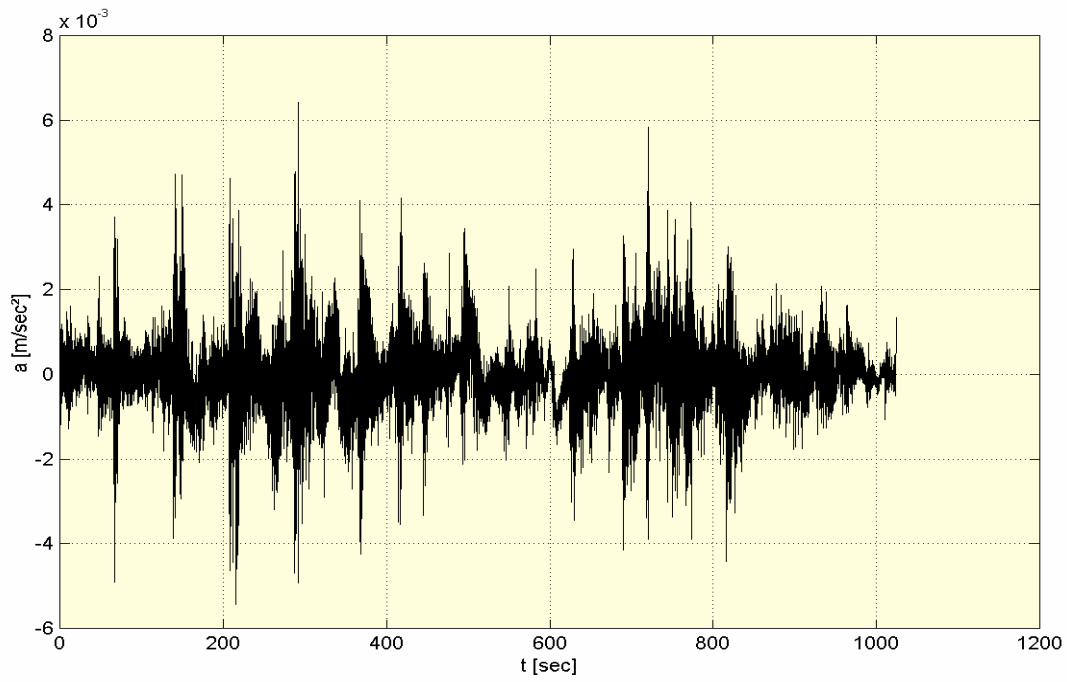
Fig. 4.6a   Resampled Transverse Acceleration-Time Measurement at Station 1 (Test1)
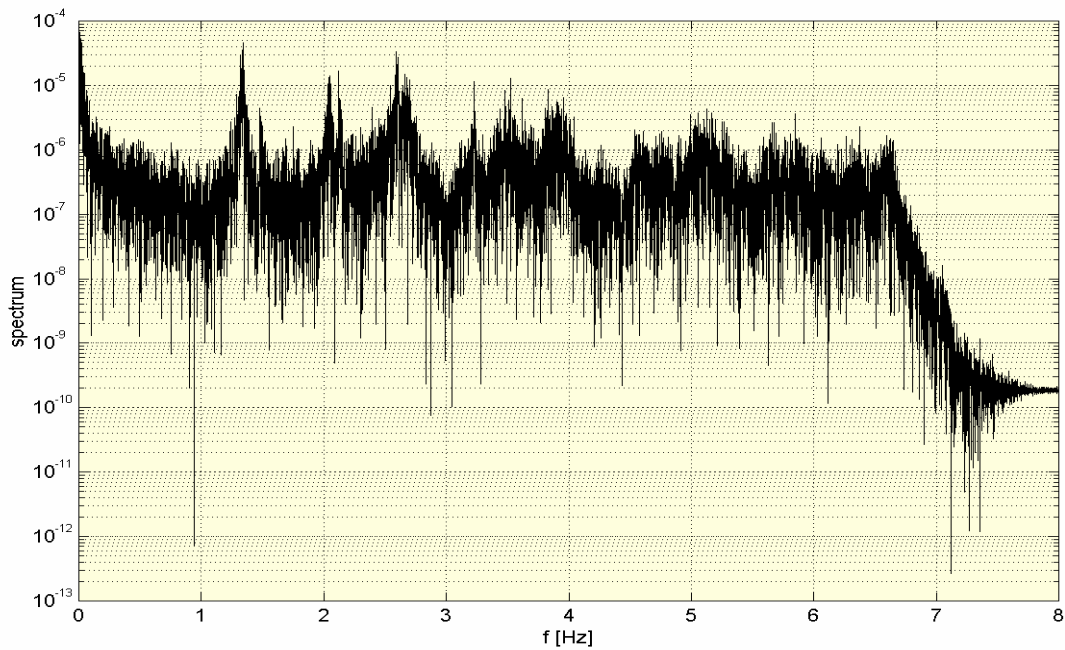
Fig. 4.6b   Resampled Transverse Power Spectral Density at Station 1 (Test1)
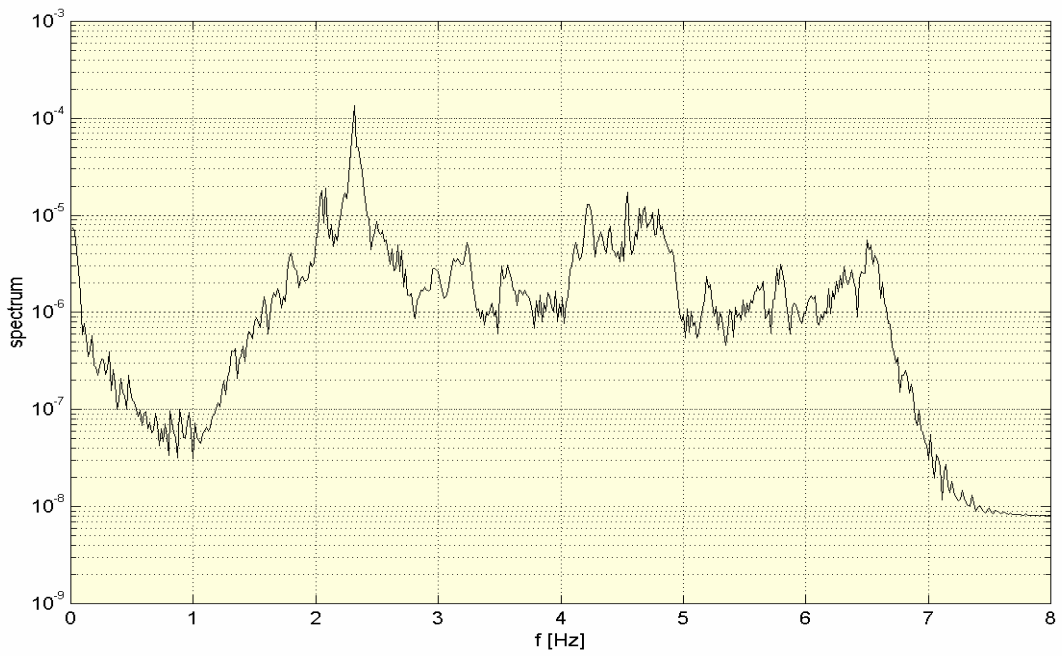
Fig. 4.7   Modified Vertical Power Spectral Density at Station 1 (Test1)
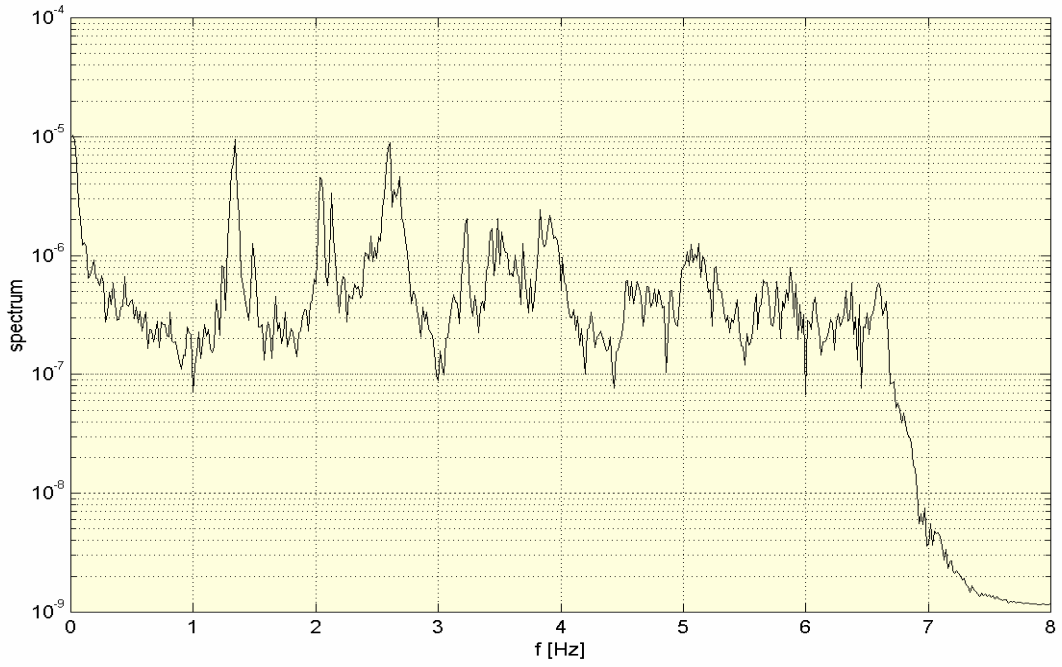
Fig. 4.8   Modified Transverse Power Spectral Density at Station 1 (Test1)

98
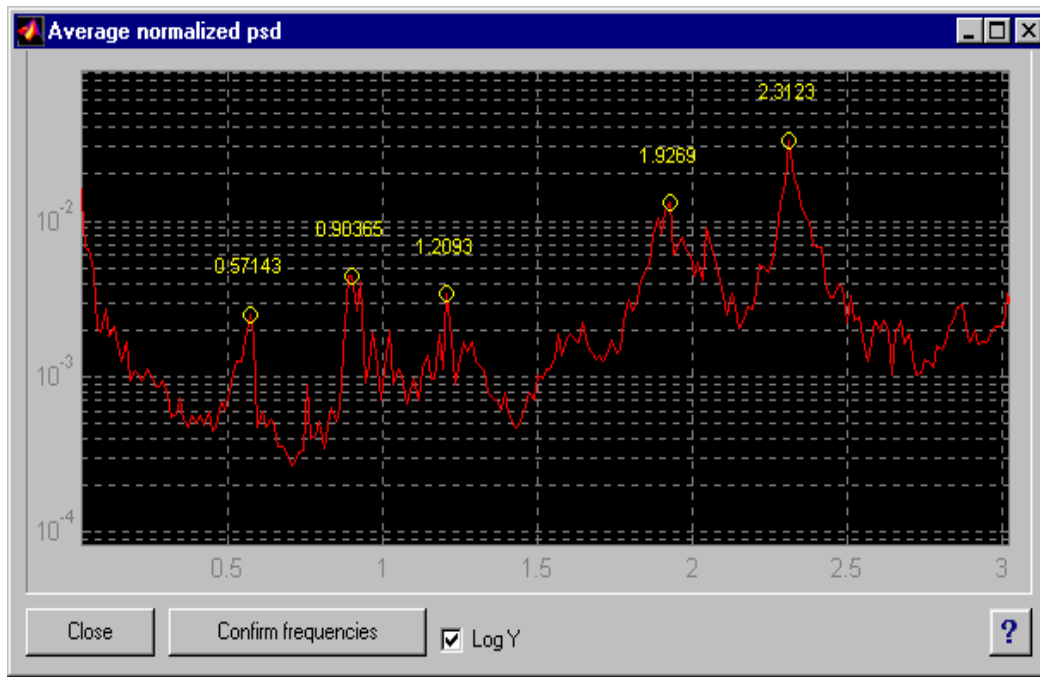
Fig. 4.9a   Vertical Average Normalized Power Spectral Density of Test1
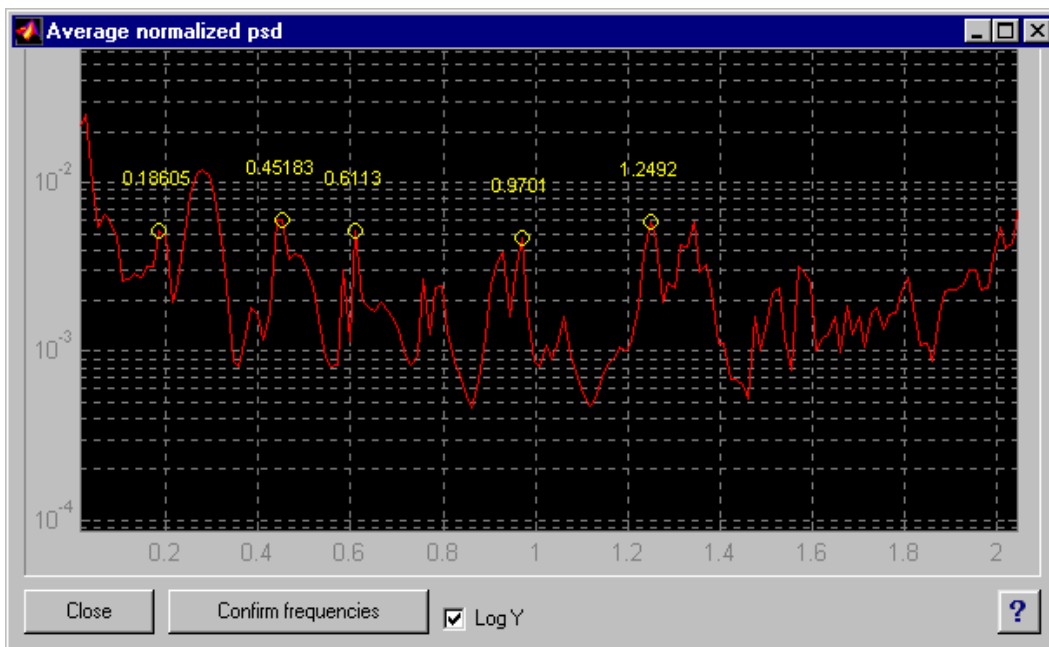
Fig. 4.9b   Transverse Average Normalized Power Spectral Density of Test1
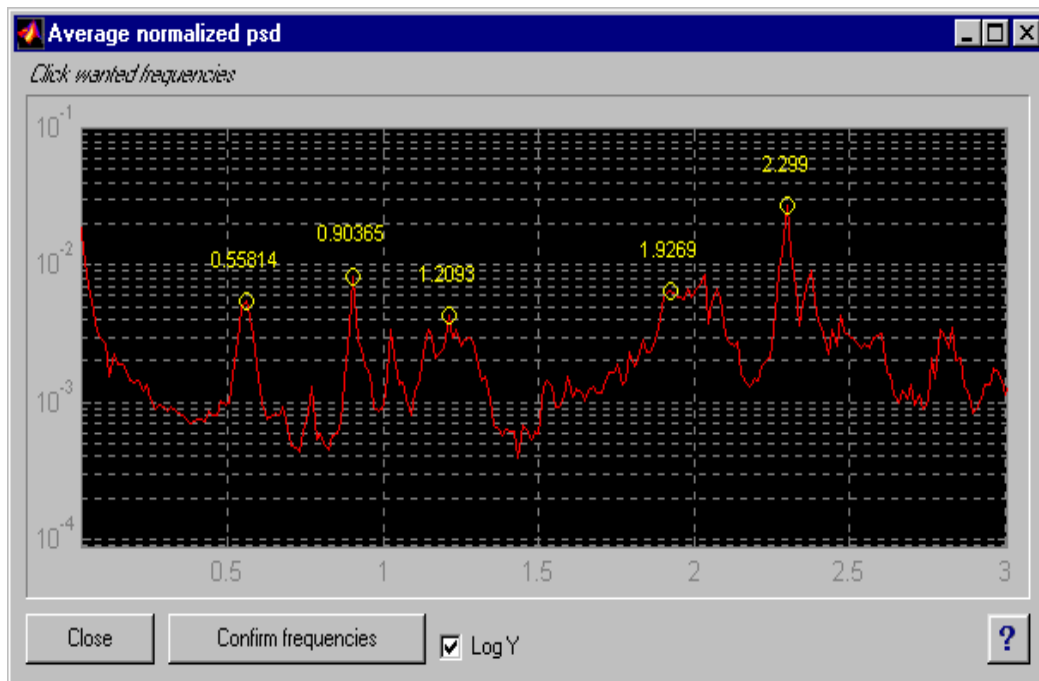
Fig. 4.10a   Vertical Average Normalized Power Spectral Density of Test2
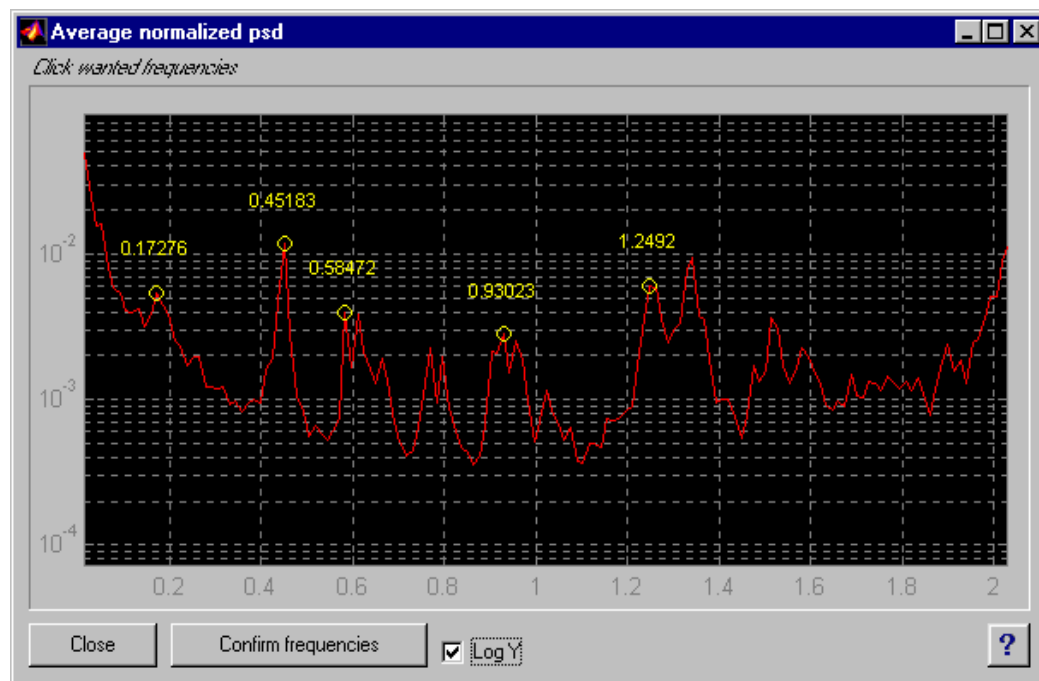
Fig. 4.10b Transverse Average Normalized Power Spectral Density of Test2

100
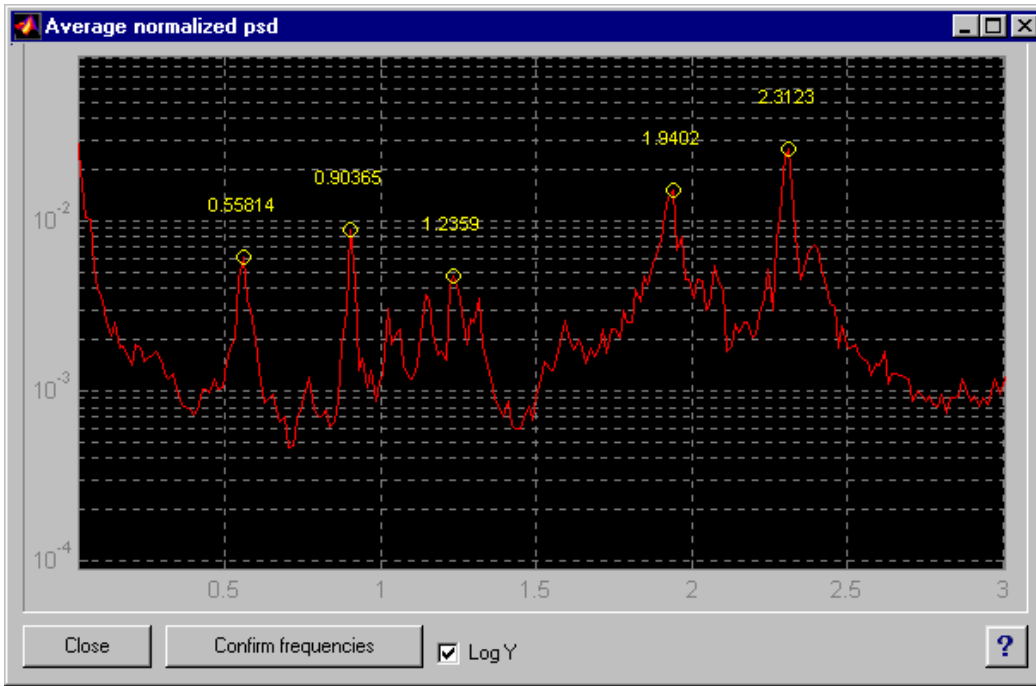
Fig. 4.11a   Vertical Average Normalized Power Spectral Density of Test3
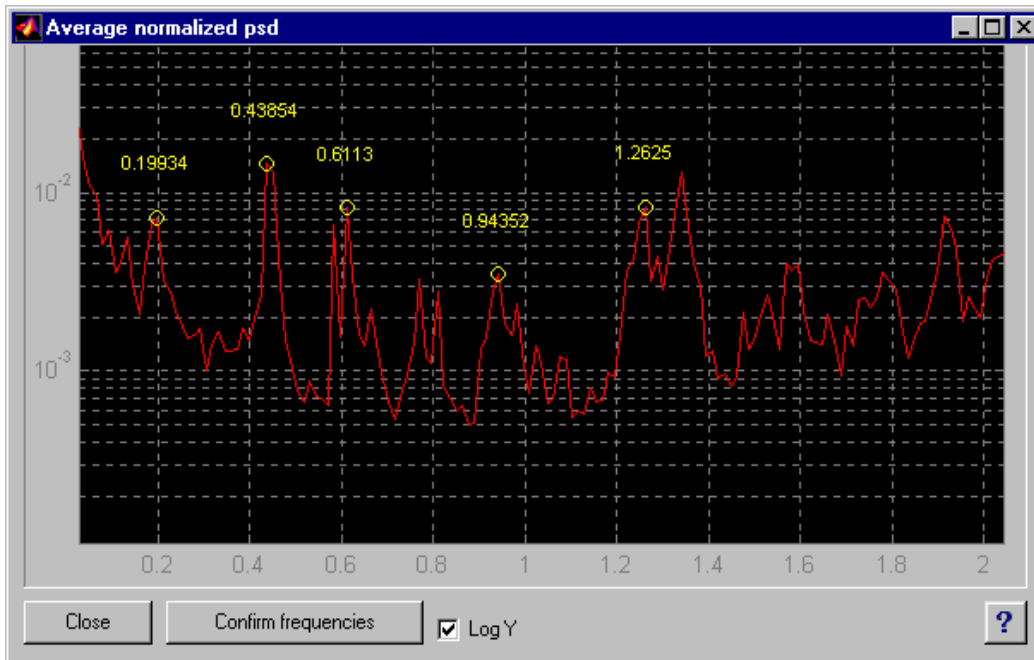
Fig. 4.11b Transverse Average Normalized Power Spectral Density of Test3

101

4.5 Finite Element Model Calibration

Now we know the real dynamic properties of the bridge through field ambient vibration testing. And we already know the structural or material parameters that may largely affect the modal properties of the bridge through parametric studies. The original finite element model can be calibrated by adjusting these parameters to match the frequencies and mode shapes best between testing and modeling. The updated structural and material parameters are summarized in Table 4.3 and Table 4.4 respectively.

Table 4.3 Calibrated Real Constants

Type	Cross-section area: m^2 (ft^2)	Inertia moment: m^4 (ft^4)		Initial strain or thickness	Structural member
		I_{zz}	I_{yy}		
1	0.027 (0.287)	3.194×10^{-4} (0.037)	9.667×10^{-4} (0.112)	-	Bottom chords
2	0.0318 (0.342)	1.079×10^{-3} (0.125)	1.510×10^{-3} (0.175)	-	Top chord
3	0.0101 (0.109)	1.033×10^{-4}	1.726×10^{-4} (0.02)	-	Verticals
4	0.0085 (0.0917)	-	-	-	Diagonals
5	0.0559 (0.602)	-	-	0.8×10^{-3}	Primary cable
6	0.00485 (0.0522)	-	-	-	Suspender
7	0.0431 (0.464)	-	-	0.8×10^{-3}	Secondary cable
8	0.00384 (0.0413)	-	-		Tie rods
9	107.777 (1160.1)	2057.19 (238350)	459.25 (53209)	-	Columns
10	0.00256 (0.0276)	-	-	0.0	Stay wire
11	0.00256 (0.0276)	-	-	-	Stabilizer cable
12	0.0141 (0.152)	2.020×10^{-4} (0.0234)	9.986×10^{-5} (0.01157)	-	Outer stringer
13	0.0171 (0.184)	4.954×10^{-4} (0.0574)	1.498×10^{-4} (0.01736)	-	Inner Stringer
14	0.0361 (0.388)	4.100×10^{-3} (0.475)	1.131×10^{-3} (0.1334)	-	Floor beam
15	-	-	-	6.096 (20)	Web wall above
16	-	-	-	3.962 (13)	Web wall below

Table 4.4　Calibrated Material Properties

Group No.	Young's modulus MPa (lb/ft^2)	Poisson's ratio	Mass density kg/m^3 (lb/ft^3)	Structural member
1	0.84×10^5 (1.754×10^9)	0.3	7849 (490)	Stiffening trusses
2	1.6×10^5 (3.342×10^9)	0.3	7849 (490)	Cables
3	2.0×10^5 (4.177×10^9)	0.3	7849 (490)	Suspenders
4	2.0×10^5 (4.177×10^9)	0.3	7849 (490)	Stay wires and tie rods
5	2.0×10^4 (4.177×10^8)	0.15	2500 (156)	Tower
6	2.1×10^5 (4.386×10^9)	0.3	19575 (1222)	Floor beams and stringers

The first five vertical frequencies and transverse frequencies coming out of the system identification through ambient vibration measurements and FEM predictions are summarized in Table 4.5 and Table 4.6. A good agreement of frequencies has been found between FEM modeling and in situ ambient measurements. As mentioned previously, a dominated mode of the Roebling suspension bridge in 3-D FEM modeling is always coupled with other mode shapes. The higher the dominated mode, the more serious the coupling. Because the experimental modal properties of the bridge come form the ambient vibration measurements, the better matching for higher modes is not expected and not realistic.

Table 4.5　Comparison of Vertical Frequencies (Hz)

Order	v1	v2	v3	v4	v5
Test	0.563	0.904	1.218	1.931	2.308
FEM	0.561	0.971	1.240	1.843	2.282

Table 4.6　Comparison of Transverse Frequencies (Hz)

Order	t1	t2	t3	t4	t5
Test	0.186	0.447	0.602	0.938	1.254
FEM	0.189	0.418	0.617	0.875	1.091

The first two vertical and transverse mode shapes of both FEM modeling and ambient testing are shown in Fig.4.12 ~ Fig.4.15. The test mode shapes are directly obtained by picking up the magnitude values of each spectral diagram at the peak points of interest and then normalized to unity. The sign of magnitudes is referred to the mode shapes of FEM results. The FEM mode shapes have been normalized according to the maximum value (unity) of the test point. In fact, the mode shapes through ambient vibration are not always that good because ambient excitation does not lend itself to frequency response functions (FRFs) or impulse response functions (IRFs) since the input

force can not be measured. Peak picking is always a subjective task. This is one of the drawbacks of structural system identification through ambient measurements.

4.6 Observations and Remarks

1. It is found that the simple peak picking technique is applicable in the identification of the Roebling suspension bridge through the ambient vibration measurements. The identified eigen frequencies from three separate ambient vibration measurements are quite stable. The peak picking method is fast and easy to apply. However, the peak picking technique has some theoretical drawbacks. Picking the peaks is always a subjective task. The operational deflection shapes are obtained instead of mode shapes. The damping estimates are unreliable in the peak picking system identification method.

2. A good agreement of frequencies has been found between FEM modeling and in situ ambient testing. The identified frequencies from three separate ambient measurements are quite stable. But the mode shapes are not too good as ambient excitation does not lend itself to frequency response functions (FRFs) or impulse response functions (IRFs) since the input force can not be measured. This is also one of the drawbacks of ambient measurements.

3. The better matching for higher modes is not expected and not realistic too, as the experimental modal properties of the bridge come form the ambient vibration measurements.

Magnitude
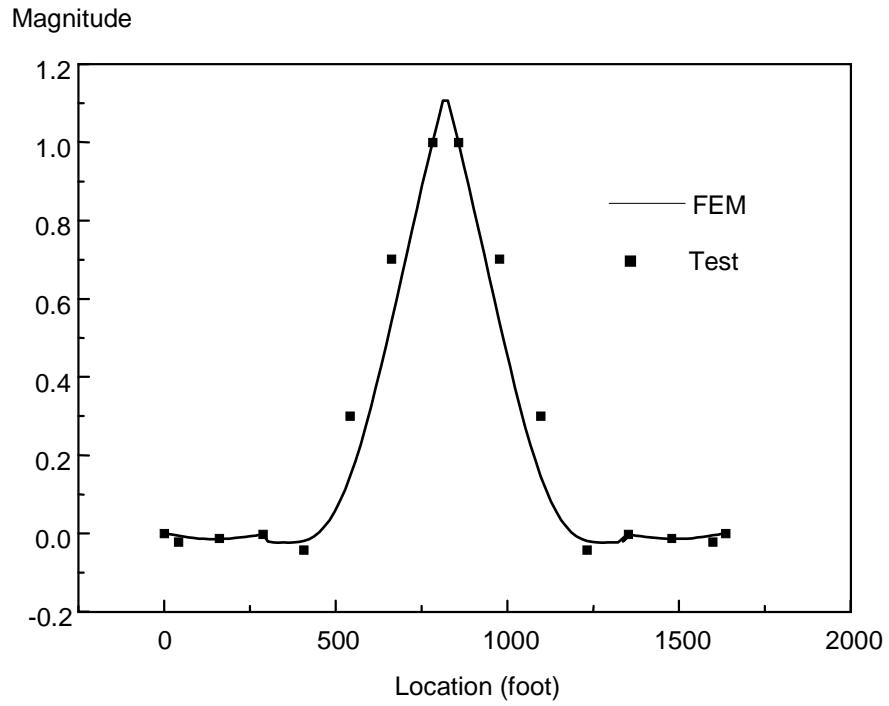
Fig. 4.12   Comparison of 1st Vertical Mode Shape

Magnitude
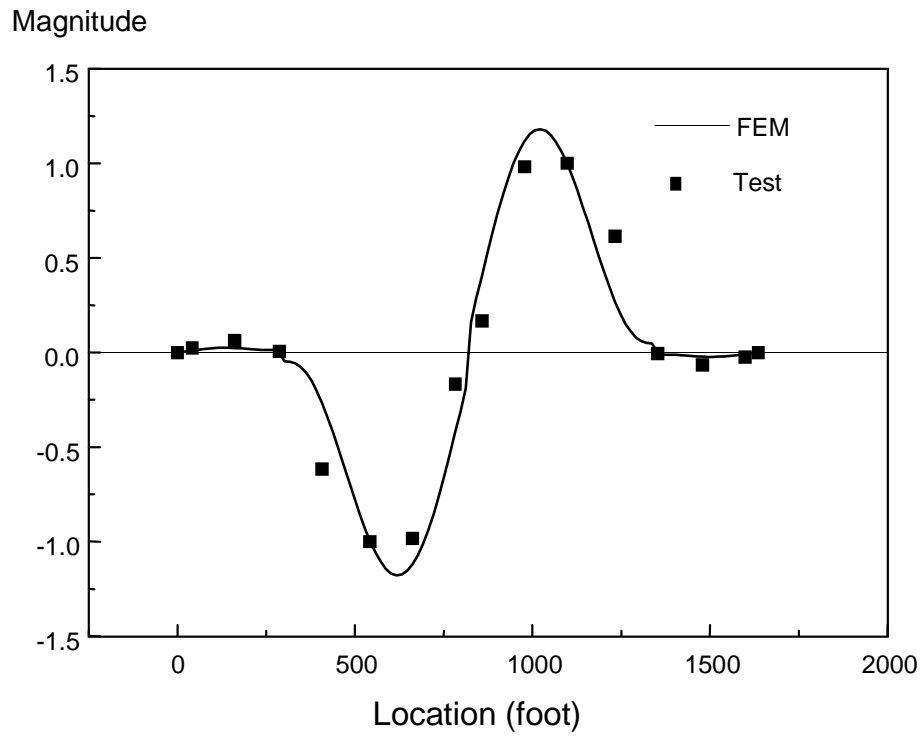
Fig. 4.13   Comparison of 2nd Vertical Mode Shape

Magnitude
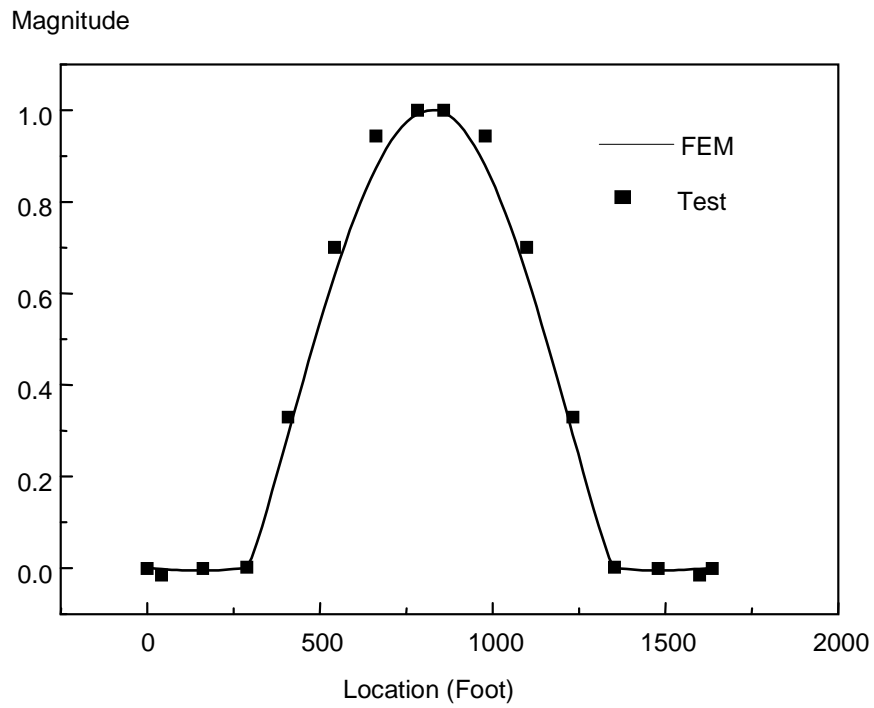
Fig. 4.14   Comparison of 1st Transverse Mode Shape

Magnitude
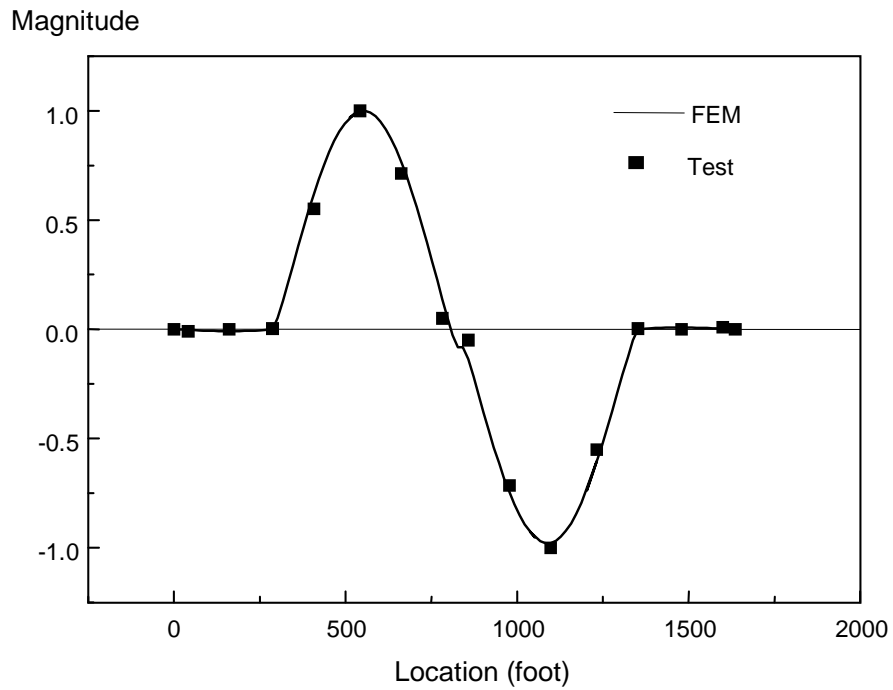
Fig. 4.15   Comparison of 2nd Transverse Mode Shapes

5. BRIDGE CAPACITY

5.1 General

An objective of performing bridge capacity evaluation is to determine the stiffness and strength of the bridge. The finite element model of the Roebling suspension bridge, once calibrated by the dynamic testing on site, is capable to evaluate the global capacity. The bridge capacity evaluation aims at finding the deflected shape and member forces due to dead load and imposed live loads on the bridge. Here, the considered live load pattern is an extreme live loading (40% in addition to the dead load). In addition, the cable area is reduced by a certain percentage (10~40%) to simulate the deterioration and corrosion of the cables. The bridge behavior under live loads is studied when the cable areas are reduced. The bridge capacity evaluation includes the maximum deflection, the capacity of the cables and the capacity of the stiffening trusses.

5.2 Bridge Capacity under Distributed Live Load Condition

As mentioned previously, 2.5Kips/ft distributed dead load is applied to the bridge deck. In addition to the dead load, a uniform deck live load of 1.0 kips/ft is considered. The value of 1.0 kips/ft is 40% of the dead load value and considered an extreme live loading. These loads are taken from the report by Hazelat and Erdel (1953). In the finite element analysis, the load is applied directly on each node of inner stringers under the assumption that the floor beam will transmit this force onto the bottom chord. The additional distributed live load of 1.0 kips/ft is then equivalent to 15 kips point load applied on each node of the inner stringers. In other words, the total nodal load of (Dead+Live) load is 52.5kips.

The cable area is reduced by a certain percentage to simulate the deterioration and corrosion of the cables. The following four cable area reduction cases have been considered:

- **Cable Case 1**: the effective sectional areas of both primary and secondary cables are reduced by 10%;
- **Cable Case 2**: the effective sectional areas of both primary and secondary cables are reduced by 20%;
- **Cable Case 3**: the effective sectional areas of both primary and secondary cables are reduced by 30%;
- **Cable Case 4**: the effective sectional areas of both primary and secondary cables are reduced by 40%;

The ultimate strengths of member materials as shown in Table 5.1 are used to judge the allowable capacity of structural members. The bridge capacity evaluation includes the maximum deflection, the capacity of the cables and the capacity of the stiffening trusses.

Table 5.1 Ultimate Strengths of Materials

Member	Primary cable	Secondary cable	Suspender	Chords	Diagonals
Ultimate Stress	96,000 *psi* (662MPa)	180,000 *psi* (1240MPa)	20,000 *psi* (138Mpa)	20,000 *psi* (138MPa)	25,000 *psi* (172MPa)

5.2.1 Maximum Deck Deflection

Shown below (Fig.5.1) is the deflected shape under dead load, an additional 40% live load and 40% cable area reduction. The additional deflections under the live load consider as a measure of the suspension bridge stiffness. Table 5.2 lists the maximum deflections at the span center. It can be observed that the reduction of the effective cable areas does increase the deck deflection significantly. Once again, it can be noted that the deflections may not increase proportionally to the load since the structure is nonlinear.

Deflection (foot)

Deck Location (foot)
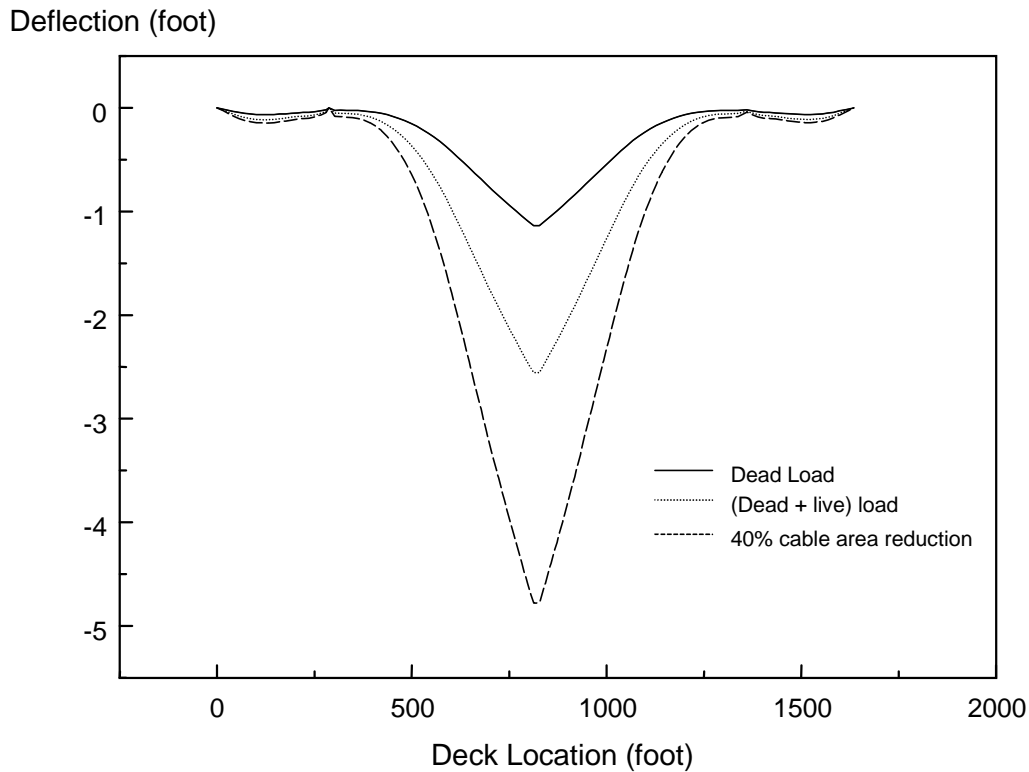
Fig. 5.1 Deck Deflected Shape under Loadings

108

Table 5.2 Maximum Deflection of Deck

Cases	Dead load	Dead+live load	Cable case 1	Cable Case 3	Cable case 3	Cable case 4
Deflection (foot)	-1.1606	-2.6079	-3.0573	-3.5733	-4.1720	-4.8778

5.2.2 Load-Carrying Capacity of the Cables

Table 5.3 lists the maximum forces and safety evaluation for the primary cable, secondary cable and suspender. It is found that the total forces in the cables would increase about 25% under the live loading of 40% dead load. The safety factors of the cables are more than three. Assuming that the ultimate strength of the primary cables has been reduced by 12.5% as estimated during the cable restoration of the 1890's, the total stress in the primary cable is still 2.8 times less than its ultimate strength.

The secondary cable was built up in 1897 after the completion of the bridge in 1867. The safety factor of the secondary cable is always much higher than other cable members as it is composed of steel wires, instead of iron wires, which almost doubles the ultimate strength. The inspection of the secondary cables (Parsons Brinckerhoff Quade & Douglas, Inc. 1988) counted twenty-one broken wires in the south anchorage for the east secondary cable. Several strands are also bulging due to corrosion caused by primarily by leakage of water through the roof. Assuming conservatively that the ultimate strength has been reduced by 40%, the increased actual stress is still more than three times less than ultimate strength.

According to the inspection on site, the primary and secondary suspension cables are in fair condition. The areas of deterioration are in the masonry anchorages. The paint system on the primary cable wrapping is in poor condition. There is also a heavy accumulation of pigeon waste on the cables in the towers. A report prepared by the Kentucky department of Highways, Division of Maintenance, suggests that this cable has lost 35% of its ultimate strength. Assuming conservatively that the effective sectional area has been reduced by 40% for both primary and secondary cables, the safety factors of cables are still more than two.

The safety of suspenders is fair according to Table 5.3. It is observed that the reduction of cable areas does not result in the significant reduction of the safety for the cable members themselves. As the most important members to sustain the loads of a suspension bridge, however, it does increase the deflections significantly. In the next section it can be seen that the reduction of cable areas does increase the forces in the stiffening truss members and reduce the safety factors significantly.

109

Table 5.3   Capacity of Cables

Member		Maximum Force (Kips)	Allowable Capacity (Kips)	Safety
Dead load	Primary cable	2,062	8,392	4.07
	Secondary cable	1,533	12,040	7.85
	Suspender	36	150	4.17
Dead load + live load	Primary cable	2,620	8,392	3.20
	Secondary cable	1,947	12,040	6.18
	Suspender	46	150	3.26
Dead load + live load + 10% cable area reduction	Primary cable	2,520	7,553	3.00
	Secondary cable	1,870	10,836	5.79
	Suspender	44	150	3.41
Dead load + live load + 20% cable area reduction	Primary cable	2,405	6,714	2.79
	Secondary cable	1,783	9,632	5.40
	Suspender	42	150	3.57
Dead load + live load + 30% cable area reduction	Primary cable	2,274	5,874	2.58
	Secondary cable	1,683	8,428	5.01
	Suspender	40	150	3.75
Dead load + live load + 40% cable area reduction	Primary cable	2,122	5,035	**2.37**
	Secondary cable	1,567	7,224	**4.61**
	Suspender	37	150	4.05

5.2.3 Capacity of the Stiffening Trusses

The magnitude of the member forces in the stiffening trusses induced due to dead and additional live loads is of interest. Table 5.4 summarizes the maximum forces in some of the typical truss members of the model. An investigation of the member forces reveals that the forces induced under a very severe uniformly distributed live loading (40% of dead load) are well within the maximum capacity of the member for most members. The critical members are the top chords.

It can be seen that the reduction of cable areas significantly increases the forces in the stiffening truss members and therefore the safety factors reduce dramatically. Assuming conservatively that the effective sectional area has been reduced by 40% for both primary and secondary cables, the induced forces in the critical truss members (top chords) almost approach the design limit. However this level of loading and cable area reduction is very extreme and considered improbable.

Table 5.4   Capacity of Stiffening Truss

Member		Maximum Force (Kips)	Allowable Capacity (Kips)	Safety
Dead load	Bottom chord	58.7	828	14.11
	Top Chord	-170.8	985	5.77
	Diagonal	34.5	330	9.57
Dead load + live load	Bottom chord	138.8	828	5.97
	Top Chord	-367.7	985	2.68
	Diagonal	79.9	330	4.13
Dead load + live load + 10% cable area reduction	Bottom chord	162.2	828	5.11
	Top Chord	-434.5	985	2.27
	Diagonal	93.8	330	3.52
Dead load + live load + 20% cable area reduction	Bottom chord	188.7	828	4.39
	Top Chord	-512.1	985	1.92
	Diagonal	109.7	330	3.01
Dead load + live load + 30% cable area reduction	Bottom chord	219.3	828	3.78
	Top Chord	-603.4	985	1.63
	Diagonal	128.2	330	2.58
Dead load + live load + 40% cable area reduction	Bottom chord	254.9	828	3.25
	Top Chord	-712.6	985	1.38
	Diagonal	150.0	330	2.20

Note: minus sign refers to compression

5.3 Observations and Comments

1. The deflections may not increase proportionally to the load since the suspension bridge is a nonlinear structure. The reduction of the effective cable areas does increase the deck deflection significantly. It can be observed that the effect of decreasing the truss stiffness does not lead to an increase in the bridge deflections as significant as a reduction of same percentage in the main cable areas. This observation once again points to the importance of the main cable in governing the stiffness of the suspension bridge.

2. The safety of primary cables, secondary cables and suspenders is fair under the extreme distributed live load condition (in addition to 40% dead load). Assuming conservatively that the effective sectional area has been reduced by 40% for both primary and secondary cables, the safety factors of cables are still more than two.

3. It is observed that the reduction of cable areas does not result in the significant reduction of the safety for the cable members themselves. As the most important members to sustain the loads of a suspension bridge, however, it does increase the deflections significantly. As a result, the reduction of cable areas increases the forces in the stiffening truss members and reduces the safety factors significantly.

4. The truss member forces induced under a very severe uniformly distributed live loading (40% of dead load) are well within the maximum capacity. The critical members are the top chords. Assuming conservatively that the effective sectional area has been reduced by 40% for both primary and secondary cables, the induced forces in the critical truss members (top chords) almost approach the design limit. However this level of loading and cable area reduction is very extreme. The margin of safety in the main cables and the suspenders is fair and this is of great significance for the safety concerns of a suspension bridge anyway.

6. CONCLUSIONS AND RECOMMENDATIONS

6.1 General

The John A. Roebling suspension bridge, completed in 1867, over the Ohio River between Covington, Kentucky and Cincinnati, Ohio, still stand today. This suspension bridge was obviously designed for live loads that are quite different from automobile traffic it carries today. It is necessary to bring the bridges up to current standards of safety. The present study focuses on the structure evaluation of the John A. Roebling suspension bridge. It has demonstrated that the dynamics-based structural evaluation method provides a 'global' way to evaluate the structural state and safety. The dynamics-based structural evaluation requires improvements in instrumentation for sensing and recording, data acquisition, algorithms for system identification, model updating and structure evaluation. The FEM model calibration through the field dynamic testing plays an important role in the dynamics-based structural evaluation. The calibrated FEM model serves as the base-line of load-carrying capacity evaluations of the bridge.

It is demonstrated that the margin of safety in the main cables and the suspenders is fair under the extremely distributed live load condition, and this is of great significance for the safety concerns of a suspension bridge. Assuming conservatively that the effective sectional area has been reduced by 40% for both primary and secondary cables, the safety factors of cables are still more than two. It is indicated that some truss members may be overstressed at an inventory loading. Hence, it is suggested that some truss members would have to be rehabilitated to carry the increased loading.

The outcome can assist in the preservation of the J.A. Roebling suspension bridge. The methodology developed could be applied to wide range of old cable-supported bridges.

6.2 Finite Element Modeling and Dynamic Properties

The complete 3-D nonlinear modeling of a suspension bridge has proved to be difficult. The smaller discretization would be computationally very large and inefficient. Convergence of such a large number of nonlinear elements is not always guaranteed. The displacement convergence criterion is effective and often results in the convergent solution. Due to the cable sagging, the static analysis of a suspension bridge is always a geometric nonlinear. The stress stiffening of cable elements plays an important role in both the static and dynamic analysis. Nonlinear static analysis without the stress stiffening effect will lead to an aborted run due to the divergent oscillation even though the displacement convergence criterion is used. Large deflection has demonstrated the limited effect on the member forces and deck deflection of the bridge under dead loads. After introducing enough amount of initial strain in the cables, the static analysis of the Roebling suspension bridge due to dead loads can be elastic and small deflection. However, the stress stiffening effect is always required to ensure the convergent solution.

The initial strain in the cables is the key factor to control the initial equilibrium configuration under dead loading. For a completed bridge, the common fact is that the initial position of the cable and bridge is unknown. The initial geometry of the bridge that we have modeled is really the dead load deflected shape of the bridge. The initial equilibrium configuration of the bridge due to dead

113

loads can be approximately achieved by manipulating the initial tension forces in the cables until a value is found that leads to the minimum deck deflection and minimum stresses in the stiffening structure.

It is demonstrated that a suspension bridge is a highly pre-stressed structure. The self-weight effect can significantly improve the stiffness of a suspension bridge. The modal or any dynamic analysis shall start from the initial equilibrium configuration due to dead loads. In other words, the modal analysis of a suspension bridge should include two steps: small deflection static analysis under dead loading and followed pre-stressed modal analysis. Namely, the modal analysis of a suspension bridge must be a pre-stressed modal analysis. In the case of the Roebling suspension bridge, the lateral stiffness benefits much more than the vertical stiffness does. The dead load effect increases the transverse natural frequency by about 20% but increases the vertical natural frequency by about 5% only. Hence, the regular modal analysis without a dead-load static analysis will under estimate the stiffness of the suspension bridge and consequently provides the more safe evaluation of the bridge.

It is observed that one dominated mode of the Roebling suspension bridge is always coupled with other modes. The dominated mode shapes of the Roebling suspension bridge in the low-frequency (0~1.0 Hz) range are in transverse direction. This reveals the fact that the lateral stiffness of the bridge is relatively weak because the lateral system of the Roebling bridge is a single truss system unlike the lateral systems of modern bridges which have major lateral load resisting systems comprising of two lateral trusses. Throughout the parametric studies the key parameters affecting the vertical modal properties of the Roebling suspension bridge are the mass, cable elastic modulus and stiffening truss stiffness. The key parameters affecting the transverse modal properties are the mass, cable elastic modulus, stiffening truss stiffness and the transverse bending stiffness of deck system.

6.3   Ambient Vibration Testing and Model Calibration

On site ambient vibration testing provides a fast and cheap way to obtain the real dynamic properties of a structure. It is found that the simple peak picking technique is applicable in the identification of the Roebling suspension bridge through the ambient vibration measurements. The identified eigen frequencies from three separate ambient vibration measurements are quite stable. But the mode shapes are not too good as ambient excitation since the input force can not be measured. This is one of the theoretical drawbacks of ambient measurements.

A good agreement of frequencies (the first two transverse and vertical) has been found between the ambient vibration testing and analytical prediction from the calibrated FEM model. The better matching for higher modes is not expected and not realistic too, as the experimental modal properties of the bridge come form the ambient vibration measurements.

6.4   Bridge Capacity under Live load

The safety of primary cables, secondary cables and suspenders is fair under the extremely distributed live load condition (in addition to 40% dead load). Assuming conservatively that the

effective sectional area has been reduced by 40% for both primary and secondary cables, the safety

factors of cables are still more than two. It is observed that the reduction of cable areas does not result in the significant reduction of the safety for the cable members themselves. As the most important members to sustain the loads of a suspension bridge, however, it increases the deflections significantly. As a result, the reduction of cable areas increases the forces in the stiffening truss members and reduces the safety factors significantly.

The truss member forces induced under a very severe uniformly distributed live loading (40% of dead load) are well within the maximum capacity. The critical members are the top chords. Assuming conservatively that the effective sectional area has been reduced by 40% for both primary and secondary cables, the induced forces in the critical truss members (top chords) almost approach the design limit. However this level of loading and cable area reduction is very extreme. The margin of safety in the main cables and the suspenders is fair and this is of great significance for the safety concerns of a suspension bridge anyway.

6.5   Recommendations

The current load limit posting for the Roebling bridge is adequate. In case the load limit will be increased in the future, it is recommended that a detailed study be conducted to evaluate the need to strengthen the top chord truss members in order to increase the loading capacity of the truss.

REFERENCES

[1]   Abdel-Ghaffar, A.M. (1978). "Free lateral vibrations of suspension bridges." *J. Struct. Engrg.*, ASCE, 104(3), 503-525.

[2]   Abdel-Ghaffar, A.M. (1979). "Free torsional vibrations of suspension bridges." *J. Struct. Engrg.*, ASCE, 105(4), 767-787.

[3]   Abdel-Ghaffar, A.M. (1980). "Vertical vibration analysis of suspension bridges." *J. Struct. Engrg.*, ASCE, 106(10), 2053-2075.

[4]   Abdel-Ghaffer, A.M. and Scanlan, R. H.(1985). "Ambient vibration studies of Golden Gate Bridge. I: suspended structure." *J. Engrg. Mech.,* ASCE, 111(4), 463-482.

[5]   Andersen, P., Brincker, R. and Kirkegaard, P.H. (1996). "Theory of covariance equivalent ARMAV models of civil engineering structures." *Proceedings of IMAC14, the 14th International Modal Analysis Conference,* Dearborn, MI, 518-524.

[6]   ANSYS5.6 (1999). U*ser's manual*, Swanson Analysis System, USA. http://www.ansys.com

[7]   Bathe, K-J. (1982). *Finite element procedures in engineering analysis*. Prentice-Hall, Inc., Englewood Cliffs, New Jersey

[8]   Bendat, J.S. and Piersol, A.G. (1993). *Engineering applications of correlation and spectral analysis.* 2nd edition, John Wiley & Sons, New York.

[9]   Bounopane, S. and Billington, D. (1993). "Theory and history of suspension bridge design from 1823 to 1940." *J. Struct. Engrg.*, ASCE, 119(3), 954-977.

[10]   Brownjogn, J.M.W. and Xia, P.Q.(2000). "Dynamic assessment of curved cable-stayed bridge by model updating." *J. Struct. Engrg.,* ASCE, 126(2), 252-260.

[11]   Casas, J.R. and Aparicio, A.C. (1994). "Structural damage identification from dynamic-test data." *J. Struct. Engrg.*, ASCE, 120(8), 2437-2450.

[12]   Chen, H.L., Spyrakos, C.C. and Venkatesh, G. (1995). "Evaluating structural deterioration by dynamic response." *J. Struct. Engrg.*, ASCE, 121(8), 1197-1204.

[13]   DADiSP (1995). *User Manual, DADiSP Worksheet, Data Analysis and Display Software*. DSP Development Corporation, Cambridge, Massachusetts.

[14]   De Roeck, G., Peeters, B. and Ren, W.X. (2000). "Benchmark Study on System Identification through Ambient Vibration Measurements." *Proceedings of IMAC-XVIII*, the 18th International Modal Analysis Conference, San Antonio, Texas, 1106-1112.

[15] De Roeck, G. and Peeter, B. (1999). *MACEC2.0 – Modal Analysis on Civil Engineering Constructions*, Department of Civil Engineering, Catholic University of Leuven, Belgium. http://www.bwk.kuleuven.ac.be/bwk/mechanics/macec

[16] Doebling, S.W., Farrar, C.R., Prime, M.B. and Shevitz, D.W. (1996). "Damage identification and health monitoring of structural and mechanical systems from changes in their vibration characteristics: A literature review." *Research report LA-13070-MS, ESA-EA*, Los Alamos National Laboratory, New Mexico, USA.

[17] Ewins, D.J. (1986). *Modal testing: theory and practice*. Research Studies Press Ltd., England.

[18] Friswell, M.I. and Mottershead, J.E. (1995*). Finite element model updating in structural dynamics*, Kluwer Academic Publishers, Netherlands.

[19] Harik, I.E., Allen, D.L., Street, R.L., Guo, M., Graves, R.C., Harrison, J. and Gawry, M.J. (1997). "Free and ambient vibration of brent-spence bridge." *J. Struct. Engrg.,* ASCE, 123(9), 1262-1268.

[20] Harik, I.E., Allen, D.L., Street, R.L., Guo, M., Graves, R.C., Harrison, J. and Gawry, M.J. (1997). "Seismic evaluation of Brent-Spence bridge." *J. of Struct. Engrg*., ASCE, 123(9), 1269-1275.

[21] Harik, I.E., Vasudevan, K., Madasamy, C., Chen, D., Zhou, L., Sutterer, K., Steet, R. and Allen, D.L. (1999). "Seismic evaluation of the US41 Southbound bridge over the Ohio River at Henderson, KY." *Research Report KTC-99-17*, Kentucky Transportation Center, University of Kentucky.

[22] Hazelat and Erdel (1953). "Report on inspection of physical condition of the Convington & Cincinnati suspension bridges over the Ohio River." Cincinnati, Ohio

[23] Hearn, G. and Testa, R.B. (1991). "Modal analysis for damage detection in structures." *J. Struct. Engrg.*, ASCE, 117(10), 3042-3063.

[24] Hermans, L., Van der Auweraer, H. and Guillaume, P. (1998). "A frequency-domain maximum likelihood approach for the extraction of modal parameters from output-only data*." Proceedings of ISMA23, the 23th International Conference on Noise and Vibration Engineering.* Volume 1, 367-376, Leuven, Belgium.

[25] James III, G.H., Carne, T.G. and Lauffer, J.P. (1995). "The natural excitation technique (NExT) for modal parameter extraction from operating structures*." International Journal of Analytical and Experimental Modal Analysis,* 10(4), 260-277.

[26] Juang, J.N. (1994). *Applied system identification*. Prentice-Hall Inc., Englewood Cliffs, New Jersey.

[27] Juneja, Y. , Haftka, R.T. and Cudney, H.H. (1997). "Damage detection and damage detectability — analysis and experiments." *J. Aerospace Engrg.*, ASCE, 10(4), 135-142.

[28] Lall, J. (1992). "Analytical modelling of the J.A. Roebling suspension bridge." A thesis submitted to the Department of Civil and Environmental Engineering, University of Cincinnati in partial fulfillment of the requirements for the degree of Master of Science.

[29] Liu, P.L. (1995). "Identification and damage detection of trusses using modal data." *J. Struct. Engrg.*, ASCE, 121(4), 599-608.

[30] Ljung, L. (1987). *System identification: theory for the user*. Prentice-Hall Inc., Englewood Cliffs, New Jersey.

[31] Maia, N.M.M. and Silva, J.M.M. Edited. (1997*). Theoretical and experimental modal analysis.* Research Studies Press Ltd., England.

[32] Mazurek, D.F. and Dewolf, J.T. (1990). "Experimental study of bridge monitoring technique." *J. Struct. Engrg.*, ASCE, 116(9), 2532-2549.

[33] Nazmy, A.S., and Abdel-Ghaffar, A.M. (1990). "Three-dimensional nonlinear static analysis of cable-stayed bridges." *Comp. and Struct.,* 34(2), 257-271.

[34] Okukawa, A., Suzuki, S. and Harazaki, I. (2000). Suspension bridges, in the Chapter 18 of Bridge Engineering Handbook, CRC Press, USA.

[35] Parsons Brinckerhoff Quade & Douglas Inc. (1988). "Bridge inspection report: John A. Roebling bridge over the Ohio River at Conviton." *Division of Maintenance*, Department of Highways, Transportation Cabinet, Commonwealth of Kentucky.

[36] Ren, W.X. (1999a). "Ultimate behavior of long span cable-stayed bridges." *J. Bridge Engrg.*, ASCE, 4(1), 30-37.

[37] Ren, W.X. and Obata, M. (1999b): "Elastic-plastic seismic behavior of long span cable-stayed bridges." *J. Bridge Engrg.*, ASCE, 4(3), 194-203.

[38] Ren, W.X. and De Roeck, G. (2000a). "Structural damage identification through changes in dynamic characteristics. I: Simulation Verification." accepted by *J. Struct. Engrg.*, ASCE.

[39] Ren, W.X. and De Roeck, G. (2000b). "Structural damage identification through changes in dynamic characteristics. II: Test Verification." accepted by *J. Struct. Engrg.*, ASCE.

[40] Ren, W.X., Shen, J.Y. and De Roeck, G. (2000c). "Structural Stiffness Matrix Identification with Maximum Likelihood Estimation Method." *Proceedings of IMAC-XVIII*, the 18th International Modal Analysis Conference, San Antonio, Texas, 418-423.

[41] Roebling, J.A. (1867). Report to the Board of Directors of the Covington and Cincinnati Bridge Company.

[42] Salawu, O.S. (1997). "Detection of structural damage through changes in frequency: a review." *Engineering Structures*, 19(9), 718-723.

[43] Spyrakos, C.C., Kemp, E.L. and Venkatareddy, R. (1999). "Validated analysis of Wheeling suspension bridge." *J. Bridge Engrg.*, ASCE, 4(1), 1-7.

[44] Steinman, D.B. (1929). *A practical treatise on suspension bridges*, 2nd Ed., Wiley, New York.

[45] Stubbs, N., Sikorsky, C., Park, S., Choi, S. and Bolton, R. (1999). "A methodology to nondestructively evaluate the structural properties of bridges." *Proceedings of IMAC17, the 17th International Modal Analysis Conference*, 1260-1268, Kissimmee, Florida, USA.

[46] The Suspension Bridge Co. (1954). Rehabilitation of Cincinnati-Covington Suspension Bridge.

[47] Van der Auweraer, H. and Hermans, L. (1999). "Structural modal identification from real operating conditions." *Sound and Vibration*, 33(1), 34-41.

[48] Van Overschee, P. and De Moor, B. (1996). *Subspace identification for linear systems: theory, implementation and applications,* Kluwer Academic Publishers, Dordrecht, Netherlands.

[49] West, H.H., Suhoski, J.E. and Geschwindner Jr., L.F. (1984). "Natural frequencies and modes of suspension bridges." *J. Struct. Engrg.*, ASCE, 110(10), 2471-2486.

[50] Wilson, J.C. and Gravelle, W. (1991). "Modeling of a cable-stated bridge for dynamic analysis." *Int. J. Earthquake Engrg. and Struct. Dynamics*, 20, 707-721.